Winter 1985

# Sedimentology, Sedimentary Petrology, and Tectonic Setting of the Lower Miocene Clallam Formation, Northern Olympic Peninsula, Washington

Kurt Soe Anderson
*Western Washington University*

WESTERN WASHINGTON UNIVERSITY

*Bellingham, Washington 98225 • [206] 676-3000*

MASTER'S THESIS

In presenting this thesis in partial fulfillment of the requirements for a master's degree at Western Washington University, I agree that the Library shall make its copies freely available for inspection. I further agree that extensive copying of this thesis is allowable only for scholarly purposes. It is understood, however, that any copying or publication of this thesis for commercial purposes, or for financial gain, shall not be allowed without my written permission.

Signature _____

Date March 25 1985

**MASTER'S THESIS**

In presenting this thesis in partial fulfillment of the requirements for a master's degree at Western Washington University, I grant to Western Washington University the non-exclusive royalty-free right to archive, reproduce, distribute, and display the thesis in any and all forms, including electronic format, via any digital library mechanisms maintained by WWU.

I represent and warrant this is my original work and does not infringe or violate any rights of others. I warrant that I have obtained written permissions from the owner of any third party copyrighted material included in these files.

I acknowledge that I retain ownership rights to the copyright of this work, including but not limited to the right to use all or part of this work in future works, such as articles or books.

Library users are granted permission for individual, research and non-commercial reproduction of this work for educational purposes only. Any further digital posting of this document requires specific permission from the author.

Any copying or publication of this thesis for commercial purposes, or for financial gain, is not allowed without my written permission.

Name: Kurt S. Anderson

Signature: [redacted]

Date: 6/8/18

# Sedimentology, Sedimentary Petrology, and Tectonic Setting of the Lower Miocene Clallam Formation, Northern Olympic Peninsula, Washington

by
Kurt Soe Anderson

Accepted in Partial Completion
of the Requirements for the Degree
Master of Science

Dean of Graduate School

Chairperson

# Sedimentology, Sedimentary Petrology, and Tectonic Setting of the Lower Miocene Clallam Formation, Northern Olympic Peninsula, Washington

A Thesis Presented to the Faculty of
Western Washington University

In Partial Fulfillment
of the Requirements for the Degree
Master of Science

by
Kurt Soe Anderson

# FRONTISPIECE

"How do we presume to claim for ourselves or for our children dirt that leaves labor over or the low hill that is an ancient broken-hearted mountain, worn away by long erosion, white tides of snow ?"

James Carroll

## ABSTRACT

The Lower Miocene Clallam Formation, located on the northern coast of the Olympic Peninsula, Washington, is an approximately 800 m thick sequence of sandstone and conglomerate that was deposited in the predominantly marine portion of a prograding delta.

As a whole, the Clallam Formation coarsens and shallows upward, progressing from fossiliferous sandstones deposited below wave base, through storm-dominated deposits characterized by climbing ripples, graded rythmites, and hummocky cross-stratification, to coarse-grained distributary mouth deposits. Within this general progression are several small-scale coarsening- and shallowing-upward cycles that reflect the occupation and subsequent abandonment of distributary channels.

Analysis of lithic and monocrystalline grain characteristics indicates that the Clallam Formation had four major types of source rocks: andesitic to dacitic volcanic rocks, chert, metamorphic rocks, and intermediate plutonic rocks. Point count data plotted on ternary diagrams indicate that modal compositions were affected by depositional mechanisms. Sandstones deposited during storm activity contain fewer lithic constituents. When data from samples unaffected by storm deposition are plotted on ternary diagrams, mean modal compositions are Q:F:L= 40:22:38; Qm:F:Lt= 28:22:50; Qp:Lv:Ls= 21:56:23. Petrologic studies indicate that one or more of Vancouver Island, the San Juan Islands, and the Cascade Range (which contain similar rock types) was the source for the Clallam Formation sandstones.

The structural and depositional events that affected the Olympic Peninsula are intimately tied to the motions of the Pacific, Farallon, and North American plates. In the vicinity of the Olympic Peninsula, basin subsidence, uplift, and structural and metamorphic events that occurred

during the Oligocene and Miocene epochs were probably the result of the morphology of the Farallon Plate, which was then being subducted under the North American plate, rather than the result of changes in its relative velocity. The passage of two fracture zones, the Aja at about 28 Ma and the Sedna at about 16 Ma, may have influenced pre- to post-Clallam Formation structural and depositional events in the vicinity of the Olympic Peninsula.

## ACKNOWLEDGMENTS

I would like to especially thank my committee members Dr. Christopher A. Suczek, Dr. David C. Engebretson, and Dr. Steve Aronoff. Dr. Suczek gave hours of guidance, and aided in the editing of the manuscript. Dr. Engebretson deserves many thanks for stimulating discussions, primarily on tectonics. I am also grateful for his motivating spirit and friendship. Dr. Aronoff was a catalyst for creative thought and also aided in writing technique and editing of the manuscript. Patty Combs deserves thanks for sharing her wisdom of the intricacies of graduate school life, and thanks to Vicki Critchlow for sharing her knowledge of processing words.

Special thanks to Dr. Joanne Bourgeois and Elana Leithold for their invaluable discussions on sedimentology in the field and at the University of Washington.

Access to the field area was provided by the Pysht Tree Farm. Special thanks to Dan Sampson for pointing out many concealed outcrops.

A warm thanks to Leif Christenson and Kate Tysiak whose hospitality allowed me to spend many enjoyable times at their cabin in the hills. I am also grateful for the friendship of the many people on "the west end", particularily Spider and Lisa who shared their home and warmth.

Thanks to Keith Pine, Peter Jewett, Lolly Shera, Jeff Jones, and Moira Smith whose commitment to tele turning, peddling, and paddling added a fullness of heart and mind which allowed this project to be completed.

Warm thanks to Keith Marcott for the endless hours of discussion on the geology of the Olympic Peninsula, and for sharing the Olympic Peninsula in both its wettest and most magical moments.

Mostly I would like to thank Chuck and JoAnn Anderson for their continual love, support, and encouragment which enabled me to broaden my education in a variety of ways and places.

This project was made possible in part by NSF grant EAR-8121957.

## TABLE OF CONTENTS

## LIST OF FIGURES

## LIST OF TABLES AND PLATES

# INTRODUCTION

The Lower Miocene Clallam Formation, on the northern edge of the Olympic Peninsula, Washington, is a sequence of sandstone and conglomerate approximately 800 m thick that was deposited in the predominantly marine portion of a delta. Deposition of the delta took place in a setting that was tectonically active throughout the Cenozoic. The depositional history of the Clallam Formation reflects the Miocene tectonic development of the Olympic Peninsula and the effects of regional and local tectonic events on the delta system. This thesis will describe the sedimentology and sedimentary petrology of the Clallam Formation and relate these to regional tectonic developments.

## Geologic Setting

The Olympic Peninsula has two major tectonostratigraphic terranes (Silberling and others, 1984); the Olympic Core terrane and the Crescent terrane (Figure 1). The Olympic Core terrane consists mostly of metamorphosed marine sedimentary rocks with some sedimentologically and structurally interbedded volcanics. The Olympic Core terrane exhibits varying amounts of metamorphism ranging from zeolite facies to lowest greenschist facies. The metamorphic grade generally decreases from east to west. The distribution of sedimentary packets is a result of underthrusting of sedimentary units in an accretionary prism (Tabor and Cady, 1978a; Figure 2). Underthrusting and accretion continued through the Late Miocene or later.

The Crescent terrane of the Olympic Peninsula consists of basalt of the Eocene Crescent Formation and overlying marine sedimentary units (Figure 1). The sedimentary units are a nearly continuous sequence of Eocene to Miocene rocks that reflect deposition during marine regression. These rocks on the northern Olympic Peninsula dip away from the Olympic core,

Figrure 1. Generalized location map showing the distribution of the Olympic terrane and Crescent terrane, some major structures, pertinent rock units, and potential source areas.

| | | |
|---|---|---|
| Astoria (?) Formation and Montesano Formation | Tam | Lower Miocene |
| Hoh Lithic Assemblage | Th | Oligocene and Miocene |
| Sooke Formation | Ts | Late Oligocene |
| Crescent Formation | Tc | Eocene |
| Metchosin Volcanics | Tmv | Eocene |
| Leech River Complex | LRC | Jurassic and Cretaceous |

| | |
|---|---|
| Leech River fault | LRF |
| Discovery Bay fault | DBF |
| San Juan fault | SJF |
| Clallam syncline | CS |
| Carmanah Point | CP |

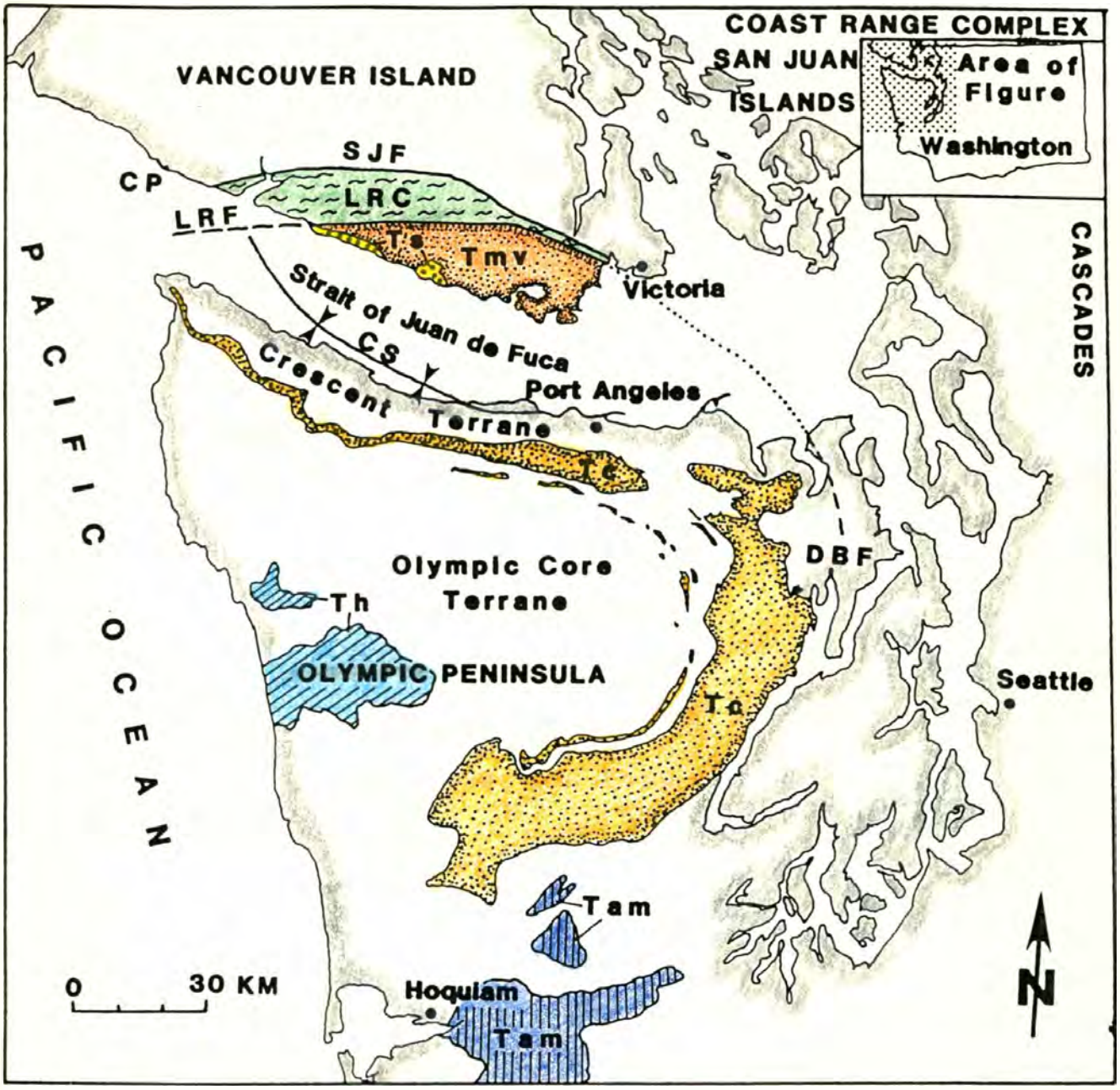
COAST RANGE COMPLEX
VANCOUVER ISLAND
SAN JUAN ISLANDS
Area of Figure
Washington
SJF
CP
LRC
LRF
Tc
Tmv
Victoria
CASCADES
PACIFIC OCEAN
Strait of Juan de Fuca
CS
Port Angeles
Crescent Terrane
Tc
DBF
Olympic Core Terrane
Th
OLYMPIC PENINSULA
Seattle
Tc
Tam
0
30 KM
Hoquiam
Tam
N

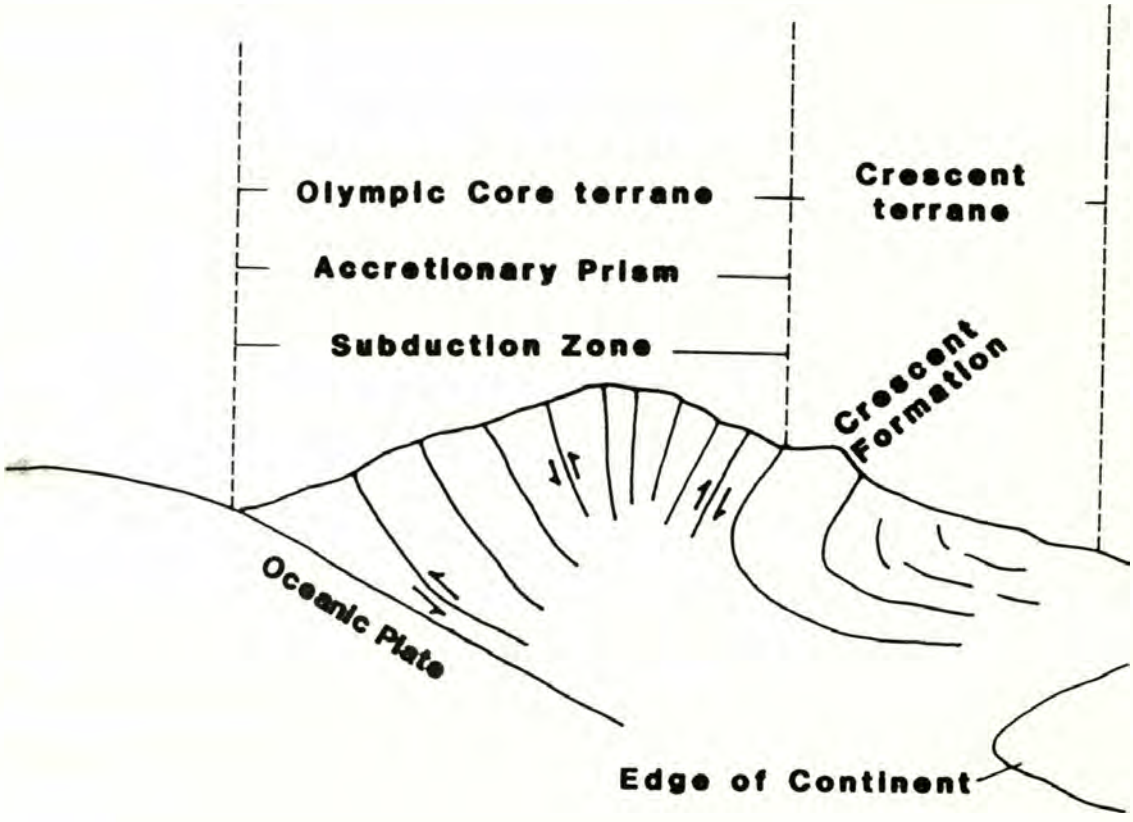


Figure 2. Generalized cross section east-west through the Olympic Mountains (modified from Tabor and Cady, 1978b).

forming the southern limb of the Clallam syncline (Figure 1). Beneath the Strait of Juan de Fuca, the sedimentary units of the Crescent terrane pinch out (Muller and others, 1983), but the Crescent Formation apparently reappears on the southern tip of Vancouver Island as the Metchosin Volcanics.

The Crescent Formation has been described as an Early Eocene seamount chain that was accreted to the continental margin (Tabor and Cady, 1978a). The timing of this accretion is not well constrained. A possible time for this accretion has been suggested by studies of movement along the Leech River fault on southern Vancouver Island and the Discovery Bay fault, its presumed equivalent on the eastern part of the Olympic Peninsula, which are felt to be the suture between the Olympic Peninsula and the North American margin (Armentrout, 1983). Motion along the Leech River fault may have been related to the accretion of the seamount chain. The period of major left-lateral movement along the Leech River fault is constrained to 40 Ma to 32 Ma by the age of metamorphism of the Leech River Complex, which has been cut by the fault (Fairchild and Cowan, 1982), and by the deposition of the Sooke Formation, which was not displaced by the fault (Fairchild, 1979). Moreover, magnetic and seismic studies (MacLeod and others, 1976) indicate that the Discovery Bay fault (Figure 1) is a southern continuation of the Leech River fault. Armentrout (1983) showed evidence that the Upper Eocene Quimper Sandstone is composed of detritus derived from both sides of the Discovery Bay fault. He postulated that the Discovery Bay fault is the suture between the Cresent terrane and the North American margin, and that, because the Quimper Sandstone overlies the Discovery Bay fault without offset, movement on the fault must have ceased by the Late Eocene. Thus, eastward movement of the Crescent terrane

may have ended by the Late Eocene (Armentrout, 1983). However, the map of the Nitinat quadrangle (Muller, 1982) shows that the Sooke Formation does not overlap the Leech River fault, indicating that motion along the Leech River fault could have continued into the Miocene. Moreover, seismic studies by Gower and others (1978) suggest that the possible extension of the Leech River fault, in the Discovery Bay and Puget Sound areas, as a series of subparallel splaying fault zones. The suture between the Crescent terrane and the North American margin may be a wide zone extending from the Discovery Bay area into Puget Sound. Thus, contraints on the timing of motion along the Discovery Bay fault may not fix the time of emplacement of the Crescent terrane.

During and following the emplacement of the Olympic Core terrane, the interaction between the Farallon and North American plates caused late Tertiary tectonic and paleogeographic developments in the Olympic Peninsula region. The Eocene through Miocene sedimentary sequences on the Olympic Peninsula reflect some of these developments. The Lower Miocene Clallam Formation represents the final shallow-water phase of a Late Eocene to Early Miocene regressive depositional trend. It is well exposed for about 12 km along the coastline of the Strait of Juan de Fuca between Slip Point and Pillar Point (Figure 3). The best exposures of the formation are on the east and west limbs of the northeast-plunging Coal Mine syncline (Figure 3; named herein) especially near the gradational contact between the Clallam Formation and the underlying Pysht Formation. The Clallam Formation sediments generally coarsen upwards, reflecting the shallowing environment of deposition.

## Structure

The major structural feature in the Clallam Formation is the northeast-plunging Coal Mine syncline (Figure 3). The southeast and northwest limbs

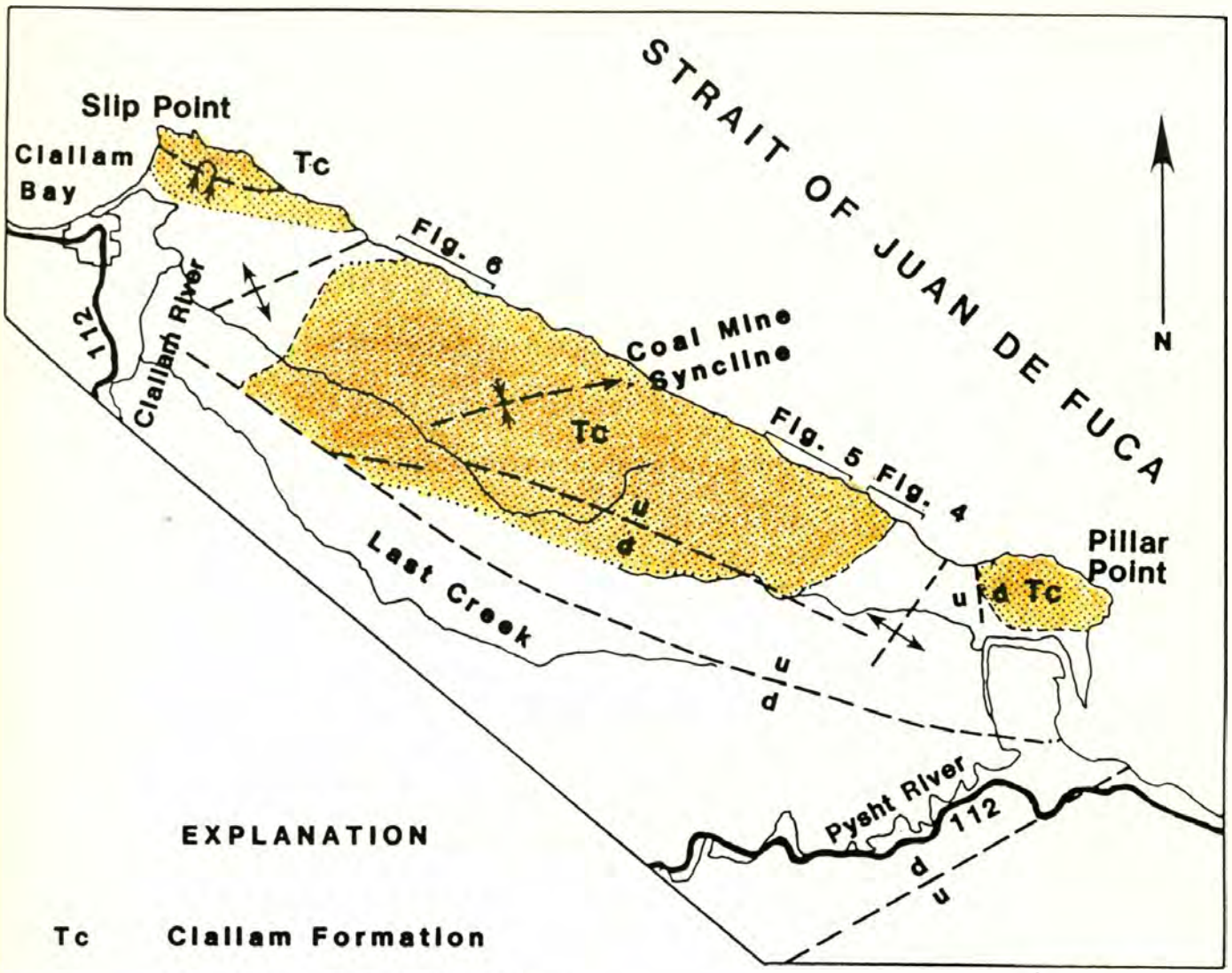


**EXPLANATION**

| | |
|---|---|
| Tc | Clallam Formation |
| ——·····—— | Contact, dashed where approximated, dotted where concealed |
| — — — — | Fault, approximately located |
| u | upthrown side |
| d | downthrown side |
| —+— | Syncline |
| —+— | Anticline |
| ⌊⌋ | Measured section |

0 1 2 3 MILES
0 1 2 3 4 5 KILOMETERS

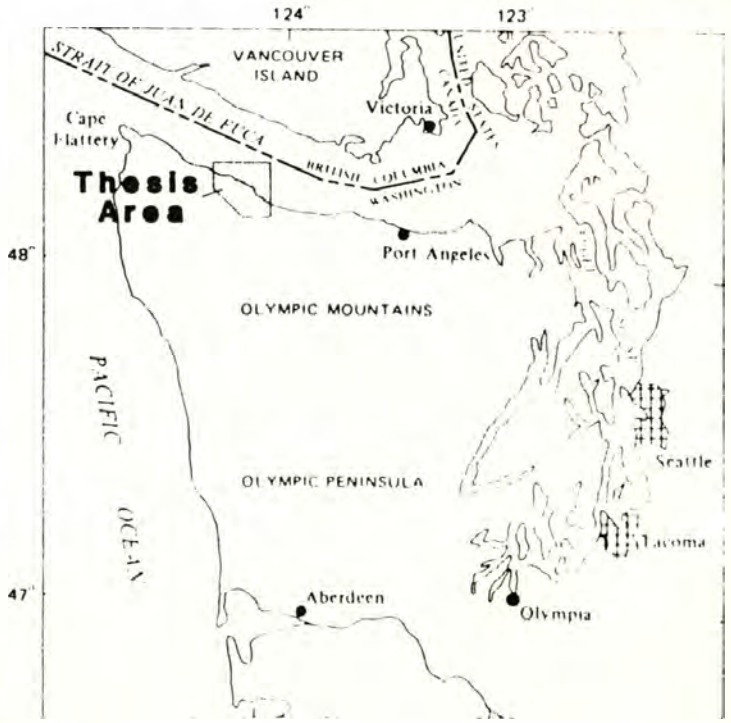


Figure 3. Map showing the location and general structure of the Clallam Formation (modified from Addicott, 1976b).

of the syncline are gently dipping, and its plunge is shallow. A series of east-west trending anticlines and overturned synclines also exists in the Clallam Formation, primarily near Pillar Point and Slip Point (Figure 3). The east-west trend of fold axes is apparent in the Pysht Formation also. Deformation in the Clallam Formation occured after the Early Miocene, but its timing is otherwise unknown.

North of the Clallam Formation is the southeast-northwest-trending Clallam syncline, which extends from west of Port Angeles to some unknown point north of Cape Flattery in the Strait of Juan de Fuca (Figure 1). The Clallam syncline reflects a period of southwest-northeast compression. The exact timing of deformation of this feature is unknown, but Muller and others (1983, Figure 12) show that deformation may have continued through the Late Miocene into the Pliocene (?). The timing and orientation of this deformation is consistant with seismic-reflection profiles showing landward- and seaward-verging thrust faults and associated anticlines involving Late Miocene and Late (?) Pleistocene strata on the continental shelf northwest of Cape Flattery (Muller and others, 1983). A period of uplift is also documented in the region of the northern Olympic Peninsula by an unconformity at the base of Upper Miocene strata near the mouth of the Strait of Juan de Fuca.

Moyer and others (1985) observed that the peripheral rocks on the northwest coast of the Olympic Peninsula have rotated about 45 degrees clockwise relative to rocks on the northeast coast near Port Angeles. The hinge point appears to have been near the position of the Clallam Formation, which may explain the intensity of its deformation. This rotation event may be related to the structures observed on the north coast of the Olympic Peninsula.

## Previous Work

The discovery of coal between Slip Point and Pillar Point in the late 1800's (Brown, 1870; Gillman, 1896; Landes, 1901) attracted the first geologists to the northern Olympic Peninsula. Arnold (1906) described the rocks of the peripheral terrane and included all of the marine shale, sandstone, and conglomerate lying stratigraphically above the Eocene Crescent Formation in his description of the Clallam Formation. He designated exposures at the top of this formation, between Clallam Bay and Pillar Point, as the type locality. Although many other early authors referred briefly to the geology of the Clallam Formation (Arnold, 1909; Reagan, 1909; Weaver, 1912; Arnold and Hannibal, 1913; Weaver, 1916a; Hertlein and Crickmay, 1925), it was Weaver (1937) who eventually restricted its areal distribution to those rocks between the mouth of the Clallam River and the town of Pysht (Figure 3), and those extending west from Clallam Bay to the mouth of the Sekiu River. Gower (1960), in his mapping of the Pysht quadrangle, moved the southernmost contact with the underlying Pysht Formation to the north of Last Creek (Figure 3). A map by Gower and Snavely (1975, unpublished) shows the boundary between the Clallam Formation and the underlying Pysht Formation nearer Reed Creek, 1 km north of Last Creek. This excludes from the Clallam Formation sections of conglomerate at Pillar Point State Recreational Area and the stretch of rocks described by Weaver (1937) that crop out from Clallam Bay west to the mouth of the Sekiu River (Addicott, 1976a). These conglomerates differ from in the Clallam Formation as now defined by containing silicic volcanic and fossiliferous sandstone clasts, and they have been placed in the upper part of the Pysht Formation.

The most detailed lithologic description and structural interpretation of the Clallam Formation is from the map by Gower (1960). Gower described

the Clallam Formation as poorly sorted, fine- to medium-grained, lithic sandstone and pebbly sandstone with abundant pebbly conglomerate layers, carbonaceous flakes, and coal stringers. He described the bedding as very thick with both high-angle and low-angle crossbedding and observed that bedding is often disrupted by soft-sediment deformation. He also observed two coal beds 10 and 19 inches thick. In a semiquantitative study of the petrology of Tertiary sedimentary rocks of the Olympic Peninsula, Pearl (1977) identified one thin section as a submature to immature, moderately sorted, medium-grained, micaceous lithic subarkose.

Historically, formation boundaries within the Crescent terrane were largely determined on the basis of paleontologic data. Early descriptions of the geology and paleontology in the Clallam Bay and Pillar Point areas disagreed as to the age and areal distribution of the Clallam Formation (Arnold, 1905, 1906; Arnold and Hannibal 1913; Reagan, 1909; Weaver, 1912, 1916a, 1916b, 1937; Dall, 1922; Etherington, 1931; Durham, 1944; Stirton, 1960; Moore, 1963). A study of benthonic foraminifera by Rau (1964) suggested that the Clallam Formation is part of the Saucesian Stage (Middle Miocene) of Kleinpell (1938). Addicott (1975, 1976b) assigned it to the Pillarian Stage, a provincial upper Lower Miocene unit based on molluscan assemblages. Furthermore, Addicott (1976b) determined that the molluscan assemblages indicate a warm water sublittoral environment with gradual shallowing up-section. In correlating Cenozoic stratigraphic units of western Oregon and Washington, Armentrout and others (1983) referred to the Pillarian Stage as Lower Miocene.

## SEDIMENTOLOGY

### Introduction

As a whole, the Clallam Formation coarsens and shallows upward. Within this general trend are several small-scale coarsening- and shallowing-upward cycles. Based on lithology and on biogenic and other sedimentary structures, the upper Pysht Formation and the Clallam Formation have six lithologic facies, five in the Clallam Formation and one in the Pysht Formation. The facies are interstratified in various combinations (see schematic columnar sections in Figures 4, 5, and 6). These facies define the parameters for recognizing individual shoaling events. Each facies was produced by a single depositional regime; these regimes varied primarily as a result of fluctuations in the position of distributary mouths, in the water depth, and in the severity of storm conditions in the prodelta and delta front portions of a prograding deltaic sequence (Figure 7). Sediments of the uppermost part of the Pysht Formation are included in this study because they are a part of the same depositional system as sediments of the Clallam Formation and are transitional with them.

Facies 1 (the planar-laminated silty sandstone facies) is transitional between the Pysht Formation mudstones and the Clallam Formation and occurs only in the Pysht Formation. The facies consists of planar-laminated silty sandstone, disrupted in a few places by burrows and interbedded with channels of fine-grained sandstone . Facies 2 (the burrowed sandstone facies) is fine- to medium-grained sandstone that, owing to bioturbation, is nearly devoid of bedding and sedimentary structures. Facies 3 (the hummocky cross-stratified and burrowed facies) is interbedded burrowed and hummocky cross-stratified medium-grained sandstone. Facies 4 (the laminated-burrowed and hummocky cross-stratified facies) is a complex sequence of fine- to medium-grained sandstones that may be parallel-

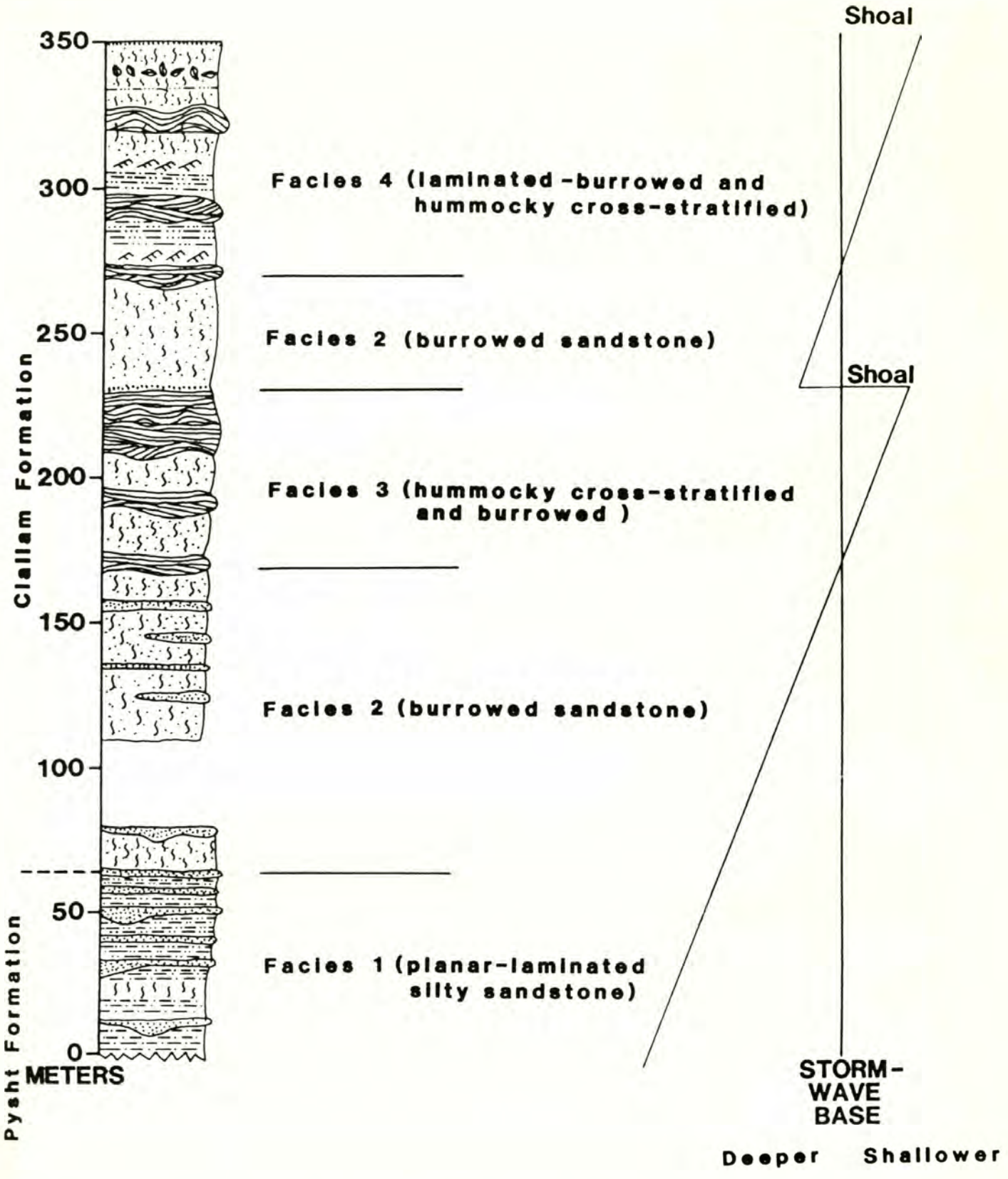


Figure 4. Schematic columnar section from the east limb of the Coal Mine syncline in the Clallam Formation showing a series of shoaling upward successions.

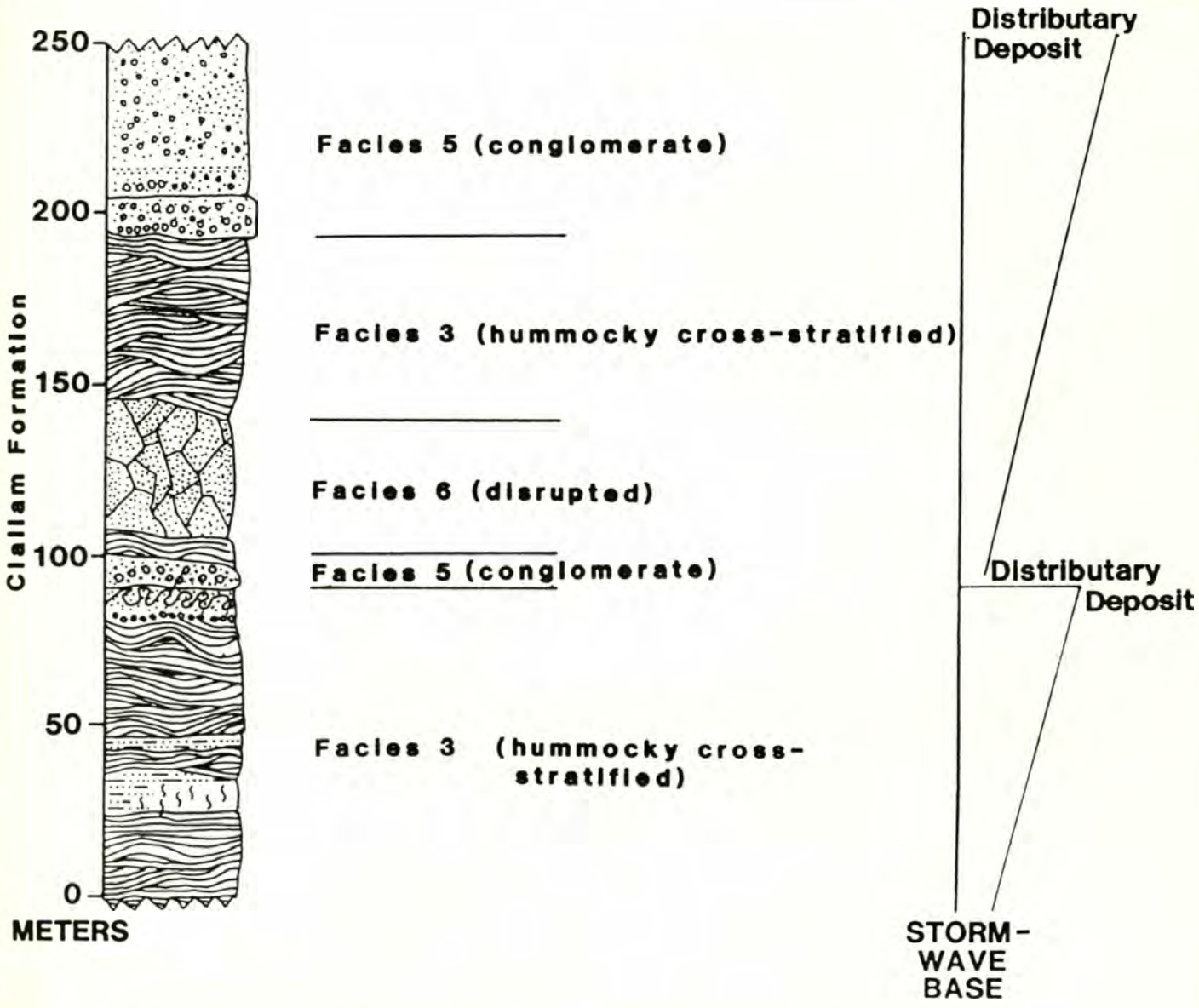


Figure 5. A continuation of the schematic columnar section shown in figure 4 from the east limb of the Coal Mine syncline in the Clallam Formation showing a series of shoaling upward successions.

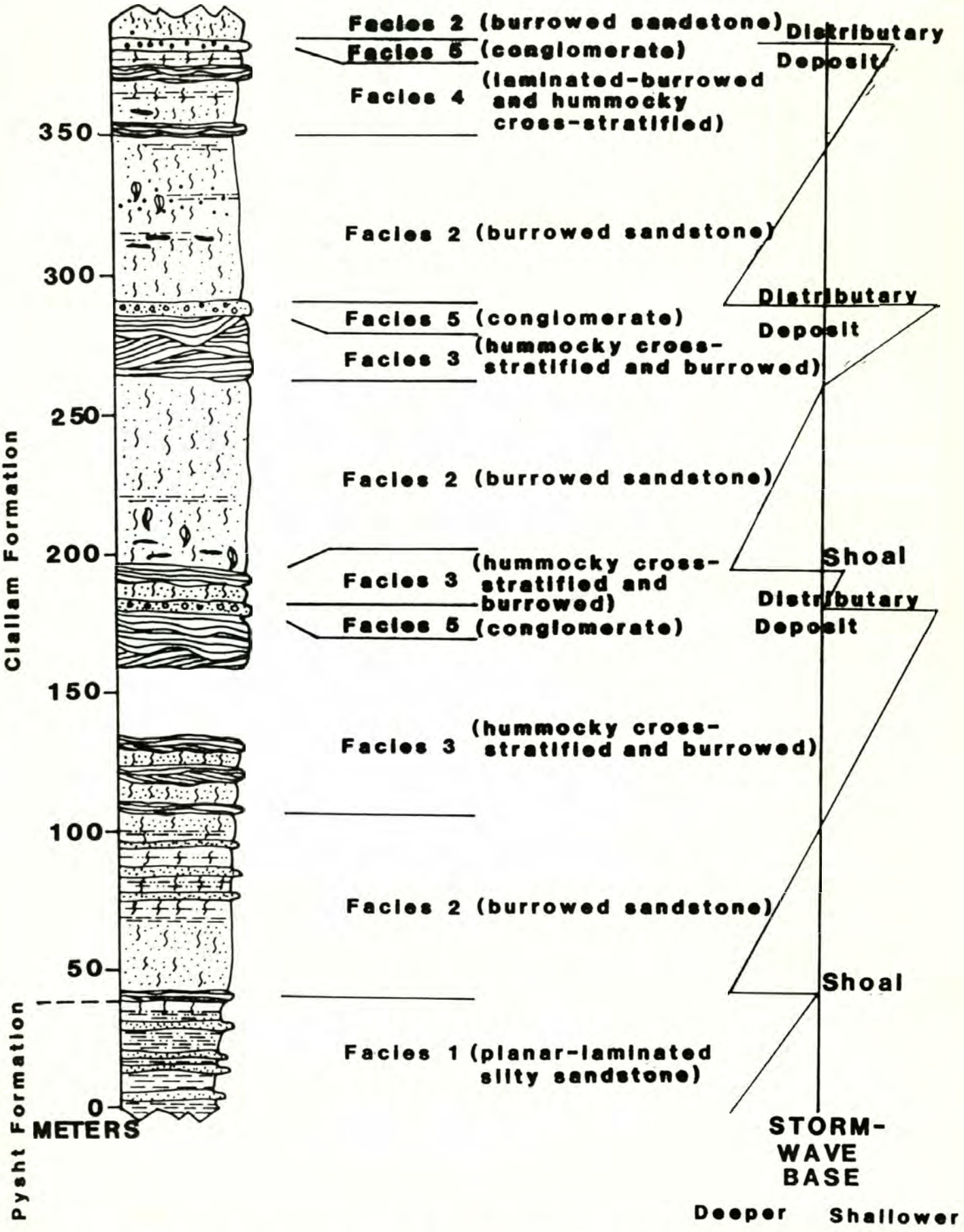


Figure 6. Schematic columnar section from the west limb of the Coal Mine syncline in the Clallam Formation showing a series of shoaling upward successions.

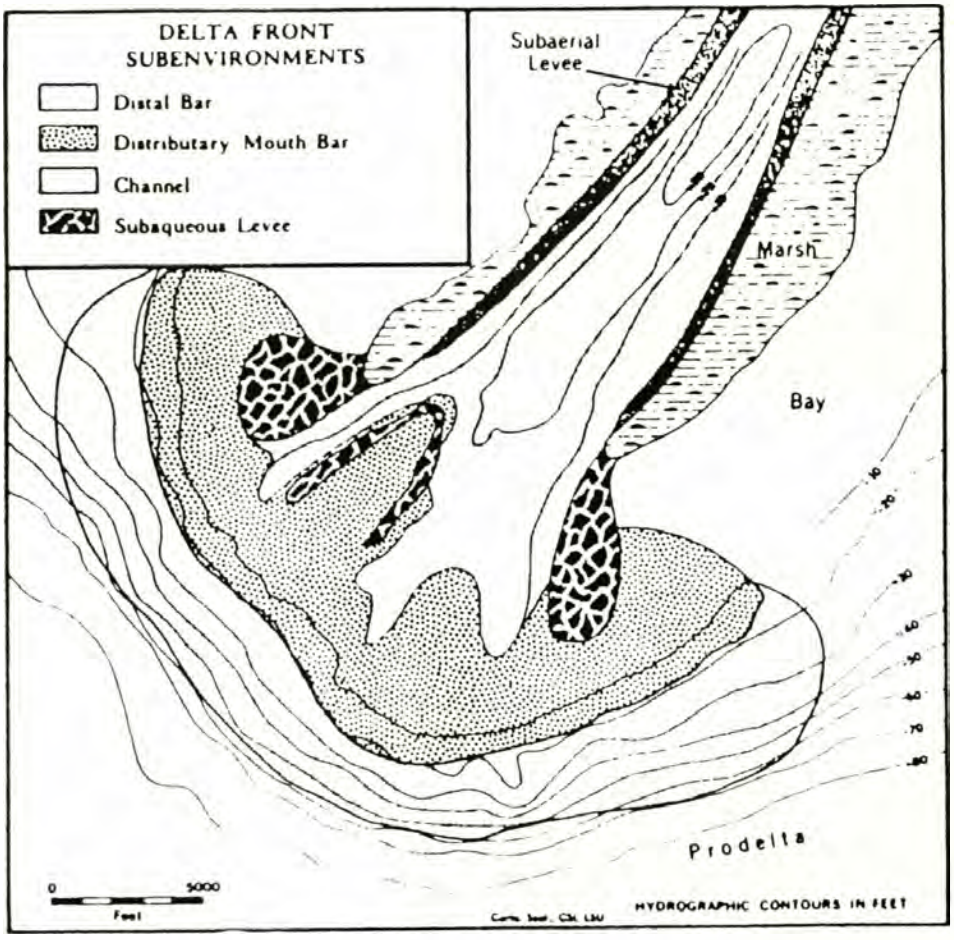


Figure 7. Subenvironments at a distributary mouth (from Reineck and Singh, 1980)

laminated, burrowed, or hummocky cross-stratified. Ripples, climbing ripples, layers rich in plant-debris, and shell layers also appear in this facies. Facies 5 (the conglomerate facies), which is most prominent near the top of the formation, is largely structureless organic-rich pebbly sandstone and conglomerate that occasionally exhibit horizontal planar bedding and trough cross-bedding. Facies 6 (the disrupted facies) is sandstone that shows evidence of postdepositional soft-sediment deformation.

## Description and Interpretation of the Facies

### Facies 1

Facies 1 crops out on the east and west limbs of the Coal Mine syncline (Figure 3). It is underlain by siltstone and mudstone of the Pysht Formation. The facies is distinguished from Facies 2, which everywhere overlies it, by the paucity of burrows and by the well-preserved bedding features (Figure 4 and 6). Three lithologic types dominate Facies 1: laminated silty sandstone, fine-grained sandstone, and medium-grained channel sandstone. The silty sandstone and fine-grained sandstone are interbedded and form laterally continuous layers (Figure 8). Some burrows and a few articulated bivalves are present.

The channel sandstones have low-angle internal laminations. They often contain layers of rounded, fine-grained, sandstone intraclasts (Figure 9). The tops of some channels are convolutely bedded. Individual channeled layers are most commonly less than 1 m thick at their thickest points (Figure 10). On the west limb of the Coal Mine syncline, the sediment is slightly finer and sandstone channels are less abundant than on the syncline's east limb. Facies 1 was deposited on a steep submarine prodelta or delta front slope below storm wave base, near an active delta

Figure 8. Interlayered silty-sandstone and fine-grained sandstone. Facies 1, east limb of the Coal Mine syncline.

Figure 9. Sandstone intraclasts in channel sandstone. Facies 1, east limb of the Coal Mine syncline.

Figure 10. Channel sandstone in Facies 1 from the east limb of the Coal Mine syncline.

distributary mouth. River sediment and storm-resuspended sediment settled from suspension to form laterally continuous laminated deposits, whereas the channels carried high-energy gravity flows that resulted in channeled sand deposits.

The lack of burrows in the laminated silty sandstone suggests either relatively high rates of sedimentation or anoxic conditions. Moore and Scruton (1957) observed that rapid deposition of laminated, unburrowed muds on the Mississippi River delta occurred adjacent to active distributaries. The thicker, fine-grained sandstone interlayered with the silty sandstone in Facies 1 is interpreted to have resulted from periodic seasonal fluctuations in sediment supply, whereas thinner interbeds probably resulted from more frequent changes in the bed or suspended load of the fluvial system.

The role of storm-wave activity in the deposition of sediments in Facies 1 was indirect. Although graded rhythmites in storm-sand layers, such as described by Reineck and Singh (1972), may be expected near a storm-dominated nearshore environment, they do not appear in this facies. If the laminated sediments in Facies 1 were derived by settling from suspension clouds, in a process similar to that described by Reineck and Singh, deposition of this facies probably proceeded in deeper water than did deposition of the graded rhythmites. Distinguishing between sedimentary features derived from storm-induced suspension and those from distributary-controlled suspension would be difficult; both may have been active in the deposition of this facies.

The lenticular, medium-grained channel sandstone layers within this facies probably were deposited by density currents other than turbidity currents. They resemble facies B2 of Walker and Mutti (1973), which is characterized by faint, parallel-stratified to massive-bedded, medium-fine

to coarse sandstone. The origin of these deposits is enigmatic. Although such deposits are found in association with submarine fans (Corbett, 1972; Piper and Normark, 1971), channeled sandstones in the Pysht and Clallam Formations are interpreted to be channels near a delta front. This interpretation is largely based on the stratigraphic positions of Facies 1 and 2, both of which are immediately overlain by distributary mouth and distal bar deposits. Because delta fronts and submarine fans are below wave base where sedimentation rates are rapid, they can be expected to contain some similar deposits.

Rapid deposition of sand in channels in Facies 1 is evidenced by low-angle internal discontinuities, basal scouring, and abundant intraclasts. Sediment transport in these channels may have proceeded during periods of disruption that created such features as slumps, convolute bedding, and disruption seen higher in the formation. Density transport of sediment through local channels may have resulted from episodic seismic events, oversteepening of submarine slopes, or rapid deposition (see the interpretation of Facies 6), all of which would be expected in the deltaic system of the Clallam Formation.

Facies 2

The burrowed sandstone facies occurs in a variety of stratigraphic positions in the Clallam Formation (Figures 4, 5, and 6). On the east limb of the Coal Mine syncline, and to some degree on the west limb, the burrowed sandstone facies is interrupted by channels of sandstone similar to those in Facies 1. On the west limb, sandstone interbeds in the burrowed sandstone facies tend to be more planar than channeled.

Facies 2 consists of organic-rich, fine- to medium-grained sandstone with fossil mollusk assemblages including gastropods, bivalves, and

scaphopods. One fossil crab was found in a Facies 2 bed on the east limb of the syncline at the 240 m interval of the stratigraphic section (Figure 4). For a discussion of the molluscan paleontology see Addicott (1976b). Many concretions contain plant and animal parts, and fossil-rich strata commonly contain abundant concretions.

Although bioturbation has disrupted most sedimentary structures, some planar beds and laminations are preserved. Typically, sediments in the silt to fine-sand range have better preserved internal features than do coarser-grained sediments. The features most often preserved are organic-rich laminations (Figure 11) and some leaf imprints on bedding planes. The medium-grained, burrowed sandstones characteristically contain fewer internal structures but a greater number of Ophiomorpha traces (Figure 12). Ophiomorpha are also common in facies that contain sections of burrowed deposits and interbeds of hummocky cross-stratification.

Both gradational and sharp contacts separate the burrowed sediments from the nonburrowed sediments (Figure 13). The contacts tend to be sharp if the deposition of bounding sediments was hydrodynamically energetic or if the change in depositional regime was abrupt.

The burrowing in Facies 2 reflects periods of slow sedimentation. The sedimentation rates were slower in Facies 2 than in Facies 1 because of abandonment or migration of the distributary mouth, which cut off most of the sediment supply. The lack of interlayered storm wave deposits suggests that sediments in this facies were deposited below storm wave base. The retention of interlayered channeled sandstone is further evidence that storm activity did not rework sediments in this facies.

Facies 3

This facies contains only two types of strata, hummocky cross-stratified and burrowed. The absence of other types of strata distinguishes this

Figure 11. Organic-rich laminae in bioturbated sandstone. Facies 2, east limb of the Coal Mine syncline.

Figure 12. Ophiomorpha traces in medium-grained burrowed sandstone. Facies 2, west limb of the Coal Mine syncline.

Figure 13. Sharp contact between burrowed and nonburrowed sediments. Facies 2, east limb of the Coal Mine syncline.

facies from the more diverse Facies 4. It differs from the other facies in having hummocky cross-stratified beds.

Hummocky cross-strata are distinguished from other cross-stratified sandstones by their low-angle scoured truncations and laterally continuous bed-forms (Figure 14). Abundant mica and plant flakes, irregularly spaced synforms, and upward-diminishing inclinations of cross-strata within sets have been observed in other areas by Dott and Bourgeois (1982) and are characteristic of hummocky cross-stratification in the Clallam Formation. The most useful feature for the recognition of hummocky cross-strata is the hummocks themselves (Figure 15). However, because of erosion prior to and during deposition, hummocks are not commonly preserved. Preservation of hummocks appears to be less common in thick sections of amalgamated hummocky cross-strata in the upper part of each occurrence of the facies. The lowest occurrence of hummocky cross-stratified beds in the Clallam Formation marks the first time flow regimes induced by storm wave action affected shelf deposition. Harms and others (1975), Dott and Bourgeois (1982), and Hunter and Clifton (1982) have interpreted hummocky cross-strata in other areas to have been created by storm waves and wind-driven currents. According to Dott and Bourgeois (1982, p. 675) hummocky cross-stratified beds form as follows:

> "Either flooding rivers or scour of the bottom by wave surges and wind-driven currents deliver much sand to the offshore... Pebbles and shells occasionally concentrated along scoured surfaces associated with hummocky stratification attest to very large flow velocities of the order of a few hundred centimetres per second, and thus great competence, during scouring events. The almost universal fine grain size of hummocky stratification must reflect efficient selective sorting of sand by suspension transport to the site of deposition. As intensity of water motion diminishes, fallout from suspension begins. Seemingly, actual deposition of the hummocky laminae involves major lateral components of oscillatory flow at the bed associated with fallout from the water column... Near the bed, falling grains encounter a zone of intense oscillatory sheet

Figure 14. Laterally continuous layer of hummocky cross-strata. Hammer pictured is about 40 cm in length. Facies 3, west limb of the Coal Mine syncline.

Figure 15. Crests of hummocky cross-strata accentuated by the low angle of dip of the beds. Hummock crests are about 1 m apart. Facies 3, east limb of the Coal Mine syncline.

> flow, which has molded the bed into undulating hummocks and swales. The result is a smooth but not perfectly flat bed with part of its irregularity from slightly earlier scour and part due to the flow itself. Sand grains are deposited in sharply defined undulating laminae. Each lamina is thought to represent deposition from a single wave or wave train. If the water disturbance fluctuates somewhat, as is the rule, the second-order scour surfaces form locally within sequences of hummocky laminae, and they are then draped by more laminae."

Beds of hummocky cross-stratification in the Clallam Formation are in some ways different from the idealized hummocky cross-stratified unit defined by Dott and Bourgeois (1980). They described the succession within the hummocky cross-stratified bed as characterized by:

> "scoured and/or sole-marked base, typical unoriented hummocky lamination, horizontal lamination, preferentially-oriented ripple cross lamination and symmetrical ripples--all overlain by burrowed mudstone or siltstone."

The hummocky units in Facies 3 of the Clallam Formation commonly contain hummocky zones succeeded only by flat laminae or partial bioturbation. This sequence resembles variations to the ideal sequence noted by Dott and Bourgeois (their Figure 5, 1982). The hummocky cross-stratification in Facies 3 is further characterized by a lack of both ripples and interbedded mudstone and by the fine- to medium sizes of the grains.

The base of Facies 3, where it overlies Facies 2, is indicated by the first occurrence of hummocky cross-stratification. Hummocky cross-stratified beds at the base of the facies begin as 15-30 cm thick, laterally continuous layers containing low-angle cross-strata that have abrupt basal contacts and abrupt or burrowed top contacts (Figure 14). Hummocks and swales in the lower part of the facies are relatively closely spaced, with crests 30-50 cm apart; higher in the stratigraphic section hummock crests are up to a few meters apart. The strata consist primarily of fine- to medium-grained sandstone. Hummocky cross-stratified beds

increase in abundance upward, both within this facies and in the Clallam Formation as a whole (Figures 4, 5, and 6). Within each occurrence of the hummocky cross-stratified and burrowed facies, hummocky cross-stratification increases upward and burrowed portions decrease. At the top of each of the hummocky cross-stratified and burrowed units, amalgamated hummocky cross-stratification predominates and few or no burrowed interbeds exist (Figure 16).

The amalgamated portions of Facies 3 range in thickness from 1 m to 50 m. These portions are devoid of burrowing except for Ophiomorpha traces. The hummock crests are usually 1 to 3 m across (Figure 15). Pebble and shell lags (Figure 17) occur in Facies 3 in the upper part of the formation on the west limb but are absent from most units on the eastern limb. Convoluted beds (Figure 18) and featureless sandstone found in many of the thicker amalgamated sequences indicate penecontemporaneous soft-sediment deformation. Throughout the stratigraphic section amalgamated units are typically overlain by coarse, poorly-sorted sandstone or conglomerate of Facies 5. The contact between the amalgamated sequences and the conglomerate is usually abrupt.

The intermittent presence of hummocky cross-stratification in the basal portion of the facies suggests that scouring by waves only occurred during major storms. However, higher in the facies, amalgamated hummocky cross-stratified beds define a zone in which scouring by storm waves was common. There, high sediment input facilitated the preservation of amalgamated units by allowing scouring to proceed without affecting the majority of the preexisting hummocky cross-stratified deposits in the sediment column. At the top of the facies the complete absence of fair-weather deposits attests to the frequency of reworking by storm waves and suggests a shallower-water environment than for the base of the facies.

Figure 16. Amalgamated hummocky cross-strata from Facies 3 on the west limb of the Coal Mine syncline. Note the relatively large distance between projected crests of hummocks. Hammer for scale.

Figure 17. Pebble lag in a section of amalgamated hummocky cross-strata. Facies 3, west limb of the Coal Mine syncline.

Figure 18. Convoluted beds interlayered with amalgamated hummocky cross-strata. Facies 3, near Slip Point.

Overall, Facies 3 represents a shallowing-upward trend, proceeding from predominantly fair-weather deposition and bioturbation, with minor storm wave influence, to primarily storm-wave deposition that has completely reworked fair-weather deposits. Because the Clallam Formation lacks wave ripples, the methods of estimating water depth described by Bourgeois (1980) and Hunter and Clifton (1982) cannot be used. However, the profusion of hummocky cross-strata in the Clallam Formation suggests an environment influenced, and in some places dominated, by open-ocean storm wave activity. If calculations using known wave heights for the present Oregon shelf are used (Bourgeois, 1980), up to 50 m of water depth would be a reasonable estimate for the depth of deposition of the hummocky cross-stratified beds observed in the Clallam Formation.

Facies 4

The first occurrence of Facies 4 is 200 m above the base of the Clallam Formation and is seen in the stratigraphically and structurally coherent sections on the east and west limbs of the Coal Mine syncline (Figure 4 and 6). Broken and incomplete sections that resemble Facies 4 occur in a few other locations. This facies is distinctive in displaying a complex series of changing lithologies and depositional sedimentary structures. Laminated, cross-laminated, rippled, burrowed, and hummocky cross-stratified siltstones and sandstones form an intricate sequence that reflects subtle changes in depositional environments (Figure 4).

At least two different types of laminated fine sandstone and siltstone are present in this facies. The first exhibits some rhythmic grading and usually occurs in 10- to 20-cm-thick layers (Figure 19). The laminated deposits characteristically display sharp contacts with underlying and overlying deposits, but their tops are often disrupted by some

Figure 19. Rhythmically graded beds with relatively low organic contents (note area near the head of the hammer for graded beds). Facies 4, east limb of the Coal Mine syncline.

bioturbation. They are distinct from, but sometimes associated with, rippled fine sandstone, hummocky cross-stratified sandstone, and bioturbated siltstone. The laminae of the second type rarely contain graded beds, are often interlayered with climbing ripples (Figure 20), and are accentuated by organic-rich layers (figure 21). Escape structures are common in both types of laminae. A possible third type of lamination is characterized by interbedded organic-rich and organic-poor siltstone that is often extensively burrowed (Figure 22). These deposits resemble those of the second type but are generally finer-grained.

Asymmetrical ripples and climbing ripples in Facies 4 are often interlayered with laminations (Figure 20). Sections of rippled laminae display erosional boundaries with underlying planar laminae or mudstone beds and may either grade into or abruptly contact the planar laminae or mudstone layers above. Some of the overlying deposits are burrowed. Frequent alternations from planar laminae to cross-laminae to burrowed strata occur within a few tens of centimeters (Figure 23).

Burrowed portions of the facies range in thickness from a few centimeters to a few meters. Individual burrows range from widely spaced (Figure 22) to so densely packed as to almost completely obliterate original stratification. Escape features are common in rapidly-deposited beds. Although most of the burrows are concentrated in siltstone and fine-grained sandstone, quite thick sections of medium-grained, bioturbated sandstone resembling Facies 2 do occur. These sandstones are placed in Facies 4 because of their associations. Concentrated layers of shells up to 0.5 m thick are common in these coarser-grained sections.

Interbedded with the planar-laminated, cross-laminated, rippled, and burrowed siltstones and sandstones are fine- to medium-grained beds of hummocky cross-stratification. Hummocky sets usually form resistant,

Figure 20. Organic-rich laminae interlayered with climbing ripples. Facies 4, east limb of the Coal Mine syncline.

Figure 21. Organic-rich laminae interlayered with cross-laminae. Facies 4, west limb of the Coal Mine syncline.

Figure 22. Burrowed organic-rich laminae. Facies 4, east limb of the Coal Mine syncline.

Figure 23. Frequent alternations from planar laminae to cross-laminae to burrowed strata. Facies 4, east limb of the Coal Mine syncline.

laterally continuous outcrops that are spaced about 1 m to 8 m apart (Figure 24). Individual beds average 0.3 m to 1 m in thickness. The beds consist of sets of laminae that truncate one another at angles of less than 20 degrees. Truncations at the bases of beds are erosional but contain no lag or sole marks. Small, less than 0.5 cm long, siltstone intraclasts often occur along second-order truncations (Figure 25). The siltstone intraclasts probably were derived from fair-weather deposits that were eroded during hydrodynamically energetic periods. The tops of the hummocky cross-stratified beds usually display planar lamination and are sometimes disrupted by convolute bedding. Unlike the hummocky cross-stratified beds in Facies 3, the bed thicknesses are relatively constant throughout the facies. Hummocks are more often preserved in Facies 4 than in hummocky cross-stratified beds elsewhere in the formation (Figure 26).

In review, this facies is a complex accumulation of various lithologies and physical sedimentary structures. This suggests a complex environment of deposition where sedimentologic features respond to minor fluctuations in depositional regime.

The deposition of sediments in Facies 4 was affected by several physical factors, including the position of the delta distributary mouth, the relative severity of storm-induced wave action, the nature of bottom currents, aggradation rates, tidal influence, and biologic activity. Deposition probably proceeded in water a few tens of meters to roughly 50 m deep in an inner shelf or outer shoreface environment.

Hummocky cross-stratification in Facies 4 is the only type of storm-wave-related bed form to be developed by the oscillitory wave action. Depending on the wave base, various forms of storm-related deposits will develope. During infrequent strong storms, pre-existing bottom sediments

Figure 24. Resistant layers of hummocky cross-strata on a wave-cut platform. Facies 4, east limb of the Coal Mine syncline.

Figure 25. Siltstone intraclasts along a second-order truncation in a hummocky cross-stratified set. Facies 4, east limb of the Coal Mine syncline.

Figure 26. Well preserved hummock with escape structure. Facies 4, east limb, Coal Mine syncline.

or fluvially-derived material will be thrown into suspension; the bottom surface will be reformed into a series of undulating hummocks and swales. As wave energy decrease the suspended sediment will settle, draping itself over erosional hummocky surfaces and forming laminated and hummocky cross-stratified layers. The paucity of ripple-laminae and cross-laminae at the top of beds in this facies suggests that bottom currents, following oscillatory flow during deposition of hummocky laminae, were very slow to nonexistent.

If storm action is less violent than that just described, the storm-wave-base will be higher. Depending on the velocity of bottom currents and on aggradation rates (a product of both fluvial and nearshore resuspended sediments), either laminated, laminated-graded rhythmite, or rippled beds will form. Storm-wave-impelled oscillatory flow does not effect this environment.

Finally during fair-weather periods, laminae develope that, in most cases, subsequently undergo bioturbation.

As discussed above, at least two different types of laminated fine sandstone and siltstone exist in Facies 4. The graded rhythmite type, is interpreted to have been deposited from fallout during the waning stages of storms. Reineck and Singh (1972) explained that sand eroded from near-shore environments is transported seaward via suspension clouds during storm activity. As wave energy decreases, material falls from suspension and is segregated into a fraction of fine-grained sediment and a fraction of sand, first forming laminated sand and then graded rhythmites. Thinning- and fining-upward laminae of this type are interpreted to represent the progressive waning of storm-induced turbulence. Due to slow bottom currents, laminated deposits are not reformed into ripples.

The second type of lamination, which is interlayered with climbing

ripple deposits, and displays little or no grading, but exhibits alternating organic-rich and fine sand-layers (Figure 21). This type of lamination is interpreted to have been deposited during the settling of suspended material derived from fluvial sources. Suspension clouds formed during fluvial flooding may have effects similar to those derived from storm-resuspended material. Leithhold and Bourgeois (1984) have noted similar occurrences in the sandstone of Floris Lake. They have interpreted these deposits as reflecting the episodic influence of tidal action on river-derived sediment by the following mechanism:

> "As the storm reached its final phases river flooding continued, and the decrease in wave action allowed for the settling of finer-grained material from suspension. During flood-enhanced ebb-tide sand was transported and deposited as the coarser member of each couplet. The superposition of flood-tidal currents essentially damped both wave and fluvial processes, and the finer, wood-rich portion of each couplet was deposited. As wave activity and flood action decreased with time the couplets, each of which represents one tidal cycle, became thinner and finer upward."

It is concluded that, because both organic rich and organic poor rhythmites occur in Facies 4, laminated and graded rhythmites in this facies represent both storm-induced and flood-induced deposits or a combination of the two depending on the relative severity of storm-activated reworking of near-shore sediments or the amount of fluvial influence. Although the presence of low-angle discontinuities between sets of laminae indicate some reworking or eroding of the laminated deposits, the retention of laminated sets suggests that bottom currents were slow enough as to not develope ripples. In addition, sedimentation rates were high enough to discourage the activity of bottom-dwelling organisms.

Climbing ripples that are interlayered with the second type of lamination (Figure 20) indicate that currents periodically flowed across the bottom. Ashley and others (1982) conducted flume simulations in which

they set out to duplicate ripple and lamination patterns observed in recent glaciodeltaic and stream deposits. They concluded that two factors, current velocities and aggradation rates, had primary influence on resultant sedimentary features.

Climbing ripples observed in the Clallam Formation closely resemble the Type B (depositional-stoss) climbing ripples described by Ashley and others (1982). This type of ripple is produced when aggradation rates are large relative to ripple migration rates. Ripple migration rates, in turn, are a function of current rates: as current rates increase, ripple migration rates increase. The interlayering with laminated deposits suggests that bottom-current velocities periodically increased to a point where they were strong enough to form climbing ripples but not strong enough to rework already-deposited sediments. Draped ripples, which usually form under hydrodynamic conditions intermediate between the conditions in which laminae and climbing ripples form, were not observed in the field. Either they do not exist, or they were not seen because of the limited exposures. Alternatively, current velocities may have fluctuated rapidly enough for conditions to proceed directly from deposition of laminae to deposition of climbing ripples and vise-versa.

Ashley and others (1982) stated that 20 cm of cross-laminated sediment can be deposited in a period of 10 hours or less in flume simulations. If the organic-rich laminated sediments that are interlayered with cross-laminated deposits were deposited at the rate of approximately one laminae in a four hour period, 20 cm of cross-laminated material deposited in ten hours would imply a large increase in sediment supply. As with storm-derived laminated sections, this sediment could come from stream flooding, from resuspension of near-shore and shelf sediments, or from a

combination of both. In Facies 4 the type of bed form constructed during a storm event depended on the velocity of bottom currents. If bottom currents were nonexistant or relatively slow, laminated sand and graded rhythmite layers would form. When bottom currents increased slightly, sediment from either a fluvial or near-shore source would fall from suspension and be molded into the Type B climbing ripples of Ashley and others (1982). Furthermore, depending on the amount of material in suspension (a product of fluvial and wave energies and thus related to grain size), laminated deposits display varying amounts of diurnal flood and ebb tide organic-rich laminations, silt-sized interbeds, and organism traces.

The burrowed portions of Facies 4 represent periods of slower deposition. In areas where internal structures have not been completely obliterated, laminations and silty interbeds are present. These deposits probably represent a continuum of the processes described above. They depict a relatively low-energy environment in which sediment input was largely derived from fair-weather fluvial suspension.

The coarser-grained burrowed sections of Facies 4 that contain shell debris layers also reflect a relatively low-energy environment. They are interpreted to have been deposited laterally distal to the mouth of a distributary where sediment was derived primarily from reworked nearshore deposits. There appears to have been little fluvial input. Owing to the high concentrations of burrowing organisms, deposits formed by storm-wave activity were destroyed and only shell lag deposits remained. The interlayering of these distal deposits with proximal deposits described earlier suggests that there were minor fluctuations in the position of the distributary mouth and that sediment input from fluvial sources was sometimes cut off.

Interbedded hummocky cross-strata present in this facies reflect the periodic reworking and redeposition of sediments by storm wave action. Beds usually contain few second-order truncations and, therefore, few hummocky sets within each bed. Also, hummocky cross-stratified beds are interbedded with substantial thicknesses of other bedforms; such thicknesses demonstrate the relative infrequency of storm-wave influence in the facies.

Facies 5

Although present throughout most of the Clallam Formation, the deposits in Facies 5 progressively alter in sedimentologic character, especially thickening, from the base of the formation to the top. At the base of the formation this facies consists of 1 to 3 m thick, tabular, and laterally-continuous beds of conglomerate and coarse sandstone. Toward the top of the formation, deposits in Facies 5 are up to several tens of meters thick and contain a greater variety of sedimentary features.

The conglomerates in Facies 5 are divided into two subfacies, a lower subfacies and an upper subfacies. Near the middle of the formation the lower and upper subfacies overlap.

Rocks in roughly the lower 450 m of the formation, belonging to the lower subfacies, generally consist of laterally continuous, coarse-grained, poorly sorted sandstone and pebbly sandstone and minor amounts of matrix-supported pebble conglomerate. Completely or partially carbonized wood fragments (usually displaying Teredo borings) are common. The tabular, laterally continuous layers of conglomerate and sandstone are most commonly internally structureless, but some indistinct planar beds and a few trough cross-beds are present. Higher in this lower part of the formation there are some conglomerate channels. The erosional nature of

the channel conglomerates is indicated by the presence of truncated beds along the basal contacts of the channels (Figure 27). The channels also contain coal breccias.

Internally featureless, very poorly sorted conglomerate and pebbly sandstone characterize most of the upper subfacies. Sets of beds in this portion of the formation are often tens of meters thick and typically contain tree stumps, wood fragments, and sandstone intraclasts (Figure 28 and 29). Interlayered with these deposits are coarse-grained sandstone, pebbly sandstone, and cobble conglomerate that contain internal structures. The latter sandstones exhibit planar beds, planar and low angle cross-beds, and, less commonly, trough cross-beds; some of them are highlighted by pebble layers (Figure 30). A few of the cobble conglomerates are graded and some are reverse graded, but this is uncommon. Organic debris is abundant in this portion of the facies, but wood fragments usually show no evidence of burrowing.

Near the top of the formation, the upper subfacies is also distinguished by interbedded silty mudstone and coal layers and by sedimentary dikes (Figures 31 and 32). The silty mudstone layers, seen in only a few areas, are highly organic. They sometimes exist as dislocated blocks within the surrounding sandstone and pebbly sandstone.

Although coal was mined near the top of the formation near the axis of the Coal Mine syncline (Hertlein and Crickmay, 1925), only one 30 cm thick coal seam is now exposed in the cliffs above the coast (Figure 31).

The deposition of conglomerates in nearshore environments is poorly understood. However, physical sedimentary features suggest that deposition of Facies 5 proceeded on a high-energy, storm-dominated coastline affected by the interaction of wave, tidal, and fluvial processes.

At least three distinct depositional styles can be identified within

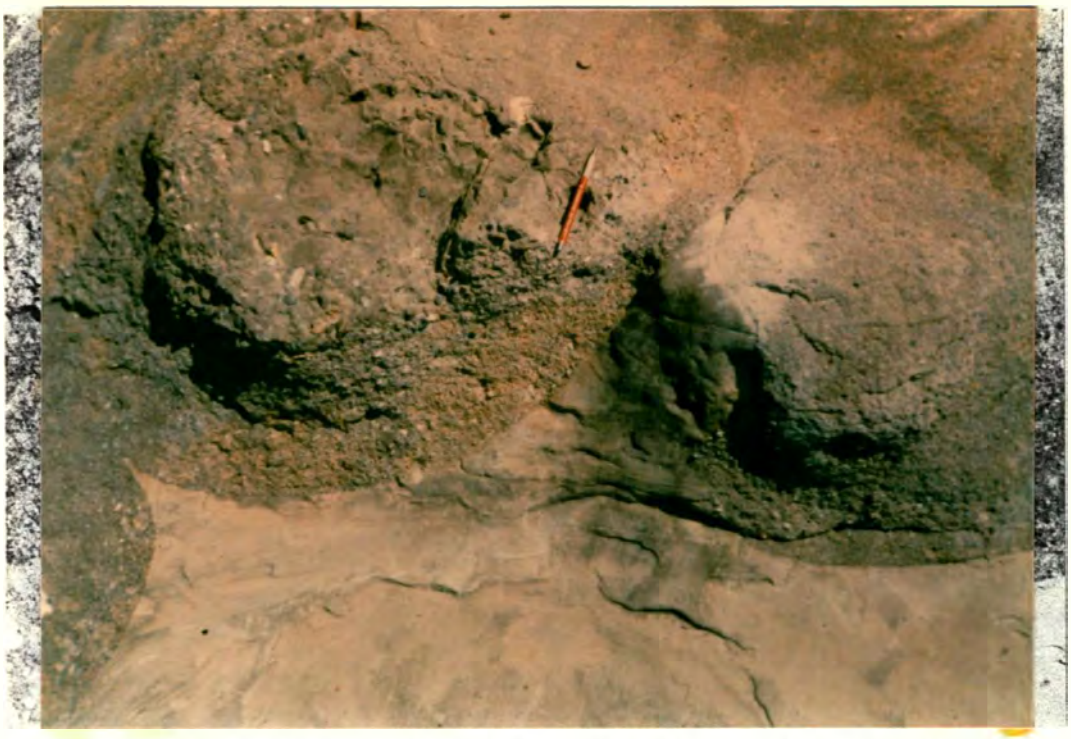

Figure 27. Channel conglomerate with flame structures, exaggerated by the low angle of dip. Facies 5, east limb of the Coal Mine syncline.

Figure 28. Wood fragment imbedded in pebbly sandstone. Facies 5 near the axis of the Coal Mine syncline.

Figure 29. Sandstone intraclasts in conglomerate. Facies 5 near the axis of the Coal Mine syncline.

Figure 30. Cross-beds in sandstone and pebbly sandstone highlighted by pebble layers. Facies 5 near the axis of the Coal Mine syncline.

Figure 31. Layer of coal about 30 cm thick. Underlain and overlain by coarse-grained sandstone. Facies 5 near the axis of the Coal Mine syncline.

Figure 32. Pebbly sandstone dike intruding sandstone. Facies 5 near the axis of the Coal Mine syncline.

this facies. One, represented by deposits in the lower subfacies, consists of tabular, laterally continuous conglomerates and pebbly sandstones that display few internal features. A second, is a thick conglomerate section that is characterized by both stratified and structureless sandstones and conglomerates. The third, represented by the upper subfacies, is a thick section of conglomerate that contains mostly unstratified but some stratified conglomerates and pebbly sandstones that are interbedded with siltstone and coal.

The conglomerate and related rocks in the lower subfacies are interpreted as having been deposited rapidly, probably near a distributary mouth. The interlayering of these tabular conglomerates with amalgamated hummocky cross-stratified beds suggests that they were deposited on the inner shelf, probably on the lower shoreface. Some reworking by waves of the tabular distributary-mouth or distal bar deposits is indicated by the occasional presence of stratified and better sorted interlayers. However, poor sorting and the rarity of burrows in the tabular conglomerate suggest rapid deposition, possibly resulting from sediment transport during river floods. For the most part these deposits have not been significantly reworked but represent constructive phases of the deltaic system.

The second depositional system contains some features common to both the upper and lower subfacies. Tabular, laterally continuous conglomerates similar to those in the lower subfacies are present but not abundant. Lenticular and internally stratified conglomerates interlayered with trough-cross-bedded and planar-bedded sandstones are also present in some locations. Most common are structureless conglomerates similar to those seen in the upper subfacies. These conglomerates attain thicknesses of several tens of meters.

The second depositional system represents fluctuating constructive and destructive phases of a prograding delta. Tabular conglomerates similar to those in the lower subfacies are probably lower shoreface deposits largely unaffected by wave reworking.

In contrast, conglomerates and associated sandstones containing many sedimentary structures are interpreted to represent the distributary mouth area where wave reworking of sediments is common; possibly a distributary mouth bar. Working by waves is indicated by trough-cross-bedded conglomerate and sandstone (Clifton, 1981; Leithold and Bourgeois, 1984) which are generally believed to represent upper shoreface deposition above fair-weather wave base.

Featureless conglomerates characteristic of the second depositional style contain large clasts of organic debris and are interpreted as proximal distributary-mouth deposits. Sedimentation rates during constructional phases of the delta system are believed to have been high enough for sediments to have retained their original depositional form and to have prevented much reworking by waves. The high rates of deposition may have been the result of direct stream input, periods of stream flooding, or a combination of the two.

Conglomerates of the upper subfacies that occur near the top of the formation formed in a variety of ways.

The conglomerates and associated sediments in the upper subfacies represent both constructional and destructional phases of a prograding, delta in a largely high-energy environment.

The planar-bedded and trough-cross-bedded sandstone and pebbly sandstone in this subfacies represent periodic wave-reworking of distributary mouth deposits.

The unsorted and unstratified conglomerates that predominate in this

subfacies are believed to have been stream derived at least in part. Large wood fragments, which are burrowed by a marine bivalve lower in the formation, are not burrowed in these deposits. In addition, interlayered fine-grained interdistributary sediments contain no marine fossils. These facts and the presence of coal seams indicate non-marine deposition.

Facies 6

The disrupted facies is primarily confined to the upper portion of the Clallam Formation. It is commonly associated with amalgamated hummocky cross-stratified layers (Figure 5). Facies 6 most often consists of fine- to medium-grained, internally featureless sandstone that is cross-cut by a network of sedimentary dikes. The dikes consist of mud and silt and may be formed by the winnowing of the surrounding sandstone host during the escape of pore water during liquefaction.

Disruption features formed during and after deposition that are interlayered with, or cross-cut, deposits in facies other than Facies 6, include convolute bedding, sedimentary dikes, and slump blocks. In some locations convolute beds alternate cyclically with hummocky cross-stratified beds. Some such cycles are intruded by sedimentary dikes and sills. Displaced and rotated blocks of strata up to several tens of meters across are present in Facies 3 and 5.

According to Pettijohn and others (1973), fine-grained sandstone and siltstone are susceptible to soft-sediment deformation owing to their low permeability. The low permeability prevents quick adjustments to external changes in pore water pressure resulting from variations in water depth in the basin, sudden changes in groundwater flow, or sudden deposition of a layer of sand on top of an uncompacted bed. Pettijohn and others also pointed out that soft-sediment deformation occurs preferentially in areas

of rapid sedimentation where sands have low porosities and where initial slopes are high.

Within the Clallam Formation, disrupted rocks are associated with hummocky cross-stratified and conglomeratic strata (Figure 5). Several of the conditions favoring sediment deformation exist in this environment. Hummocky cross-stratified beds reflect rapid deposition of large amounts of sediment. Rapid deposition, coupled with the relatively steep submarine slopes associated with deltaic environments, overloading by coarse-grained distributary deposits, and tectonic activity in the area were all conducive to the soft-sediment deformation that is exhibited throughout the Clallam Formation.

Disruption upslope from the deposits in Facies 1 and 2 may have been the source of gravity-derived channel deposits observed in Facies 1 and 2. Either episodic seismic events or pounding from wave activity may have acted as a catalyst to initiate disruption of sediments. This may have resulted in spontaneous liqufaction, convolution, or intrusion of sedimentary dikes and sills. In turn, liquefaction and disruption may have released sediment down-slope to form channeled gravity flows.

## Discussion

The Clallam Formation represents a prograding, coarse-grained, primarily wave- and river-controlled delta front and prodelta. Its internal stratigraphic characteristics resulted from periodic abandonment and reoccupation of distributary channels combined with regional uplift, eustatic sea level changes, and local basin subsidence.

The pattern of stratification of the six facies in the Pysht and Clallam Formations indicates several cycles of shallowing and coarsening upward events within an overall shallowing and coarsening upward sequence (Figures 4, 5, and 6). The relative grain sizes and amount of organic

material indicate the nearness of a distributary mouth to individual depositional sites. The repeated cycles of shallowing- and coarsening-upward reflect the occupation and subsequent abandonment of distributary channels. As the distributary channel was prograding, the input of sediment was large, but as the distributary channel over extended itself, the channel was abandoned. Near the distributary mouth, the high sediment input resulted in sediment loading and subsequent subsidence. If the distributary channel were abandoned and the sediment supply cut off, sediment accumulation would not have kept up with local subsidence. As a result, deeper water sediments would have been deposited on top of the once active distributary mouth deposits (Figures 4, 5, and 6). As the whole delta region prograded, the distributary mouth deposits and the overlying sediments were deposited in progressively shallower water.

Shoaling can be attributed to basin filling, uplift of the basin, or eustatic sealevel change. Vail and others (1977) indicated that there were two episodes of rising sea level and one period of falling sea level while the Clallam Formation was being deposited. The vertical change in facies in the Clallam Formation reflects shoaling as the delta prograded seaward. On the present west coast of North America, storm-wave reworking of sediments is active in 10 to 50 m of water (Bourgeois, 1980). Amalgamated beds, particularily in areas experiencing rapid sedimentation, probably form in a more restricted range of water depths. Hence, for accumulations of amalgamated hummocky cross-stratification to reach 50 m or more in thickness (Figure 5 and 6), some balance amoung progradation, eustatic sea level change, and uplift rates must be met. This balance may be acquired during periods of rising sea level if progradation and rising sea level rates are the same; if uplift and progration rates, combined, are the same

as rising sea level rates; or if local basin subsidence, owing to sediment loading, acts in conjunction with a rising sea level to counteract regional uplift and progradation. During periods of falling sea level, the sea level change would act with progradation and regional uplift. Thus only local basin subsidence could counteract the effects of these factors and make possible the balance necessary for the accumulation of tens of meters of amalgamated hummocky cross-stratification in the Clallam Formation.

## PETROLOGY AND PETROGRAPHY

### Introduction

The Clallam Formation consists of feldspathic and lithic wackes and arenites (classification of Dott, 1964; Figure 33). To facilitate recognition of compositional variations caused by differences in grain size, amount of cementation, and mode of deposition point count data were separated by facies and plotted individually on ternary diagrams (Figures 34, 35, and 36). Each corner of the ternary diagrams coresponds to the grain parameters set in Table 1. Petrologic interpretations were based primarily on the composition and characteristics of lithic and monocrystalline grains (see Appendix 1). Modal analysis, while aiding in the recognition of compositional variations, was also used to support petrologic interpretations.

Most samples analyzed petrographically were taken from resistant portions of the outcrop which contain more calcite cement than most of the surrounding rock. Some comparisons have been made between concretionary and nonconcretionary samples. The results of these comparisons will be discussed in context within the facies in which the samples belong.

One hundred and fifty thin sections were analyzed for cementation characteristics, sorting, grain size, maturity, and general composition. From these were selected representative samples for modal analysis. One half of each thin section was stained for the identification of plagioclase and potassium feldspars. Counts of 300 points were conducted on the stained half of the thin section to determine overall composition. Counts of 200 points on the unstained half of the thin section allowed for the identification of populations of lithic constituents. A spacing of 1.0 mm was used for the 300-point counts. This allowed counts to cover a maximum amount of area without duplicating points on any single grain. A

TABLE 1: Grain parameters (modified from Ingersoll and Suczek, 1979)

| | | |
|---|---|---|
| Q = Qm + Qp | where | Q = total quartzose grains<br>Qm = monocrystalline quartz grains<br>Qp = polycrystalline aphanitic quartz grains including chert |
| F = P + K | where | F = total feldspar grains<br>P = plagioclase feldspar grains<br>K = potassium feldspar grains |
| Lt = L + Qp | where | Lt = total aphanitic lithic grains<br>L = unstable aphanitic lithic grains |
| L = Lv + Ls + Li | where | Lv = volcanic-hypabyssal aphanitic lithic grains<br>Ls = sedimentary aphanitic lithic grains<br>Li = intrusive aphanitic lihtic grains |
| Ls = Lslt + Lcs + Lm | where | Lslt = silt-sized aphanitic lithic grains<br>Lcs = clay-sized aphanitic lithic grains<br>Lm = metamorphic aphanitic lithic grains |

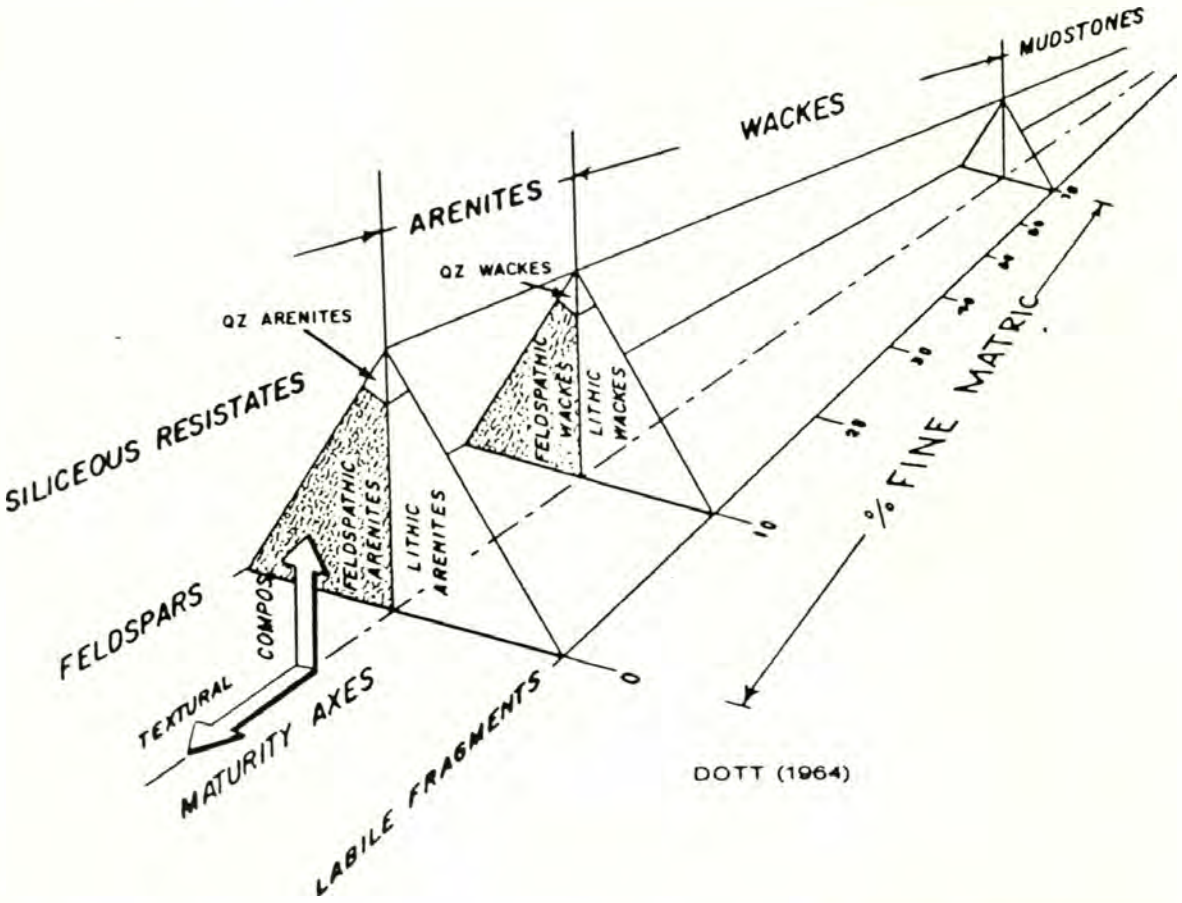


Figure 33. Sandstone classification used in this report (from Dott, 1964).

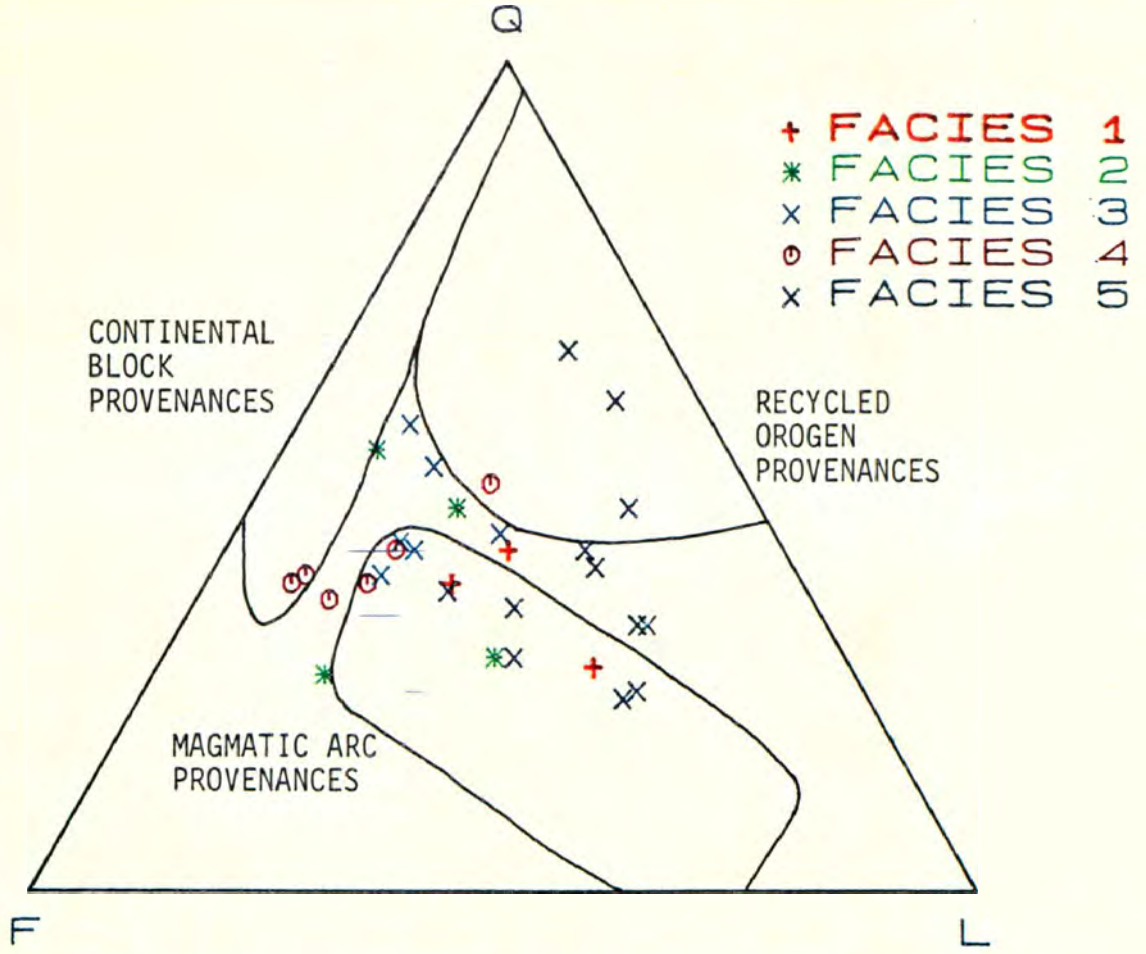


QFL PLOT: FACIES 1-5

Figure 34. QFL ternary diagram showing compositions of sandstones from the Clallam Formation. The outlined fields are tectonic provenance areas from Dickinson and Suczek (1979).

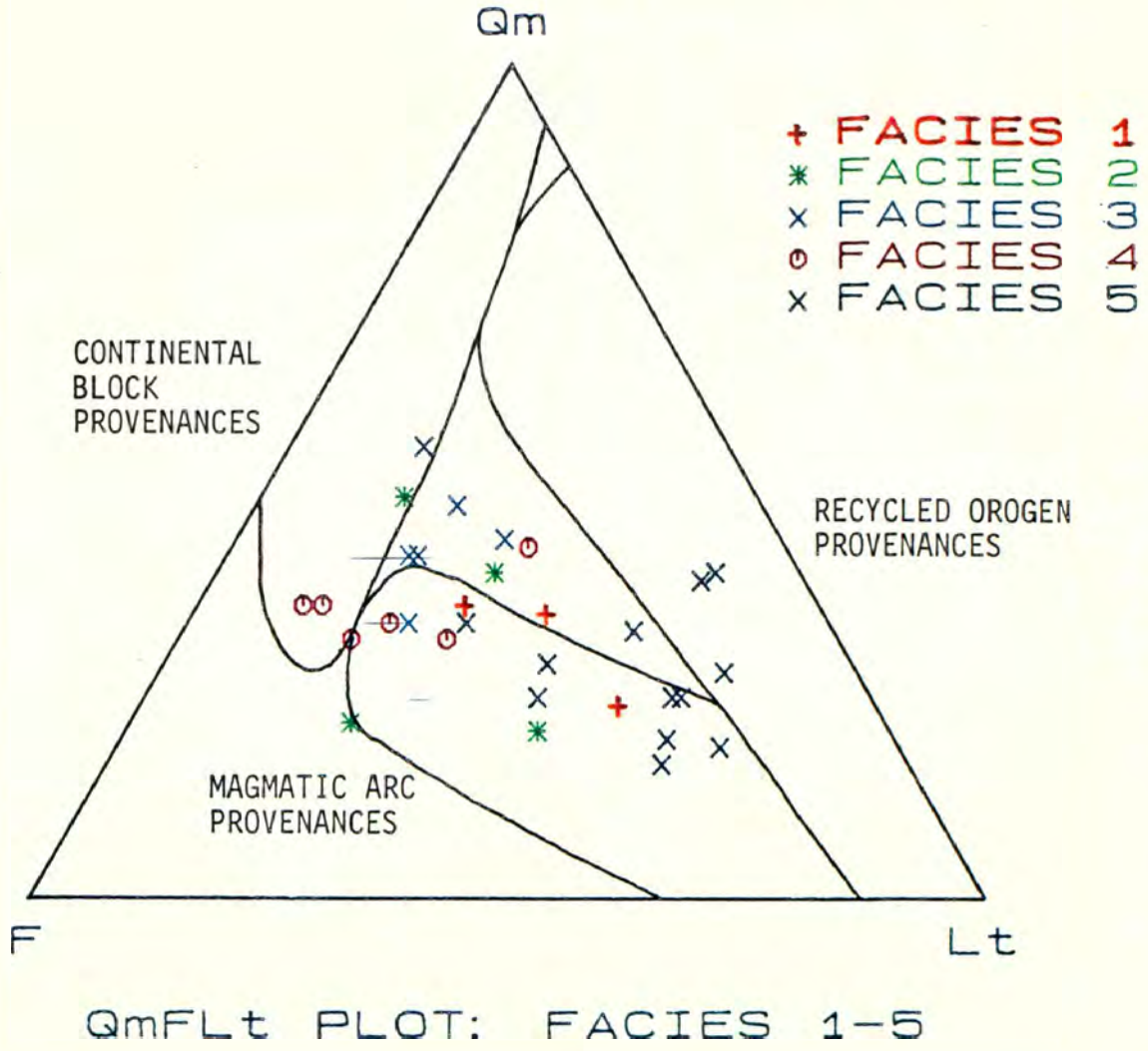


Figure 35. QmFLt ternary diagram showing compositions of sandstones from the Clallam Formation. The outlined fields are tectonic provenance areas from Dickinson and Suczek (1979).

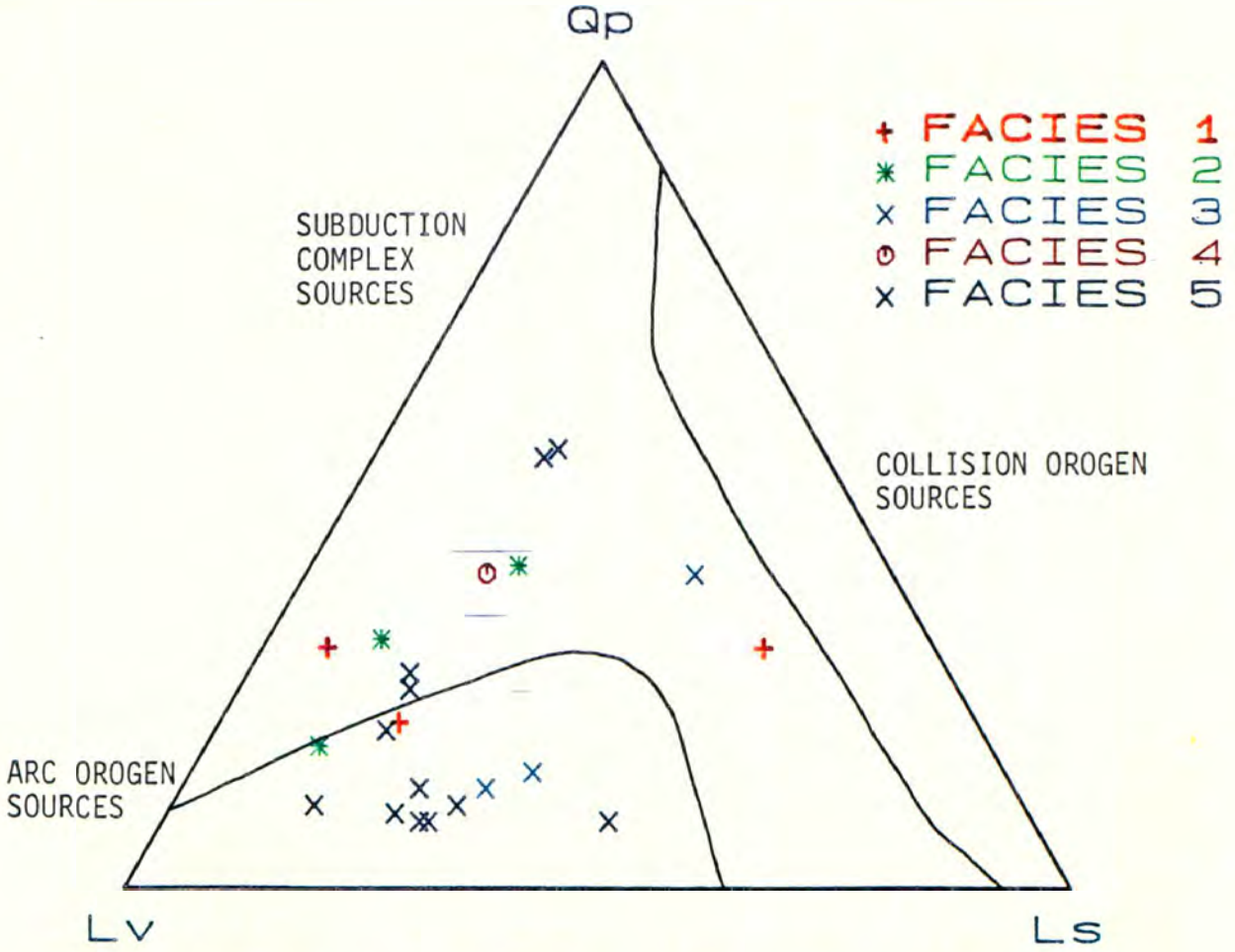


Figure 36. QpLvLs ternary diagram showing compositions of sandstones from the Clallam Formation. The outlined fields are tectonic provenance areas from Dickinson and Suczek (1979).

spacing of 0.5 mm was used on most lithic counts to enable 200 points to be counted on the unstained half of the thin section. A 1.0 mm spacing was used on a few samples containing numerous lithic grains. The Gazzi-Dickinson method of point counting was used in the present study. This method successfully eliminates the effect of breakage of fragments into constituent grains but does not eliminate actual mineralogic changes with grain size (Ingersoll and others, 1984).

Categories are:

Qm: Monocrystalline quartz, including individual grains and fine- sand-sized or larger grains located within rock fragments.

P: Plagioclase feldspar, including individual grains and fine-sand-sized or larger grains located within rock fragments.

K: Potassium feldspar, includes individual grains and fine-sand-sized or larger grains within rock fragments.

Lithics: all unstable, polycrystalline, lithic fragments. Fine-sand-sized or larger phenocrysts were counted as separate grains.

Qp: Polycrystalline quartz, including aggregates of quartz crystals and chert. If part of the grain is fine-sand-sized or larger, that part is counted as Qm.

Mafics: All mafic and heavy minerals.

Cement: Calcite cement.

Misc: Includes miscellaneous grains that cannot be identified or do not fit in any of the above catagories.

Lithic catagories counted include:

Qa: Polycrystalline quartz, including aggregates of quartz crystals of probable metamorphic or intrusive origin.

Chert: This includes microcrystalline quartz with up to 15 percent

impurities.

Lv: Volcanic lithics, including all types of volcanic lithics.

Lslt: Siltstone lithics, including siltstone lithics and claystone lithics with greater than 15 percent silt-sized grains.

Lcs: Claystone lithics, including all claystone lithics with less than 15 percent silt-sized grains wihtout metamorphic fabric.

Lm: Metamorphic lithics, including all lithics containing metamorphic mineral assemblages or metamorphic textures, with the exception of chert and polycrystalline quartz with less than 15 percent impurities.

Li: Intrusive lithics, including all fine-grained intrusives and grains with granophyric textures.

Misc: This includes miscellaneous grains that cannot be identified or that do not fit in any of the above categories.

A complete explanation and description of the individual categories is included in Appendix 1.

## Descriptive Petrography

### Facies 1

The rocks of Facies 1 are moderately- to well-sorted (classification of Pettijohn and others, 1973), very fine-grained to fine-grained subrounded to angular feldspathic arenites. Most grains float in calcite cement. The lithic grains are more rounded than are the monocrystalline grains. Some alignment of platey grains is common (Figure 37). In contrast to the channel deposits, the laminated deposits contain greater amounts of organic matter, and their lithic grains are smaller.

The mode of deposition and the lack of abrasion during deposition of the laminated deposits compared to the channeled deposits (refer to the Description and Interpretation of the Facies section) accounts for the abundance of sedimentary lithics in Facies 1 deposits.

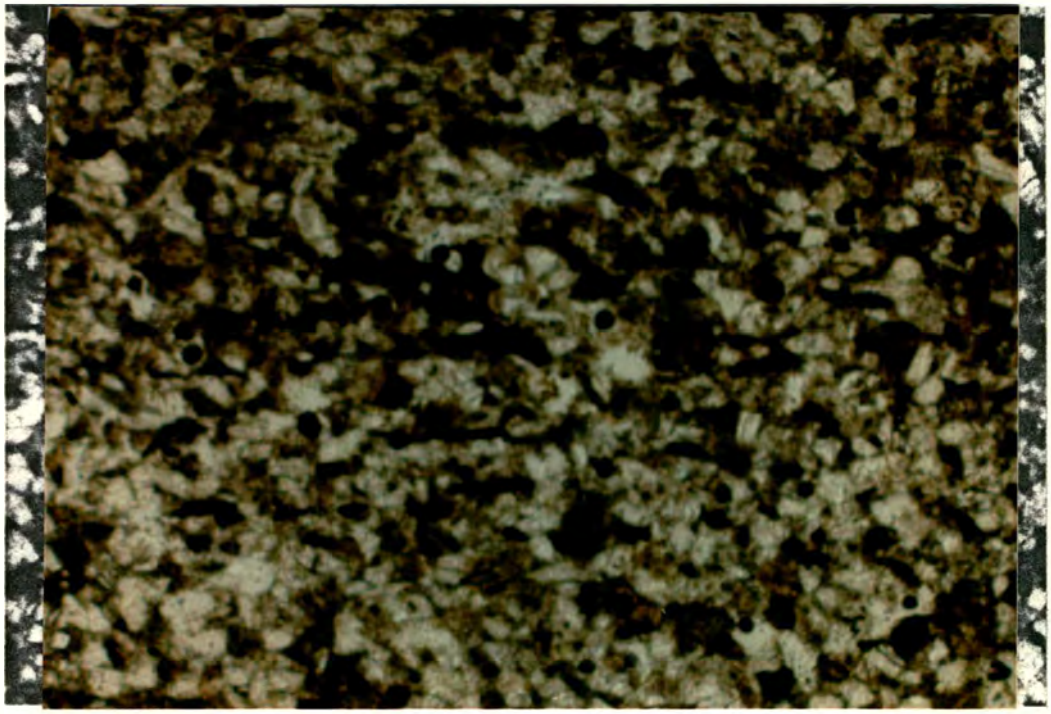

Figure 37. Alignment of platey grains. Sample 32-12-22-11. Field of view: 3.4 x 2.3 mm.

Facies 2

Burrowing in Facies 2 obliterate most sedimentary structures and bedding characteristics; thus two or more different primary depositional environments may be grouped into this facies. The variety of petrographic characteristics appears to support this. Rocks in Facies 2 are moderately sorted, very fine- to medium-grained feldspathic arenites and wackes. Individual grains in arenites are usually floating in calcite cement. In contrast, wackes exhibit tangential, long, concave-convex, and some sutured grain contacts. Matrix in the wackes includes psuedomatrix, epimatrix, and protomatrix. Both the arenites and wackes consist of subangular to angular grains; the lithic grains are generally more rounded than are the monocrystalline grains.

Facies 3

The rocks in Facies 3 are characteristically well sorted, subangular to angular, fine-grained feldspathic arenites. Most of the grains float in calcite cement. Lithic fragments tend to be subrounded. Grains not floating in cement, display tangential, long, and occasional concave-convex contacts.

Facies 3 data on the QFL and QmFLt ternary diagrams (Figure 34 and 35) are displaced away from the L and Lt corners of the diagram. This displacement is in contrast to the data in Facies 5. Samples from Facies 5, owing to their environment of deposition, are the most reliable provenance indicators.

The displacement of points in Facies 3 away from the L and Lt corners of the ternary diagrams is ascribed to the energetic mode of deposition and the relatively small grain size of samples. Resuspension of sediments during storm activity selectively abrades and dismantles less durable

grain constituents such as lithic fragments. This process essentially decreases the percentage of lithic grains and increases relative percentages of Q and F. Furthermore, very fine-grained lithic fragments have been preferentially replaced by calcite cement. Taking these factors into account, the positions of Facies 3 data points on the QFL and QmFLt ternary diagrams do not represent true provenance affinities. More likely they have very similar affinities as those in Facies 5, where lithic grains have not been preferentially removed.

Facies 4

Owing to the diverse depositional mechanisms that are present in Facies 4, petrographic characteristics are quite variable. Of the six samples selected for point counting three are from laminated deposits, which generally tend to be very-fine grained feldspathic arenites and wackes; two are from hummocky cross-stratified deposits and are fine-grained feldspathic arenites; and one is a medium-grained, bioturbated, feldspathic arenite. All but the bioturbated sample are moderately to well sorted; the bioturbated sample is poorly sorted. The grains are generally subangular and float in calcite cement. Feldspathic wackes contain little calcite cement, and the grains commonly either float in psuedomatrix, epimatrix, or protomatrix or have tangential, long, or concave-convex grain contacts.

Many of the fine-grained rocks from Facies 4 have so few lithic fragments that seperate lithic counts could not be made on them. When lithic counts in the total grain point count fall below 5 percent of the total grain population, the slide does not contain enough lithic grains to conduct a separate lihtic point count. The one sample for which lithics were counted displays no affinity for a distinct provenance on the QpLvLs ternary diagram.

Although data points from Facies 4 are displaced away from the L and Lt corners of the QFL and QmFLt ternary diagrams in a similar fashion as those from Facies 3, displacement of data from particular sediment types, such as laminated deposits, are not sufficient to allow comparisons between the positions of data points and depositional mechanisms.

Facies 5

Facies 5 samples selected for petrographic analysis are very coarse-grained to medium-grained lithic arenites and feldspathic arenites. The coarser grained samples are poorly sorted, and the medium-grained samples are moderately to well sorted. Lithic fragments are subrounded to rounded, and the remainder of the grains are subangular to angular. Although some grain contacts are tangential, long, and concave-convex, many grains are floating in calcite cement. All samples but the ones containing extreme amounts of calcite cement are grain-supported.

When compared to Facies 1, 2, 3, and 4, the lack of fine-grained sedimentary lithic fragments in the lithic-rich, coarse-grained sandstone and conglomerate of Facies 5 is enigmatic. Facies 2, 3, and 4 contain few sedimentary lithic grains but do contain intraclasts. Facies 1 contains higher amounts of sedimentary lithic than the other four facies. It may be that lithics in Facies 1 and 5 have separate origins: those in Facies 5 being derived from a fluvial source, and those in Facies 1 being intraclasts derived from the reworking of partially consolidated strata by storm waves. The presence of coarse-grained sedimentary clasts in Facies 5 and the lack of sedimentary clasts in Facies 3 and 4 would suggest that most fluvially-derived sedimentary fragments in Facies 5 were unable to survive the abrasive processes active in a wave dominated, nearshore and shelf environment.

## Discussion

The Facies 5 data appear to be most reliable for petrologic interpretations because lithic grains in Facies 5 samples have not been removed by nearshore abrasion or diagenic processes. The primary factors responsible for the possible displacement of the data points in Facies 1 through 4 relative to those in Facies 5 are the effects of varying depositional environments, relative grain sizes, and diagenesis. As mentioned in the discussion of individual facies, abrasion and subsequent removal or dismantling of unstable grains is common in high-energy nearshore and shelf environments. Lithic fragments, specifically portions of fragments with aphanitic ground masses, are selectively broken down in high energy environments; the data plotted on the ternary diagrams are conseqently biased away from the L and Lt corners. Decreasing grain sizes, independant of depositional mechanisms, also effect the percentage of lithic constituents. Most of this biasing occured during diagenisis. During calcite cementation, fine-grained lithic fragments are selectively altered to calcite, thereby removing lithic fragments from the grain populations. Calcite-cemented concretions have fewer lithic grains than do their host rocks. Some lithic fragments in Facies 5 samples have been partially altered to calcite, but the grains can still be identified (Figure 38). Thus, the effects of cementation on modal compositions are negligable in samples from Facies 5. In samples from Facies 1 through 5, modal compositions are not affected as much by calcite cementation during diagenesis as they are by depositional mechanisms.

Four major types of source rocks contributed detritus to the Clallam Formation. These are andesitic to dacitic volcanic rocks, chert, metamorphic rocks, and plutonic rocks. Volcanic rocks, chert, and metamorphic rocks appear in sandstones of the Clallam Formation as lithic

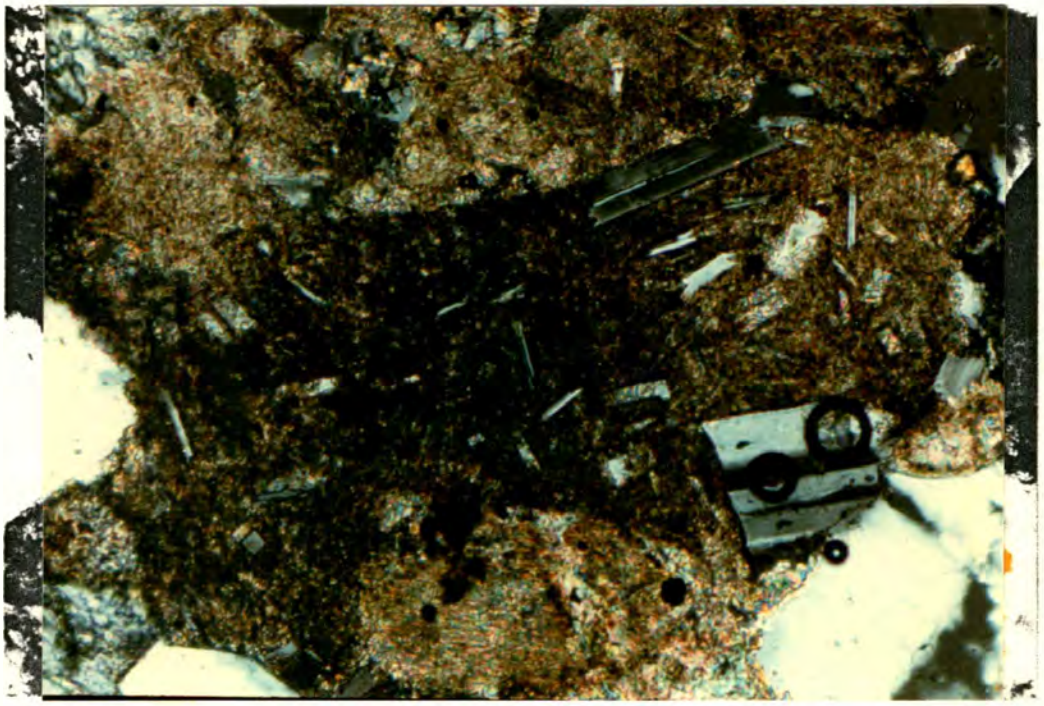

Figure 38. Volcanic lithic being altered to calcite. Sample 32-11-32-6. Field of view .85 x .58 mm.

grains; and plutonic rocks are apparent in modal grain distributions as abundant quartz, plagioclase, hornblende, biotite, and minor amounts of potassium feldspar grains, which suggest a quartz monzonite to granodiorite composition.

## PROVENANCE

Provenance determinations for the Clallam Formation are based on petrographic results, as statistically reliable paleocurrent data are unavailable. The Clallam Formation contains detritus from four major types of source rocks (see Petrology and Petrography section, and Appendix 1). These are andesitic to dacitic volcanic rocks, chert, metamorphic rocks, and plutonic rocks.

### Tectonic Provenance As Determined From Detrital Modes

Provenance determinations were based on petrographic observation of lithic fragments, monocrystalline grain characteristics, and ternary diagram plots. Dickinson and Suczek (1979), by comparing grain populations from known tectonic settings, divided ternary diagrams into several tectonic provenance areas (Figures 34,35, and 36), the boundaries of which were formed by comparing several sand-grain populations from both recent and ancient sedimentary deposits whose tectonic settings were known. The compositions of sandstones from deposits of unknown origin, when plotted on their ternary diagrams, allow general interpretations concerning provenance and tectonic setting.

Data from Facies 1-5 plotted on the ternary diagrams (Figures 34, 35, and 36) indicate that those facies have variable provenance signatures. Because these variances can be categorized by depositional facies and not by stratigraphic position, the compositional differences among the sandstones, as shown on the ternary diagrams, are attributed to changing depositional mechanisms and not various provenance areas.

In the same section it was reasoned that samples from Facies 5 were the most reliable indicators of provenance. For this reason, only the positions of Facies 5 data were selected for provenance determinations using the Dickinson and Suczek method, data points from Facies 1,2,3, and

4 are included so comparisons of the composition of grain populations between facies can be made.

The ternary diagrams together demonstrate a distinct affinity for the magmatic arc provenanc and a less convincing affinity for the subduction complex provenance. In addition, some data plot in an area intermediate between these two provenance areas. Samples from the magmatic arc provenance contain abundant intermediate volcanic lithics, while those that show subduction complex affinity contain abundant chert fragments. The sample data in areas intermediate between the two provenance areas contain a large amount of volcanic lithics but are drawn toward the area of subduction complex provenance because they also contain significant amounts of chert.

It is concluded that data plotted on the three ternary diagrams suggest a magmatic arc and, less clearly, a subduction complex provenance. These suggested provenance areas are consistant with the four major source areas suggested by petrographic observation of lithic and monocrystalline grain characteristics.

## Possible Source Areas

Table 2 summarizes the potential source areas that may have contributed detritus to the Clallam Formation. Although the specific rocks that produced the Clallam Formation sediment have been eroded, other parts of their lithostratigraphic units may remain. Besides, looking for present-day rocks similar to those that may have existed in the Miocene is still the most useful method that can be used for assessing provenance. Terranes that are today adjacent to the Clallam Formation and that contain at least one of the four major rock types that are the sources for the Clallam Formation include the San Juan Islands, Vancouver Island, the Coast Range

TABLE 2. Major rock types and possible sources.

| | PLUTONICS | ANDESITIC AND DACITIC VOLCANICS | METAMORPHICS | CHERT |
|---|---|---|---|---|
| CASCADES (Misch, 1977; Gresens, 1982) | Mount Stewart batholith | equivalents of the Eocene to Miocene intermediate volcanics in central Washington | Yellow Aster complex, Shuksan Metamorphic Suite, Cascade River Schist, Skagit Gneiss | Chilliwack Group, Cultus Formation Nooksack Group |
| SAN JUAN ISLANDS (Brandon and others, 1983) | Decatur Terrane | Constitution Formation, Haro Formation, Spieden Group | Garrison Schist, Constitution Formation | Deadman Bay Volcanics, Orcas Chert, Constitution Formation, Lopez Complex, Decature Terrane Garrison Schist |
| VANCOUVER ISLAND (Muller, 1982) | Island Intrusives, Wark Gneiss, Colquitz Gneiss, Westcoast Complex | Bonanza Group, Myra Formation | Leech River Complex, Westcoast Complex, Pacific Rim Complex | Pacific Rim Complex |
| COAST RANGE COMPLEX (Monger, 1982) | Coast Plutonics | | | |

Complex, and the North Cascades. Sand in the Clallam Formation may have been derived from one or more of these potential source areas.

Because few metasedimentary or basalt clasts resembling rocks in the Olympic Mountains were found in the sandstone of the Clallam Formation, detritus probably did not come from the Olympic Core terrane or Crescent terrane.

The relative geographic positions of the four potential source areas has not changed much since the Early Miocene. The position of Vancouver Island relative to the San Juan Islands, the Coast Range Complex, and the North Cascades is constrained by the deposition of the Nanaimo Group (Pacht, 1984). The Upper Cretaceous Nanaimo Group contains detritus from each of these areas, indicating that Vancouver Island, the San Juan Islands, the Coast Range Complex, and the North Cascades were fixed with respect to one another by the Upper Cretaceous (Pacht, 1984). Before the Early Miocene, juxtaposition of all four potential source areas was complete. However, the position of the Crscent terrane, in which the Clallam Formation is included, relative to the four potential source areas, is uncertain (see Introduction). The Clallam Formation may have been located west or southwest of its present position.

San Juan Islands

The geologically complex San Juan Islands (Figure 1) contain six major terranes that were juxtaposed by thrusting in post- mid- Cretaceous time. These are the Sinclair, Decatur, Lopez, Constitution, Eagle Cove, and Roche Harbor terranes (Whetten and others, 1978). Together, these six terranes contain rock types similar to all four major source rocks for sand in the Clallam Formation. However, in some of the six terranes numerous additional lithologies present are not found in the Clallam Formation. Therefore, unless all of the rock types that do not appear in

the Clallam Formation were eliminated during transport, those terranes with other stable rock types are unlikely sources. For example, the Decatur Terrane, a potential plutonic source, contains the required intermediate plutonics, but, as an ophiolite complex, it also contains gabbro dikes, mafic volcanics, and sandstones. Many rock types not present in the sandstones of the Clallam Formation occur in most of the other units as well.

Potential sources for andesitic and dacitic volcanic rocks in the San Juan Islands are plagued by a separate problem. The primary candidates for these sources are sedimentary formations from which magmatic-arc volcanic fragments would have been reworked and transported to the Clallam Formation. This it is not probable. The volcanic grains in the Clallam Formation appear too fresh to have been reworked from the Mesozoic formations in the San Juan Islands. Furthermore, the variety of grain sizes in the Clallam Formation could not have been derived from the predominately sand-sized volcanic sediments in the San Juan Islands.

Units in the San Juan Islands containing metamorphic rocks and chert do not contain rock types other than those present in the Clallam Formation sandstones, and they also contain metamorphic mineral assemblages similar to those seen in the Clallam Formation. Metamorphic and chert rocks in the San Juan Islands are potential source rocks.

Vancouver Island

The rocks of the Insular Belt in the Canadian segment of the Cordillera on Vancouver Island (Figure 39) are another potential source for all four lithic grain types present in the Clallam Formation (Table 2).

The Jurassic Island Intrusives, widespread throughout southern Vancouver Island, are composed of biotite-hornblende granodiorite and quartz

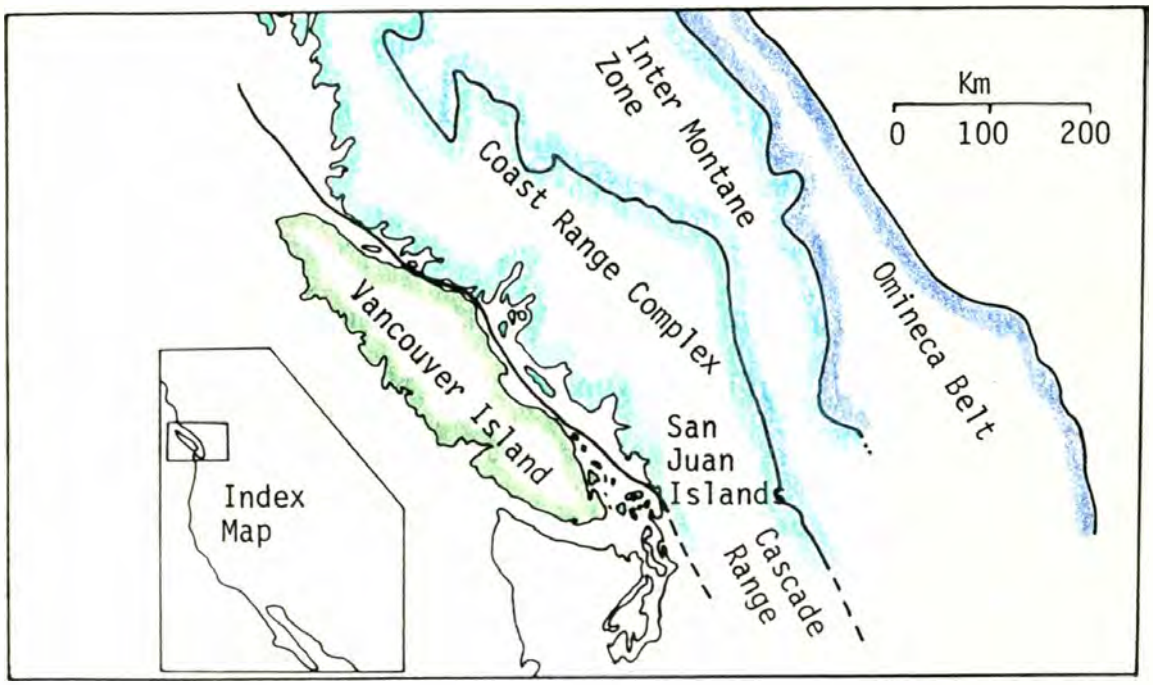


Figure 39. Location map showing potential source areas (modified form Tennyson and Cole, 1978).

diorite. They are a potential source for plutonic fragments. Portions of the Paleozoic Wark Gneiss and Colquitz Gneiss contain the requisite quartz, plagioglase, biotite, and hornblende assemblages and are also potential plutonic sources. The Westcoast Complex intrusives contain plagioclase grains that are more calcic than those seen in the Clallam Formation and are a more suitable contributor of metamorphic fragments.

Potential volcanic source rocks include the Devonian or Silurian Myra Formation of the Sicker Group and the Jurassic to Cretaceous Bonanza Group. The Myra Formation consists of silicic tuff, breccia, and flows with interbeds of black argillite and graywacke. The Myra Formation has less potential as a source area than does the Bonanza because it contains relatively few flow rocks and has rock types not found in the Clallam Formation. Bonanza Group volcanic rocks are abundant on the southern portion of Vancouver Island and contain intermediate volcanic lithologies similar to those found in the Clallam Formation.

A number of rock units on Vancouver Island, including the Leech River Complex (Figure 1), the Westcoast Complex, and the Pacific Rim Complex, contain the requisite metamorphic assemblages. The lack of high-grade metamorphic mineral assemblages in these rock units is consistant with grain lithologies in the Clallam Formation.

The Pacific Rim Complex is the most probable potential source of chert on the southern portion of Vancouver Island. Ribbon-cherts in the Pacific Rim Complex are interbedded with varying amounts of argillite, and directly overlie the Bonanza Volcanics (Muller, 1973).

Coast Range Complex

The Coast Range Complex, part of the Canadian Cordillera (Figure 39), consists primarily of Cretaceous and lower Tertiary granitic rocks and older high-grade metasediments. Although the granitic rocks appear to be

more silicic than the components found in the Clallam Formation, they are still considered a possible source for plutonic fragments. It is unlikely, however, that the high grade metasediments contributed fragments, because no granulite-facies metamorphic minerals appear in the Clallam Formation. Although the Coast Range Complex represents a magmatic and volcanic arc complex, it is unlikely that substantial amounts of volcanic rocks survived beyond the early Tertiary because uplift of 5 to 25 km and subsequent erosion in the early Tertiary was extensive enough to have exposed the granulite-facies metamorphic rocks (Monger and others, 1982). Moreover, during the deposition of the Upper Cretaceous Nanaimo Group, sediments derived from the Coast Range Complex were composed predominantly of plutonic material (Pacht, 1984). Therefore by the Miocene, the volcanic rocks had been eroded and only plutonic rocks, and possibly a few granulite facies metasediments, were exposed. Compositionally, plutonic rocks of the Coast Range Complex are unfavorable as source rocks since they have low P/F ratios; few grains of potassium feldspar are found in the Clallam Formation.

Cascades

Since the deep-seated Tertiary plutonics in the Cascades were probably not exposed in the Early Miocene, older plutonic sources in the Cascades have to be considered for source rock potential. The Mesozoic Mount Stuart batholith is the largest of the older plutonic complexes in the Cascades. Smaller areas of plutonics would require a specific point source to have supplied the sands in the Clallam Formation, and are less likely candidates for provenance. The Mount Stuart batholith is primarily granodiorite and was exposed in the Tertiary (Tabor and others, 1984). Some of the intermediate orthogneisses in the Cascades are also possible

sources of quartz, plagioclase, biotite, and hornblende.

Thick sequences of Eocene to Miocene volcanics are wide-spread in central Washington (Gresens, 1982). Calc-alkaline volcanics coeval with the central Washington volcanics may have extended over large portions of the northern Washington Cascades before uplift and erosion of the North Cascades. Although most of the uplift and erosion of the Cascades was during the Pliocene and Pleistocene (Mackin and Cary, 1965), some erosion of the active Oligocene and Miocene magmatic arc would have been expected. Thus far, no record of volcanic detritus derived from the Oligocene and Miocene volcanism has been found west of the North Cascades.

Pre-Tertiary rocks now dominate the North Cascades. The Yellow Aster Complex, Shuksan Metamorphic Suite, Cascade River Schist, and Skagit Gneiss all contain the requisite metamorphic minerals that qualify them as potential source rocks for the Clallam Formation. Unfortunately, they also contain high grade metamorphic minerals, such as lawsonite and glaucophane, that do not appear in the Clallam Formation. These minerals may have been lost in transport.

The main chert-bearing units in the North Cascades are the Chilliwack Group, Cultus Formation, and Nooksack Group.

## Discussion

Not one, but several source areas are suggested by petrographic and petrologic studies. The three regions that are the most likely source areas appear to be Vancouver Island, the Cascades, and the San Juan Islands. The Coast Range Complex may have contributed plutonic fragments but not metamorphic, chert, and volcanic rock types. Metamorphic and chert fragments may have been derived from the San Juan Islands, but volcanic and plutonic fragments probably came from elsewhere. All four lithic types are represented in the Cascades and on Vancouver Island. Owing to the

lithologic similarities between the Cacades, Vancouver Island, and the San Juan Islands it is difficult to single out one of these areas as the most likely source. Sediments in the Clallam Formation may have come from one or more of the three areas mentioned above.

## DEPOSITION AND TECTONICS

To characterize the tectonic framework of the Clallam Formation in space and time, discussion of known and postulated relationships of relevant rock units, structures, and plate reconstructions is required.

### Deposition

When characteristics of nearby and contemporary rock units are investigated some important constraints appear. These rock units are the Astoria (?) Formation in southwest Washington, the Hoh lithic assemblage in the western core of the Olympic Peninsula, and the Sooke Formation on the southern tip of Vancouver Island (Figure 1, p. 3). Also of importance is the younger Middle and Upper Miocene Montesano Formation which overlies the Astoria (?) Formation in southwest Washington.

The Astoria (?) Formation is a marine to partly non-marine unit that is composed of volcaniclastic and feldspathic sandstone interbedded with shales (Wolfe and McKee, 1972). Although more detailed petrologic studies of the Astoria (?) Formation are needed, what is known about the sediments in the Astoria (?) Formation suggest that they were not derived from the Olympic Core terrane. Interlayered tuffs suggest a volcanic source, probably from the active Cascade volcanoes to the east. A Cascade source would suggest that, during the Early Miocene, the major drainage pattern or paleoslope in southwest Washington was generally from east to west. The relative positions of the Clallam and Astoria (?) Formations suggests that the strand line in the Early Miocene was roughly northwest-southeast (Figure 40).

Further north, on the western edge of the Olympic Peninsula, rocks of the Upper Oligocene to Middle Miocene Hoh lithic assemblage crop out (Figure 1). The Hoh lithic assemblage consists primarily of sandstone, siltstone, and shale, and small amounts of shear-bounded exotic basalt

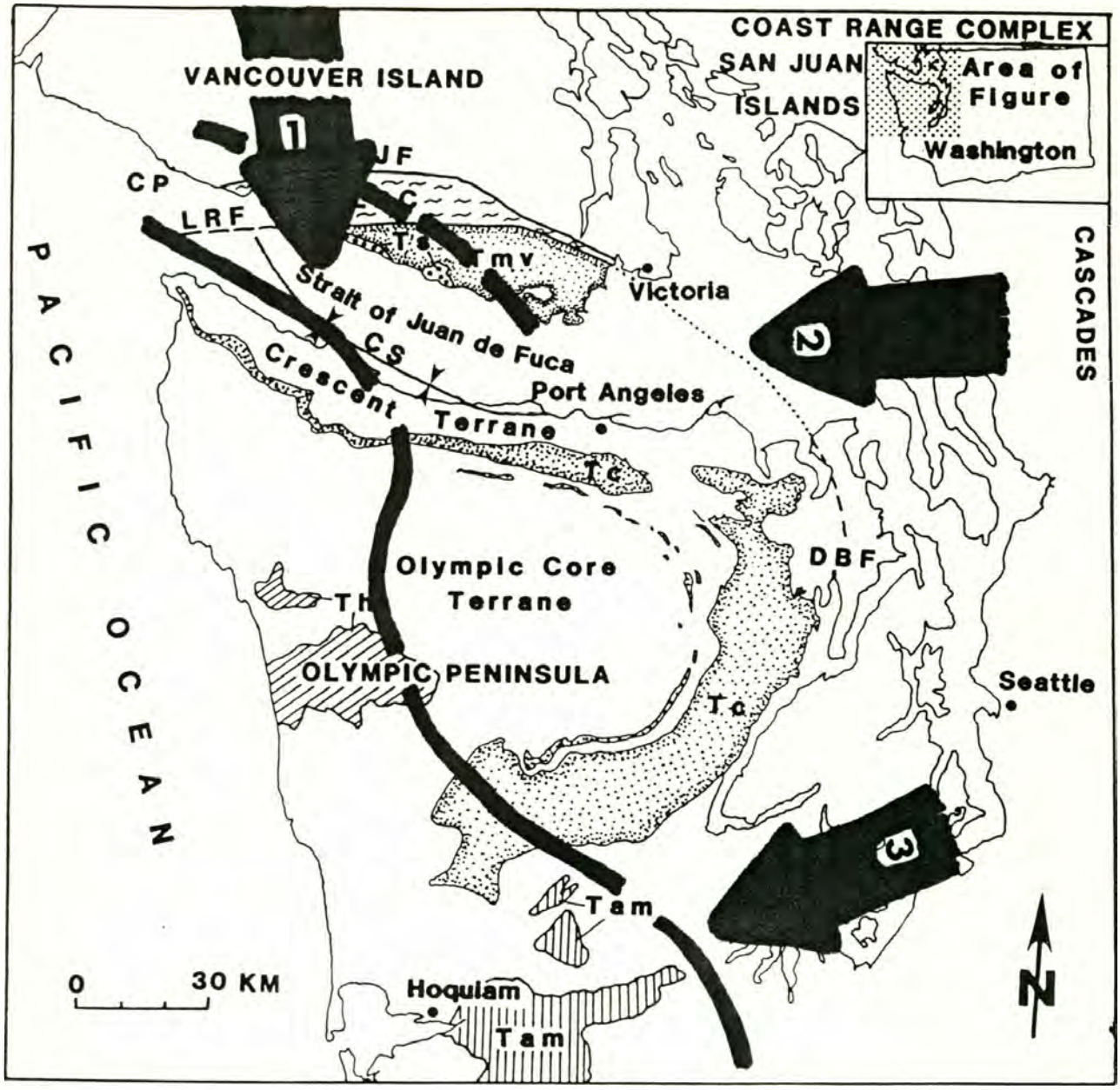


Figure 40. Possible directions of transport of sediment into the Clallam Formation. Dashed line is the inferred Late Oligocene position of the strandline. The dark solid line is the possible position of the strandline in the Early Miocene. Note the progradation of the strandline toward the southwest. Large arrows show the possible direction of transport into the Clallam Formation from Vancouver Island (arrow 1) and the Cascades (arrow 2), and into the Astoria (?) Formation (arrow 3).

masses. The assemblage is highly faulted and folded but is only locally strongly deformed or penetratively sheared (Tabor and Cady, 1978). Rocks of the Hoh lithic assemblage are part of the Olympic core accretionary prism accreted in the post-Late Oligocene to Middle Miocene. The time, age, and location of the Hoh lithic assemblage imply that somewhere west of the locations of shallow marine to nonmarine depositon represented by the Clallam and Astoria (?) Formations, turbidites were actively being deposited, followed closely by accretion to the overiding plate. Because the turbidites are now part of the accretionary prism just east of the subduction zone, it is likely that prior to accretion the turbidites were deposited on a trench-slope, in a trench-slope basin, or in the trench. Subsequent accretion implies that underthrusting in the Olympic Core terrane continued through the Middle Miocene.

Rocks of the Upper Oligocene or Lower Miocene Sooke Formation are located north of the Clallam Formation on the southern tip of Vancouver Island (Figure 1). A Late Oligocene (late Zemorian) age was based on studies of coquinas of littoral shells, and an Early Miocene age is deduced from observations of microflora from carbonaceous silts (Muller, 1982). In this study, the Late Oligocene age for the Sooke Formation will be used, because Addicott (1976b), who studied both faunal assemblages, mentioned that the Clallam Formation and Sooke Formation faunal assemblages are not coeval. The Sooke Formation unconformably overlies the Metchosin Volcanics and Sooke Gabbro on Vancouver Island, and the Hesquiat Formation on an island near Carmanah Point (Figure 1). The Sooke Formation consists of sandstone, minor conglomerate, and lenticular coquinas of bivalves and gastropods that indicate a near-shore origin. On Vancouver Island, the Sooke Formation was in part derived locally from the Metchosin

Volcanics and Sooke Gabbro (Muller, 1982). Near Carmanah Point the Sooke Formation was derived in part from the underlying Hesquiat Formation (Muller, 1982).

The location, age, and composition of the Sooke Formation places important constraints on the provenance of the Clallam Formation. Because the Sooke Formation contains material derived from the Metchosin Volcanics and Sooke Gabbro, these rock units must have been exposed just prior to, and probably during, Clallam Formation deposition. Because very few or no fragments from the Metchosin Volcanics occur in the sandstones of the Clallam Formation, a drainage system supplying sediment to the Clallam Formation from Vancouver Island must have been located west of the Metchosin Volcanics.

The Middle Miocene to Pliocene Montesano Formation in southwest Washington is included in this discussion primarily because it documents the uplift of the Olympic Peninsula. The Montesano Formation unconformably overlies older rock units and consists primarily of shallow marine sandstone and siltstone. The sandstone contains abundant lithic fragments derived from the Olympic Peninsula (Bigelow, personal communication), which must have been uplifted by that time. As discussed in the section on Provenance, the Olympic core is not a possible source area for the Clallam Formation. Petrologic studies of the Montesano Formation reflect a distinctive compostional signature characteristic of an Olympic Core terrane provenance. Because this compositional signature is not seen in the Clallam Formation or the Astoria (?) Formation it is inferred that the Olympic core area was either submergent or represented a gentle lowland during the Early Miocene (Figure 41).

## Possible Source Areas

The petrologic evidence for possible source areas was discussed in the

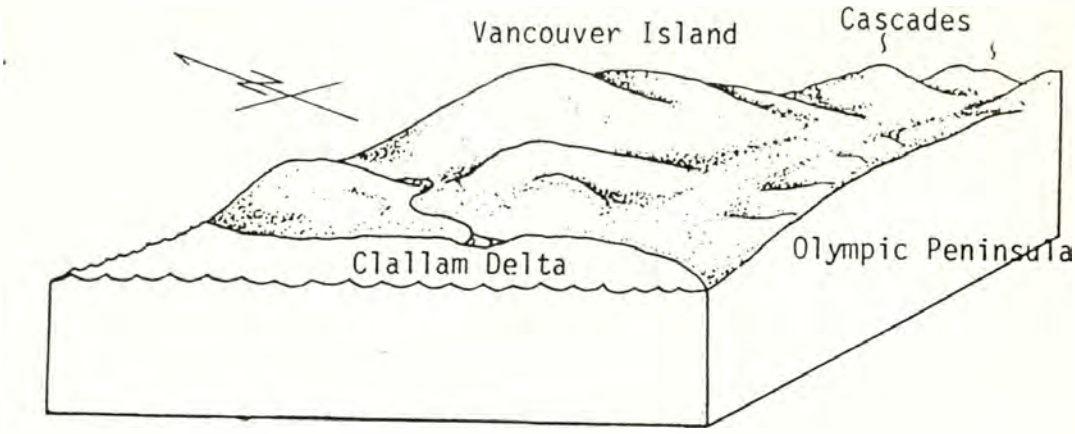


Figure 41.a. Paleogeographic reconstruction with Vancouver Island source area. River system flowing from the northwest on Vancouver Island. Olympic Peninsula may have been a lowland south of the Clallam delta.

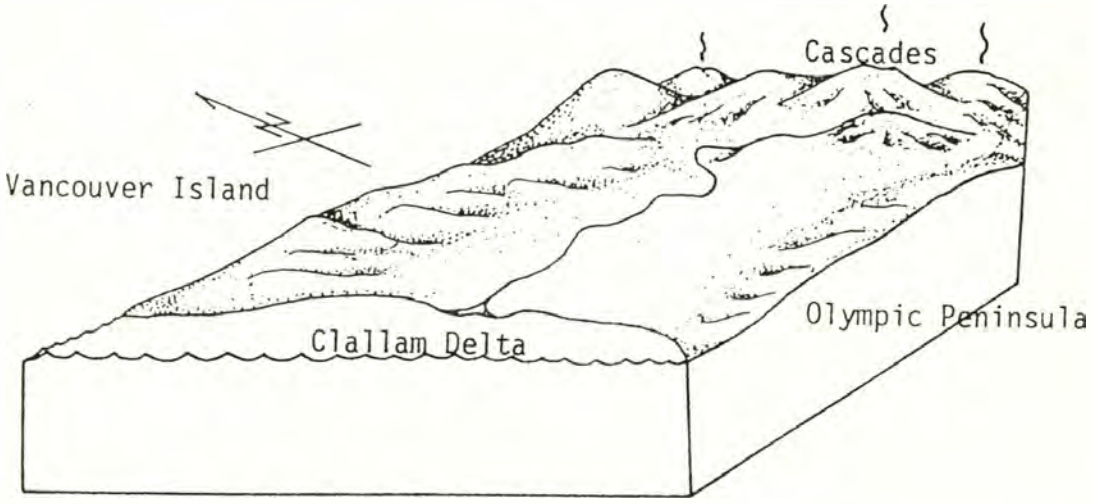


Figure 41.b. Paleogeographic reconstruction with Cascades source area. River system flowing from the east in the Cascade volcanic arc. Olympic Peninsula may have been a lowland south of the Clallam delta.

Provenance section. Other evidence is discussed below.

The location of Vancouver Island in relation to the Clallam Formation allows for a relatively simple paleogeographic reconstruction (Figure 41). With continued sediment imput from Vancouver Island, the strand line could have prograded to the southwest, from the location of the Sooke Formation on southern Vancouver Island in Late Oligocene, to a position near the Clallam Formation in the Early Miocene (Figure 40). Although the Olympic core probably was not subareally exposed until the Middle Miocene, the strand line may still have bulged slightly to the west of the Clallam and Astoria (?) Formations (Figure 40). Although storm wave deposits contained in the Clallam Formation suggest an environment influenced by ocean storm waves, a local embayment south of Vancouver Island at the time of deposition of the Clallam Formation is a possible senario. Because basalt fragments are rare in the Clallam Formation, the major stream system carrying sediment to the Clallam Formation must have been located west of the Metchosin Volcanics (Figure 41). The close proximity of Vancouver Island would have been conducive to supplying abundant coarse-grained sediment to the Clallam depositional system.

If the North Cascades or the Coast Plutonic Belt were the source for the sediment of the Clallam Formation, the probable orientation of the strand line would not change (Figure 40). The major differences would have been in the distance of sediment transport and the paleogeography of the Strait of Juan de Fuca. A fluvial system with drainage from the Cascades would have been flowing from the northeast to southeast across the Puget lowlands (Figure 41). The transport of cobble-sized material roughly 180 km from the Cascades would require a large fluvial system. Although the submature to immature textures and compositions characteristic of the

sandstones of the Clallam Formation suggest a closer source, the distance of transport from the Cascades is not prohibitive. If the Cascades were the source, the topography north of the present location of Port Angeles must have been relatively gentle, and the stream system would have flowed between Vancouver Island and the still relatively lowlying Olympic Peninsula (Figure 41). This stream system may have been roughly paralleled by another stream system feeding the Astoria (?) Formation in southwest Washington.

## Discussion of Tectonics

The structural and depositional events that affected the Olympic Peninsula are, on a broad scale, intimately tied to the relative motions and reconstructions of the Pacific, Farallon, and North American plates (Table 3). Prior to deposition of the Clallam Formation, the Pacific-Farallon-North American triple junction probably migrated to a position north of the Olympic Peninsula. This migration would have brought the Farallon plate into contact with the North American plate in the vicinity of the Olympic Peninsula (Engebretson and others, in press). From roughly 43 Ma to the Recent the Farallon (Juan de Fuca)-Pacific ridge system is estimated to have been very near the edge of North America (Engebretson, 1982; Engebretson and others, in press; Figures 42 and 43). The nearness of the ridge means that relatively young, and therefore buoyant, oceanic plate was being subducted beneath the continental margin.

The Eocene through Miocene sedimentary rocks on the northern coast of the Olympic Peninsula represent a marine regression with localized fluctuations in water depth (Addicott, 1976a). This regression may reflect the continued uplift of the Olympic Peninsula region due to the subduction of relatively young oceanic crust and the continual underplating of sedimentary packets to form the Olympic Core terrane.

TABLE 3. Timing of pre- and post-Clallam Formation events in relation to plate reconstructions.

| TIME | STATE OF PLATES | EVENTS |
|---|---|---|
| Before Clallam Formation deposition | slow down in plate motions<br><br>passage of PA-FA-NA triple junction<br><br>passage of Aja fracture zone, and possible anomalous crust | underthrusting of sediments to form core of Olympics, Eocene through Miocene<br><br>29 Ma metamorphic event in Olympic core<br><br>calc-alkaline volcanism and plutonism in North Cascades<br><br>deposition of the Sooke Formation |
| 25 Ma | | |
| During Clallam Formation deposition | | deposition of the Astoria (?) Formation<br><br>deposition of the Clallam Formation |
| 20 Ma | | |
| After Clallam Formation deposition | passage of Sedna fracture zone, and possible anomalous crust<br><br>closest proximity of PA-FA ridge, youngest subducting plate | 17 Ma metamorphic event in Olympic core<br><br>clockwise rotation of northwestern Crescent terrane<br><br>deformation of Clallam Formation<br><br>deposition of Montesano Formation (15-6 Ma)<br><br>formation of the Clallam syncline<br><br>uplift of the Clallam Formation<br><br>regional unconformity at base of Upper Miocene strata (11 Ma) |

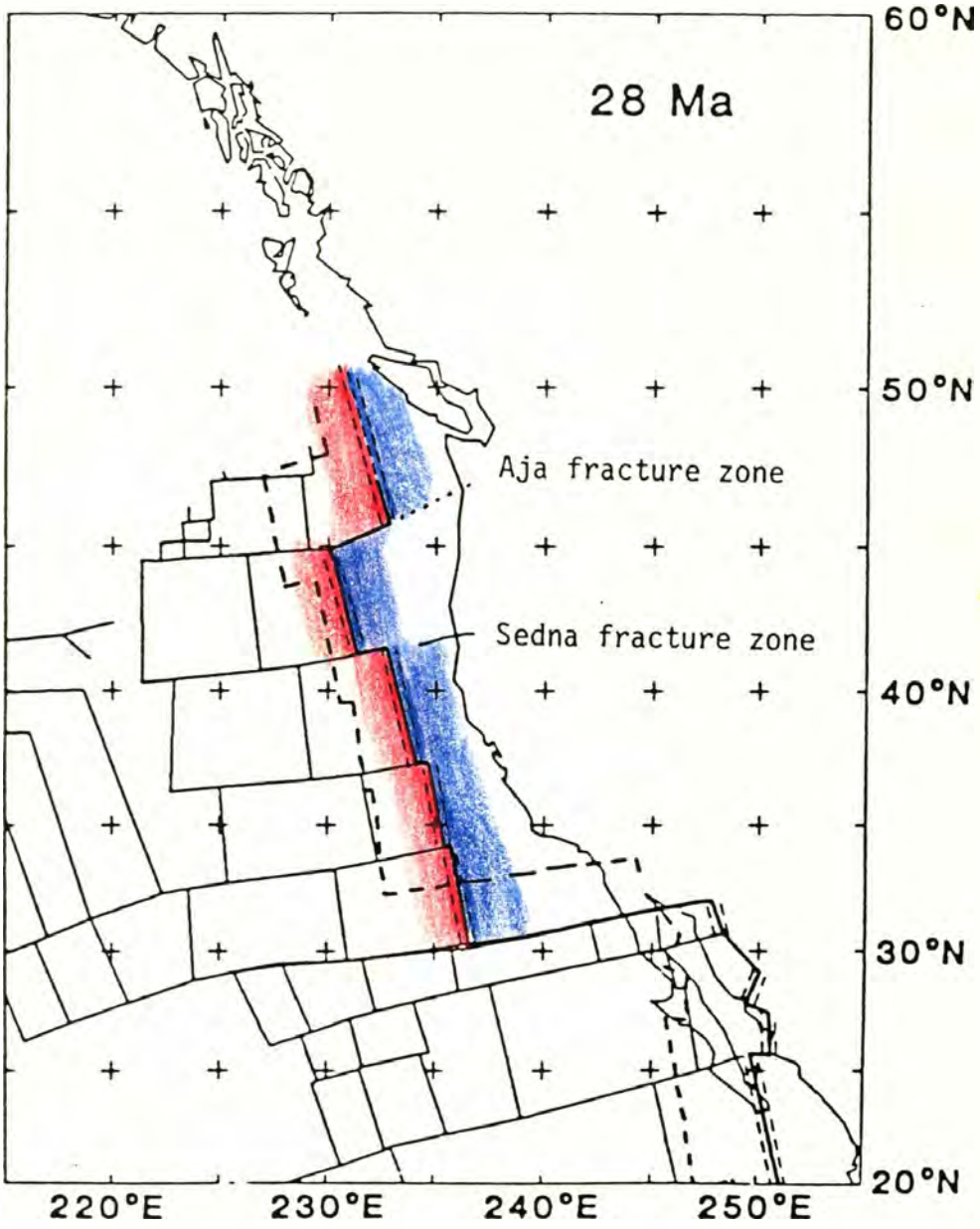


Figure 42. 28 Ma plate reconstruction of western North America and northeastern Pacific (modified from Engebretson, 1982). Pacific plate in red, Farallon plate in blue. Dotted line intersecting the Olympic Peninsula indicates inferred extension of the Aja fracture zone.

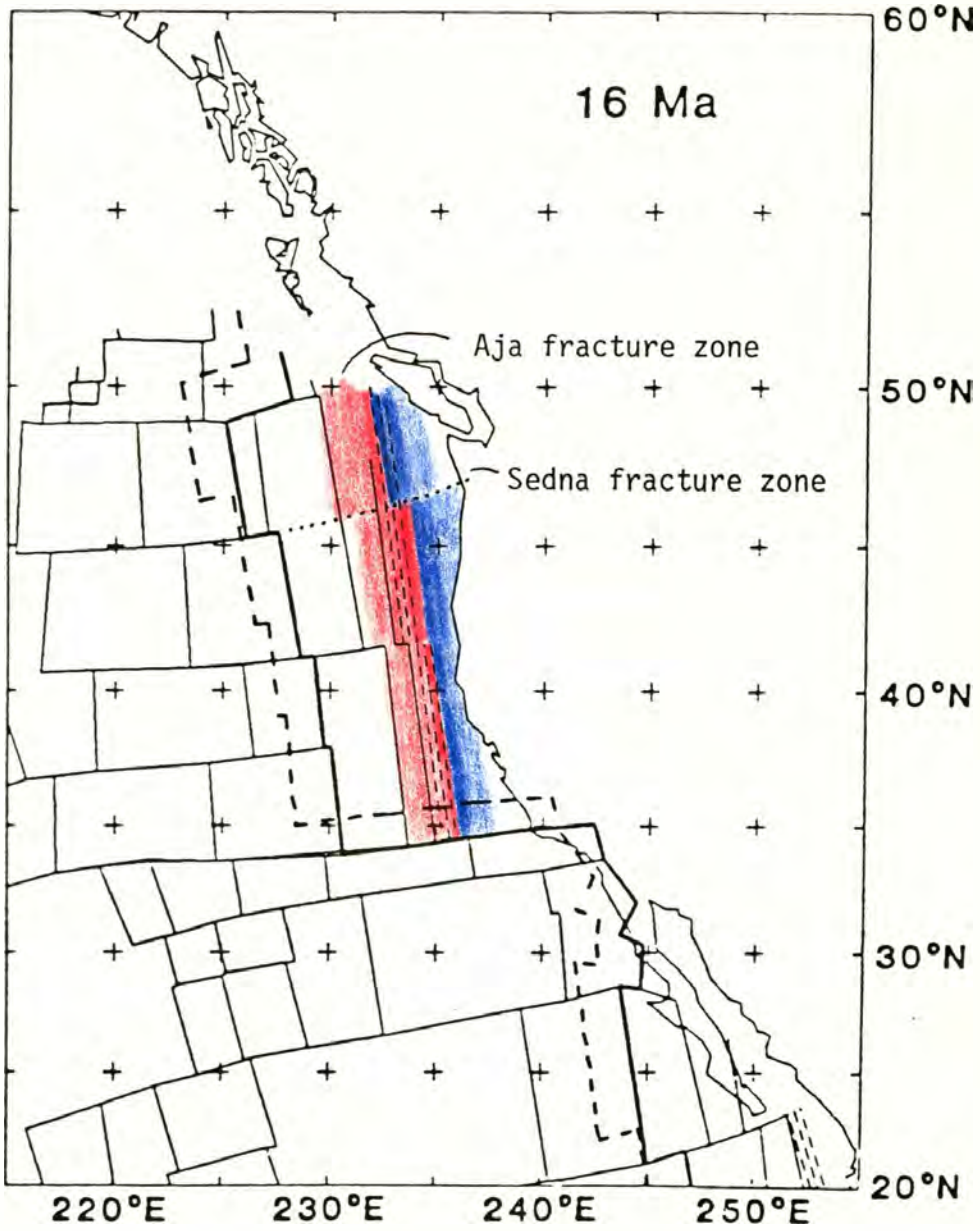


Figure 43. 16 Ma plate reconstruction of western north America and northeastern Pacific (modified from Engebretson, 1982). Pacific plate in red, Farallon plate in blue. Dotted line intersecting the Olympic Peninsula indicates inferred extension of the Sedna fracture zone.

Subsidence, uplift, and structural and metamorphic events may result from changes in the relative motion or morphology of a subducting plate. The relative velocity of the Farallon plate did not change significantly with respect to North America after about 40 Ma (Engebretson, 1982; Figure 44), so only morphologic changes in the Farallon plate could be the cause of the observed changes. The morphologic changes in the plate probably acted in conjunction with other factors such as underplating, sediment loading, and changes in eustatic sealevel to influence subsidence, uplift, and structural events.

For example, the passage of a fracture zone would bring oceanic plate of a different age into contact with the continental margin (Figure 45). Figure 42 shows plate geometries at 28 Ma when the Aja fracture zone was migrating along the Olympic Peninsula. In this reconstruction, a change from younger to older oceanic crust would occur near the study area as the fracture zone moved northward and the distance of the ridge from the North American continent was increased (Figure 42). After the passage of the fracture zone, the plate being subducted would be older and more dense than before, and subsidence of basins near the plate margin may be expected. Alternatively, if the subducting fracture zone was associated with anomalous, relatively buoyant crust the continental region would be expected to be uplifted as the buoyant feature was subducted, and then to subside as the older and more dense plate is subducted. Anomalous crust along the fracture zone may be thicknesses of basalt formed during a reorganization of plates, diapiric intrusions into the fracture zones of mantle-derived serpentinized peridotite, minor alkali basalts, and tectonized hydrothermally altered rocks (Bonatti and Honnorez, 1976), or a variety of metamorphic rock types (Fox and others, 1976). Cooling of low

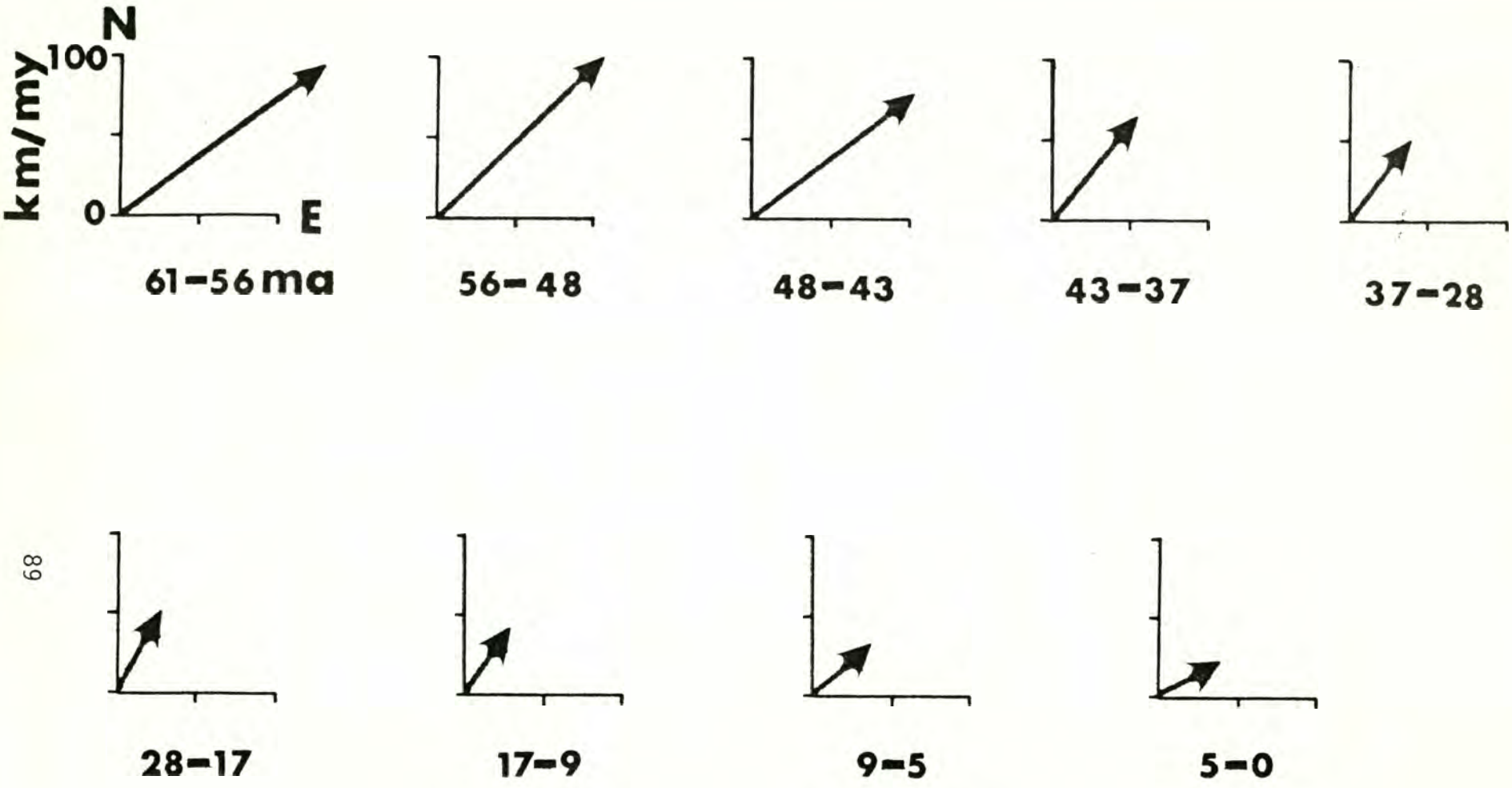


Figure 44. Relative velocity vectors for Farallon motion with respect to North America at about 48 N and 236 E longitude. Vertical and horizontal axes measure north and east components of motion respectively in km/my (model from Engebretson, 1982).

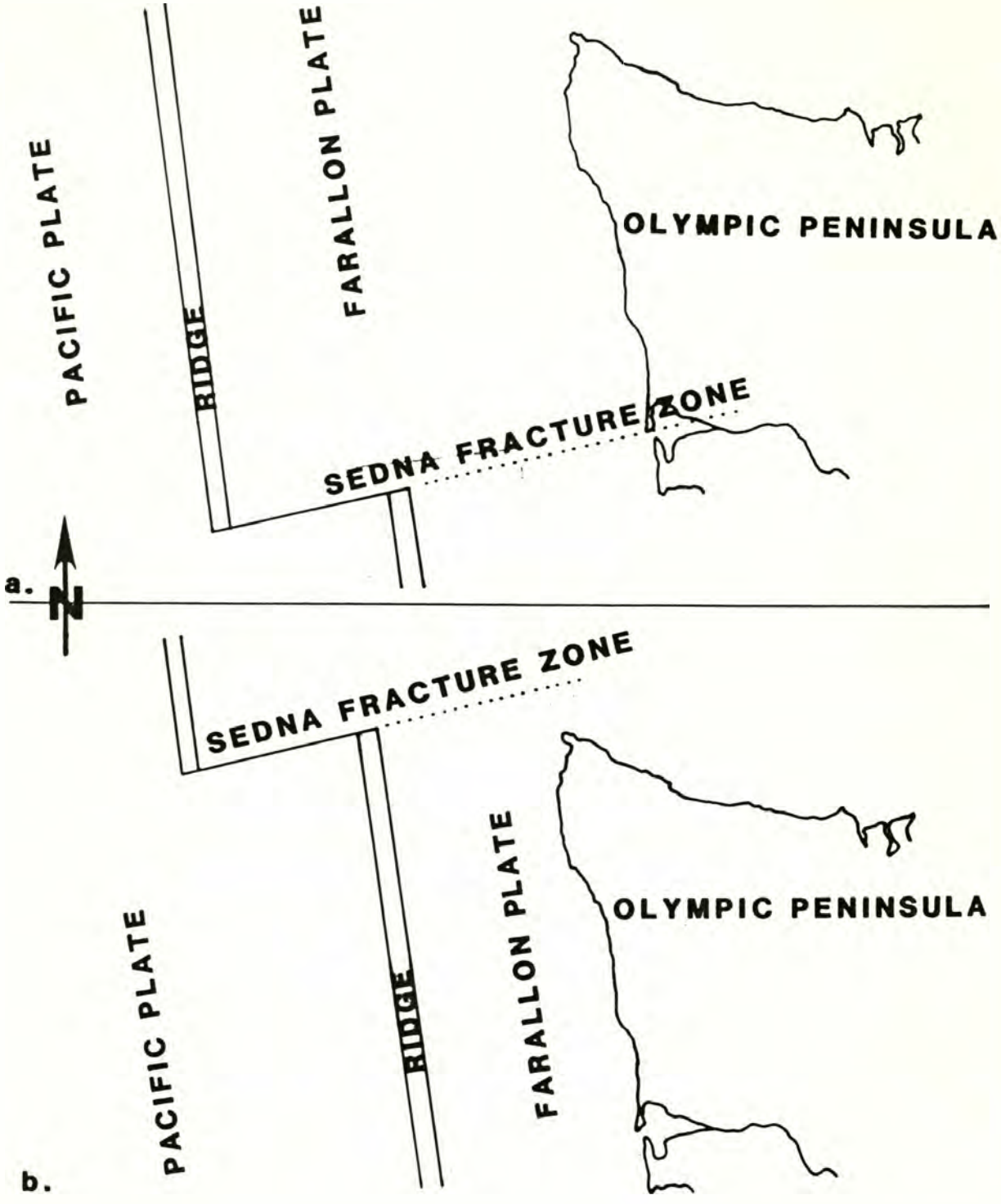


Figure 45. Northward migration of the Sedna fracture zone. Close-up of reconstruction in Figure 49. a) About 18 Ma, older, less buoyant crust being subducted. b) About 15 Ma, fracture zone migrates northward past the Olympic Peninsula, younger, more buoyant plate subducted beneath the Olympic Peninsula.

grade metamorphic rocks in the Olympic Core terrane at 29 Ma (Tabor, 1972) may reflect the temporary uplift of the Olympic Core terrane as anomalous crust on the downgoing plate was subducted.

After the deposition of the Clallam Formation, several events affected the area of the Olympic Peninsula: at 17 Ma a second period of cooling of metamorphic mineral assemblages in the Olympic core occurred (Tabor, 1972), and at 11 Ma deposition of unamed Late Miocene and Pliocene (?) sediments resumed in the area of the northern Olympic Peninsula forming a a regional unconformity (Snavely and others, 1980). Other events post dating the deposition of the Clallam Formation are the deformation of the Clallam Formation, formation of the Clallam syncline, clockwise rotation of the northern peripheral rocks, uplift of the Clallam Formation, and deposition of the Montesano Formation.

During this period of time the passage of the Sedna fracture zone, south of the Aja fracture zone (Figure 43), may have decreased the distance between the Pacific-Farallon ridge system and the Olympic Peninsula to the east. Increased coupling between the Farallon and North American plates may have been caused then by the density contrast between the older, denser subducting plate north of the fracture zone and the younger, and therefore more buoyant, subducting plate south of the fracture zone (Figure 43). Coupling between the two plates may have caused the northward rotation of the northwest end of the Crescent terrane as the fracture zone, and thus the zone of coupling migrated northward. During this period of subduction of young and buoyant plate, there may also have been an increase in the amount of sediment being obducted because of an increase in coupling at the plate boundary. The underthrusting of sediment beneath the Crescent terrane may have increased compression in the area of obduction and pushed the relatively thin northwestern part of the Crescent

terrane northward.

## A Model

Relating observed structural and depositional events to plate reconstructions is, at this point, difficult. However, a synopsis of a possible tectonic scheme follows.

43-28 Ma. The passage of the Pacific-Farallon-North American triple junction at about 43 Ma may have resulted in the implacement of the Cresent Formation volcanics (Marcott, 1984). At about this time, underthrusting of sediments to form the core of the Olympic Mountains was initiated through interaction of the Farallon and North American plates. Underthrusting continued at least through the Miocene. A slowdown in Farallon-North American convergence between 43 and 28 Ma coincided with calc-alkaline plutonism and volcanism in the Cascade Range (Wells and others, 1984).

32-20 Ma. The passage of the Aja fracture zone at about 28 Ma (Figure 42), possibly including anomalous crust, may have resulted in the uplift and cooling of metamorphic minerals in the Olympic Core terrane (Tabor, 1972). This uplift may have been followed by subsidence, resulting from the relatively older and denser oceanic crust being subducted to the south of the fracture zone. Deposition of the Sooke Formation on Vancouver Island occurred between about 32 and 25 Ma, possibly with progradation of the strand line toward the southwest. This was followed by deposition of the Clallam Formation, between 25 and 20 Ma, on the northwest Olympic Peninsula and the Astoria (?) Formation in southwest Washington between, about 25 and 15 Ma. Subsidence and

burial of the Clallam Formation followed, allowing for the compaction and eventual deformation at a later time.

20-11 Ma. Underthrusting and gradual uplift of the Olympic Core terrane continued. The passage of the Sedna fracture zone (Figure 43), possibly with anomalous crust, at about 17 Ma may have resulted in the subduction of younger, more buoyant crust beneath the Olympic Peninsula, possibly causing the clockwise rotation of the northern Crescent terrane, deformation of the Clallam Formation, uplift of the Olympic Core terrane, and subsequent cooling of metamorphic minerals in the Olympic Core terrane (Tabor, 1972). Continued uplift resulted in a regional unconformity in the Middle Miocene (about 15-11 Ma) in the north, and the initiation of Montesano Formation deposition in the south at about 15 Ma.

11 Ma-Present. Sedimentation resumed near the mouth of the Strait of Juan de Fuca in the Late Miocene (about 11 Ma)(Snavely and others, 1980). Northeast-directed compression has continued into the Recent, possibly forming the Clallam syncline and the seaward- and landward-verging thrust faults in Late Miocene to Late (?) Pleistocene sediments near the mouth of the Strait of Juan de Fuca (Muller and others, 1983).

## SUMMARY

The Lower Miocene Clallam Formation is an approximately 800 m-thick sequence of sandstone and conglomerate that was deposited in the predominantly marine portion of a prograding, wave- and fluvially-controlled delta. The Clallam Formation represents the final shallow-water phase of an Eocene to Miocene regression that is represented by a nearly continuous sequence of Eocene to Miocene sedimentary rock units. As a whole, the Clallam Formation coarsens and shallows upward. Within this general progression are several small-scale coarsening- and shallowing-upward cycles. Based on lithology, and on biogenic and other sedimentary structures, there are six lithologic facies in the upper Pysht Formation and the Clallam Formation: five in the Clallam Formation and one in the Pysht Formation. The facies differ as a result of fluctuations in the positions of distributary channels, in water depth, and in the severity of storm conditions. Grain sizes and amount of organic material increase towards distributary mouths. The repeated shallowing- and coarsening-upward cycles reflect the occupation and subsequent abandonment of distributary channels. As the distributary channel prograded, the input of sediment was large; but, as the distributary channel overextended itself, a breech caused abandonment of the channel. The abandoned distributary mouth area subsided. Later, relatively deeper water sediments were deposited. As the whole delta region prograded, the distributary mouth deposits and the overlying sediments were deposited in progressively shallower water.

Petrographic and petrologic studies of the Clallam Formation indicate that depositional facies control grain composition. Sediment from Facies 1 through 4 contains fewer lithic grains than sediment from Facies 5. These differences between Facies 1 through 4 and Facies 5 are a function of

varying depositional regimes, the relative grain sizes, the effects of diagenesis, or a combination thereof. Lithic fragments, especially portions of fragments with aphanitic groundmasses, are selectively broken down in high energy environments, such as those in Facies 1 through 4, resulting in the lower lithic counts in those Facies. During calcite cementation of the Clallam Formation, fine-grained lithic fragments were selectively replaced by calcite. Although calcite cement occurs in some samples from Facies 5, its effect on their modal compositions is negligible; because none of the grains in these coarse-grained sandstones have been completely replaced by calcite. Thus they can still be identified. The compositional differences between concretionary and nonconcretionary fine-grained samples is less than the compositional differences between samples from different facies, so most of the change in composition is the result of depositional mechanisms rather than of diagenetic effects.

The Clallam Formation petrology suggests that source rocks were of four different types: andesitic to dacitic volcanic rocks, chert, metamorphic rocks, and plutonic rocks. Volcanic rock fragments, chert, and metamorphic rock fragments appear in the sandstones of the Clallam Formation as lithic grains, and plutonic rocks are apparent in modal grain distributions as abundant quartz, plagioclase, hornblende, diorite, and minor amounts of potassium feldspar, which suggest a quartz monzonite to granodiorite composition for the plutonic source rocks. Point-count data plotted on ternary diagrams suggest a magmatic arc provenance and, less convincingly, a subduction complex provenance (following the parameters set forth by Dickinson and Suczek, 1979). The samples from a magmatic arc source area contain abundant intermediate volcanic lithics, while those that show

subduction complex affinity contain abundant chert fragments.

Several possible source areas nearby today are suggested by petrographic and petrologic studies. The three most likely source areas appear to be Vancouver Island, the Cascades, and the San Juan Islands.

The depositional and structural events of the Olympic Peninsula are intimately tied to the relative motions and reconstructions of the Pacific, Farallon, and North American plates. Prior to deposition of the Clallam Formation, the Pacific-Farallon-North American triple junction migrated from south of the Olympic Peninsula to a position north of the Olympic Peninsula. During and after deposition of the Clallam Formation, the Farallon plate interacted with the North American plate in the vicinity of the Olympic Peninsula. Basin subsidence, uplift, and the structural and metamorphic events that occurred after about 40 Ma were probably the result of changes in the morphology of the subducting Farallon plate rather than changes in its relative velocity. Morphologic changes could have occurred at fracture zones. If the passage of a fracture zone brings older, denser crust into contact with a continental margin, subsidence may be expected. In contrast, if the passage of a fracture zone brings younger, more buoyant crust into contact with the continental margin, subduction would be more difficult and an increase in compression and resulting uplift might be expected. The passage of two fracture zones, the Aja at about 28 Ma and the Sedna at about 16 Ma, may have influenced the structural and depositional events in the vicinity of the Olympic Peninsula.

## REFERENCES CITED


Addicott, W. D., 1975, Provincial age and correlation of the Clallam Formation, northwestern Washington: Geological Society of America Abstracts with Programs, v. 7, no. 3, p. 289.

Addicott, W. D., 1976a, New Molluscan assemblages from the upper member of the Twin River Formation, western Washington: Significance in Neogene biostratigraphy: United States Geological Survey Journal of Research, v. 4, p. 437-447, 7 figures.

Addicott, W. D., 1976b, Molluscan Paleontology of the Lower Miocene Clallam Formation, northwestern Washington: United States Geological Survey Professional Paper 976, 44 p., 9 pls.

Armentrout, J. M., 1983, Mineralogic terrains and tectonic timing--Quimper Peninsula, northeast Olympic Peninsula, Washington (abst.): Pacific Northwest Regional Meeting, American Geophysical Union, Program with Abstracts, p. 8.

Armentrout, J. M., Hull, D. A., Beaulieu, J. D., and Rau W. W., 1983, Corrlelation of Cenozoic stratigraphic units of western Oregon and Washington: State of Oregon Department of Geology and Mineral Industries, Oil and Gas Investigation 7, 90 p.

Arnold, R., 1905, Coal in Clallam County, Washington: United States Geological Survey Bulletin 260, p. 413-421.

Arnold, R., 1906, Geological reconnaissance of the coast of the Olympic Peninsula, Washington: Geological Society of America Bulletin, v. 17, p. 451-468, 1 map.

Arnold, R., 1909, Paleontology of the Coalinga district, Fresno and Dings Counties, California: United States Geological Survey Bulletin 396, 173 p., 30 pls.

Arnold, R., and Hannibal, H., 1913, The marine Tertiary stratigraphy of the north Pacific Coast of America: American Philosophical Society Proceedings, v. 52, no. 212, p. 559-605.

Ashley, G. M., Southard, J. B., and Boothroyd, J. C., 1982, Deposition of climbing-ripple beds: a flume simulation: Sedimentology, v. 29, p. 67-79.

Bonatti, E., and Honnorez, J., 1976, Sections of the Earth's crust in the equatorial Atlantic: Journal of Geophysical Research, v. 81, no. 23, p. 4104-4119.

Bourgeois, J., 1980, A transgressive shelf sequence exhibiting hummocky stratification: The Cape Sebastian Sandstone (Upper Cretaceous), southwestern Oregon: Journal of Sedimentary Petrology, v. 50, p. 681-702.

Brandon, M. T., Cowan, D. S., Muller, J. E., and Vance, J. A., 1983, Pre-Tertiary geology of San Juan Islands, Washington, and southeast Vancouver Island, British Columbia: Geological Association of Canada, Mineralogical Association of Canada, and Canadian Geophysical Union Joint Annual Meeting, Field Trip No. 5, 65 p.

Brown, R., 1870, On the geographical distribution and physical characteristics of the North Pacific Coast: Edinburgh Geological Society Trans., v. 1, p. 305-325.

Clifton, H. E., 1981, Progradational sequences in Miocene Shoreline deposits, southeastern Caliente Range, California: Journal of Sedimentary Petrology, v. 51, p. 165-184.

Corbett, K. D., 1972, Features of thick-bedded sandstones in a proximal flysch sequence, Upper Cambrian, southwest Tasmania: Sedimentology, v. 19, p. 99-114.

Dall, W. H., 1922, Fossils of the Olympic Peninsula (Washington): American Journal of Science, ser. 5, v. 4, p. 305-314.

Dickinson, W. R., 1970, Interpreting detrital modes of graywacke and arkose: Journal of Sedimentary Petrology, v. 40, p. 695-707.

Dickinson, W. R., and Suczek, C. A., 1979, Plate tectonics and sandstone compositions: American Association of Petroleum Geologists Bulletin, v. 63, p. 2164-2182.

Dott, R. H., 1964, Wacke, graywacke and matrix-what approach to immature sandstone classification?: Journal of Sedimentary Petrology, v. 34, p. 625-632.

Dott, R. H., Jr., and Bourgeois, J., 1980, Hummocky cross stratification-Importance of variable bedding sequences analogous to the Bouma sequence ¼abs. : Geological Society of America Abstracts with Programs, v. 11, p. 414.

Dott, R. H., Jr., and Bourgeois, J., 1982, Hummocky stratification: Significance of its variable bedding sequences: Geological Society of America Bulletin, v. 93, p. 663-680.

Durham, J. W., 1944, Megafaunal zones of the Oligocene of northwestern Washington: California University Publications, Department of Geological Sciences Bulletin, vo 27, no. 5, p. 101-211, pls. 13-18.

Engebretson, D. C., 1982, Relative motions between oceanic and continental plates in the Pacific Basin: Ph.D. thesis, Stanford University, Stanford California, 211 p.

Engebretson, D. C., Gordon R. G., and Cox, A., in press, Relative motions between oceanic and continental plates in the Pacific basin: Geological Society of America Special Paper.

Etherington, T. J., 1931, Stratigraphy and fauna of the Astoria Miocene of southwest Washington: California University Publications, Department of Geological Science Bulletin, v. 20, no. 5, p. 31-42, 14 pls.

Fairchild, S. H., 1979, The Leech River unit and Leech River fault, southern Vancouver Island, British Columbia: unpublished M.S. thesis, University of Washington, 170 p.

Fairchild, S. H., and Cowan, D. S., 1982, Structure, petrology, and tectonic history of the Leech River complex northwest of Victoria, Vancouver Island; Canadian Jounal of Earth Sciences, v. 19, p. 1817-1835.

Fox, P. J., Schreiber, E., Rowlett, H., and McCamy, K, 1976, The geology of the Oceanographer fracture zone: A model for fracture zones: Journal of Geophysical Research, v. 81, no. 23, p. 4117-4128.

Gillman, S. C., 1896, The Olympic Country: National Geographic Magazine, v. 7, p. 133-140.

Gower, H. D., 1960, Geologic map of the Pysht quadrangle, Washington: United States Geological Survey Geological Survey Quadrangle Map GQ-120, scale 1:62,500.

Gower, H. D., Yount, J. C., and Crosson, R. S., 1978, Seismotectonic map of the Puget Sound region, Washington: United States Geological Survey Miscellaneous Geologic Investigations Map.

Gresens, R. L., 1982, Early Cenozoic geology of central Washington state: 1. Summary of sedimentary, igneous, and tectonic events: Northwest Science, v. 56, no. 3, p. 218-229.

Harms, J. C., Spearing, D. R., Southard, J. B., and Walker, R. G., 1975 Depositional environments as interpreted from primary sedimentary structures and stratification sequences: Society of Economic Paleontologists and Mineralogists, Short Course Notes, no. 2, 161 p.

Hertlein, L. G., and Crickmay, C. H., 1925, Marine Tertiary of Oregon and Washington: American Philosophical Society Proceedings, v. 64. no.2, p. 245, 261-264.

Hunter, R. E., and Clifton, H. E., 1982, Cyclic deposits and hummocky cross stratification of probable storm origin in Upper Cretaceous rocks of the Cape Sebastian area, southwestern Oregon: Journal of Sedimentary Petrology, v. 52, p. 127-143.

Ingersoll, R. V., Bullard, T. F., Ford, R. L., Grimm, J. P., Pickle, J. D., and Sares, S. W., 1984, The effect of grain size on detrital modes: A test of the Gazzi-Dickinson point-counting method: Journal of Sedimentary Petrology, v. 54, no. 1, p. 103-116.

Ingersoll, R. V., and Suczek, C. A., 1979, Petrology and provenance of Neogene sand from Nicobar and Bengal Fans, DSDP sites 211 and 218: Journal of Sedimentary Petrology, v. 49, p. 1217-1228.

Kleinpell, R. M., 1938, Miocene stratigraphy of California: Tulsa, Oklahoma, American Association of Petroleum Geologists, 450 p.

Landes, H., 1901, Annual Report: Washington Geological Survey, v. 1, p. 279-281.

Leithold, E. L., and Bourgeois, J., 1984, Characteristics of coarse-grained sequences deposited in nearshore, wave-dominated environments-- examples from the Miocene of southwest Oregon: Sedimentology, v. 31, p. 749-775.

Mackin, J. H., and Cary, A. S., 1965, Origin of Cascade landscapes: Washington Division of Mines and Geology, Information Circular 41, 35 p.

MacLeod, N. S., Tiffin, D. L., Snavely, P. D., Jr., and Currie, R. G., 1977, Geologic interpretation of magnetic and gravity anomalies in the Strait of Juan de Fuca, U.S.-Canada: Canadian Journal of Earth Sciences, v. 14, p. 223-238.

Marcott, K., 1984, The sedimentary petrography, depositional environment and tectonic setting of the Aldwell Formation, northern Olympic Peninsula, Washington: M.S. thesis, Western Washington University, Bellingham Washington, 78 p.

Misch, P., 1977, Bedrock geology of the north Cascades: in Brown, E. H., and Ellis, R. C., eds., Geological Excursions in the Pacific Northwest: Western Washington University Publication, p. 1-63.

Moore, D. G., and Scruton, P. C., 1957, Minor internal sedimentary structures of some Recent unconsolidated sediments: American Association of Petroleum Geologists Bulletin 41, p. 2723-2751.

Moore, E. J., 1963, Miocene molluscs from the Astoria Formation in Oregon: United States Geological Survey Professional Paper 419, 109 p.

Monger, J. W. H., Price R. A., and Tempelman-Kluit, D. J., 1982, Tectonic accretion and the origin of the two major metamorphic and plutonic welts in the Candian Cordillera: Geology, v. 10. p. 70-75.

Moyer, R. D., Engebretson, D. C., Young, M. N., and Beck, M. E., Jr., 1985, Paleomagnetic and structural evidence for differential rotation of the northern Olympic Peninsula, Washington: in abstracts with Programs, v. 17, no. 6.

Muller, J. E., 1973, Geology of Pacific Rim National Park: in Report of Activities, April to October 1972, Geological Survey of Canada, Paper 73-1A, p. 29-37.

Muller, J. E., 1982, Geology of Nitinat Lake map area: Geological Survey of Canada, Open File Map 821, scale 1:125,000.

Muller, J. E., Snavely, P. D., Jr., and Tabor, R. W., 1983, The Tertiary Olympic terrane, southwest Vancouver Island and northwest Washington (Field Trip Guide): Geological Association of Canada, Victoria, 59 p.

Pacht, J. A., 1984, Petrologic evolution and paleogeography of the Late Cretaceous Nanaimo Basin, Washington and British Columbia: Implications for Cretaceous tectonics: Geological Society of America Bulletin, v. 95, p. 766-778, 15 figs., 3 tables.

Pearl, J. E., 1977, Petrology of Tertiary sedimentary rocks in the northernmost part of the Olympic Peninsula, Washington: San Jose State University, San Jose, California, M.S. thesis, 91 p.

Pettijohn, F.J., Potter, P. E., and Siever, R., 1973, Sand and sandstone: Springer-Verlag, New York-Heidelberg-Berlin, p. 372-373, 618 p.

Piper, D. J. W., and Normark, W. R., 1971,Re-examination of a Miocene deep-sea fan and fan-valley, Southern California: Geological Society of America, Bulletin, v. 82, p. 1823-1830.

Rau, W. W., 1964, Foraminifera from the northern Olympic Peninsula, Washington: United States Geological Survey Professional Paper 374-G, p. G1-G33.

Reagan, A. B., 1909, Some notes on the Olympic Peninsula, Washington: Kansas Academy of Science Trans., v. 22, p. 131-238, 6 pls.

Reineck, H. E., and Singh, I. B., 1972, Genesis of laminated sand and graded rhythmites in storm-sand layers of shelf mud: Sedimentology, v. 18, p. 123-128.

Reineck, H. E., and Singh, I. B., 1980, Depositional sedimentary environments: New York, N. Y., Springer-Verlag, 549 p.

Silberling, N. J., Jones, D. L., Blake, M. C., Jr., and Howell, D. G., 1984, Lithotectonic terrane maps of the North American Cordillera, in Silberling, N. J., and Jones, D. L., eds., Lithotectonic terrane maps of the North American Cordillera: United States Geological Survey Open-File Report 84-523, p. C1-C43.

Snavely, P. D., Jr., Niem, A. R., MacLeod, N. S., Pearl, J. E., and Rau, W. W., 1980, Makah Formation--a deep marginal basin sedimentary sequence of late Eocene and Oligocene age in the northwestern Olympic Peninsula, Washington: United States Geological Survey Professional Paper 1162-B, 28 p.

Stirton, R. A., 1960, A marine carnivore from the Clallam Miocene formation, Washington, its correlation with nonmarine faunas: California University Publications Geological Science, v. 36, no. 7, p. 345-368.

Snavely, P. D., Jr., and Wagner, H. C., 1982, Geologic cross section across the continental margin of southwestern Washington: United States Geological Survey Open-File Report 82-459, 10 p.

Tabor, R. W., 1972, Age of the Olympic metamorphism, Washington--K-Ar dating of low-grade metamorphic rocks: Geological Society of America Bulletin, v. 83, p. 1805-1816.

Tabor, R. W., and Cady, W. M., 1978a, The structure of the Olympic Mountains, Washington--Analysis of a subduction zone: U. S. Geological Society Professional Paper 1033, 38 p.

Tabor, R. W., and Cady, W. M., 1978b, Geologic map of the Olympic Peninsula: Map 8-994, United States Geological Survey, Reston, Virginia.

Tabor, R. W., Frizzell, V. A., Jr., Vance, J. A., and Naeser, C. W., 1984, Ages and stratigraphy of lower and middle Tertiary sedimentary and volcanic rocks of the central Cascades, Washington: Application to the tectonic history of the Straight Creek fault: Geological Society of America Bulletin, v. 95, p. 26-44, 9 figs., 2 tables.

Tennyson, M. E., and Cole, M. R., 1978, Tectonic significance of Upper Mesozoic Methow-Pasayten sequence, northeastern Cascade range, Washington and British Columbia, in Howell, D. G., and McDougal, K. A., eds., Mesozoic paleogeography of the western United States: Society of Economic Paleontologists and Mineralogists Pacific Coast Paleogeography Symposium 2, 573 p.

Vail, P. R., Mitchum, R. M., Jr., and Thompson, S., III, 1977, Global cycles of relative changes of sea level, in Payton, C. E., ed., Seismic stratigraphy- applications to hydrocarbon exploration: American Association of Petroleum Geologists Memoir 26, p. 83-98.

Walker, R. G., and Mutti, E., 1973, Turbidite facies and facies associations, in Middleton, G. V., ed., Turbidites and deep-water sedimentation: Short course notes, Pacific Section, Society of Economic Paleontologists and Mineralogists, p. 119-157.

Weaver, C. E., 1912, A preliminary report on the Tertiary paleontology of western Washington: Washington Geological Survey Bulletin 15, 80 p., 15 pls.

Weaver, C. E., 1916a, The Tertiary formations of western Washington: Washington Geological Survey Bulletin 13, 327 p.

Weaver, C. E., 1916b, Tertiary faunal horizons of western Washington: Washington University Publications Geology, v. 1, p. 1-67, pls. 1-5.

Weaver, C. E., 1937, Tertiary stratigraphy of western Washington and northwestern Oregon: Washington University Publications Geology, v. 4, 266 p.

Wells, R. E., Engebretson, D. C., Snavely, P. D., Jr., and Coe, R. S., 1984, Cenozoic plate motions and the volcano-tectonic evolution of western Oregon and Washington: Tectonics, v. 3, no. 2, p. 275-294.

Whetten, J. T., Jones, D. L., Cowan, D. S., and Zartman, R. E., 1978, Ages of Mesozoic terranes in the San Juan Islands, Washington, in Howell, D. G., ed., Mesozoic paleogeography of the Western United States: Pacific Coast Paleogeography Symposium No. 2, Society of Economic Paleontologists and Mineralogists, p. 117-132.

Wolfe, E. W., and McKee, E. H., 1972, Sedimentary and igneous rocks of the Grays River quadrangle, Washington: United States Geological Survey Bulletin 1335, 70 p.

APPENDIX 1: Description and discussion of grain categories.

Monocrystalline Grains

Qm: Monocrystalline Quartz. Monocrystalline quartz shows both undulose and straight extinction. A plutonic source is indicated by assemblages of quartz, plagioclase, hornblende, and biotite (Figure 46). Crystals of quartz were not found in the volcanic lithics, nor were embayed quartz grains observed. Vacuole-rich quartz, suggesting a hydrothermal vein source, constitutes a minor portion of the grain population.

P: Plagioclase Feldspar. The compositon of the plagioclase grains was determined using the A-normal method and the Michel-Levy statistical method. The Michel-Levy method was only used on lithic grains containing enough plagioclase laths to obtain a statistically accurate composition.

The plagioclase crystals exist in three forms: 1) altered individual grains, 2) fresh individual grains (Figure 47), and 3) grains contained in volcanics (Figure 48) and other lithic fragments. The altered plagioclase is albitic. Either these grains were originally albite that became weathered or metamorphosed, or they were albitized and then altered. The fresh plagioclase grains exhibit two compositional ranges: those in the oligoclase to albite range, and those in the andesine to labradorite range. The former are probably plutonic or volcanic in origin, and the latter probably volcanic in origin. Plagioclase grains in the volcanic fragments constitute the majority of lithic-hosted plagioclase. Such grains range in compositon from albite to labradorite, but the vast majority are in the oligoclase to andesine range. Plagioclase also exists in metamorphic aggregates and plutonic fragments containing potassium feldspar, hornblende, and biotite. Both twinned and untwinned varieties of plagioclase occur. Normally zoned plagioclase is common in the volcanic

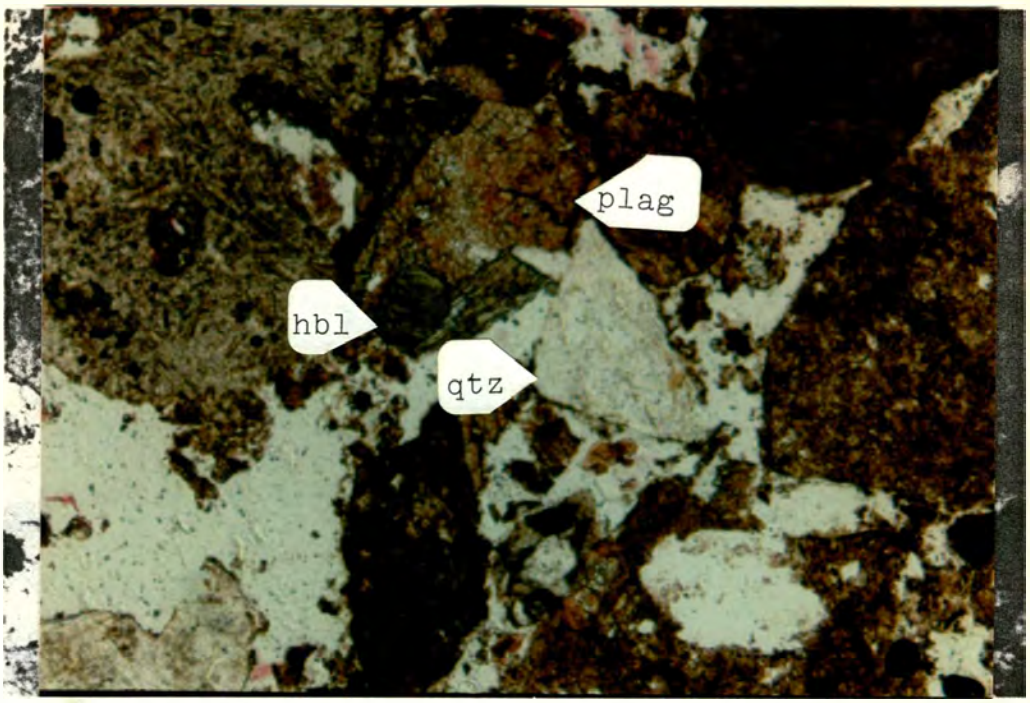


Figure 46.a. Assemblage of quartz (qtz), plagioclase (plag), and hornblende (hbl). Sample 32-11-32-9. Field of view 2.1 x 1.5 mm. Plain light.

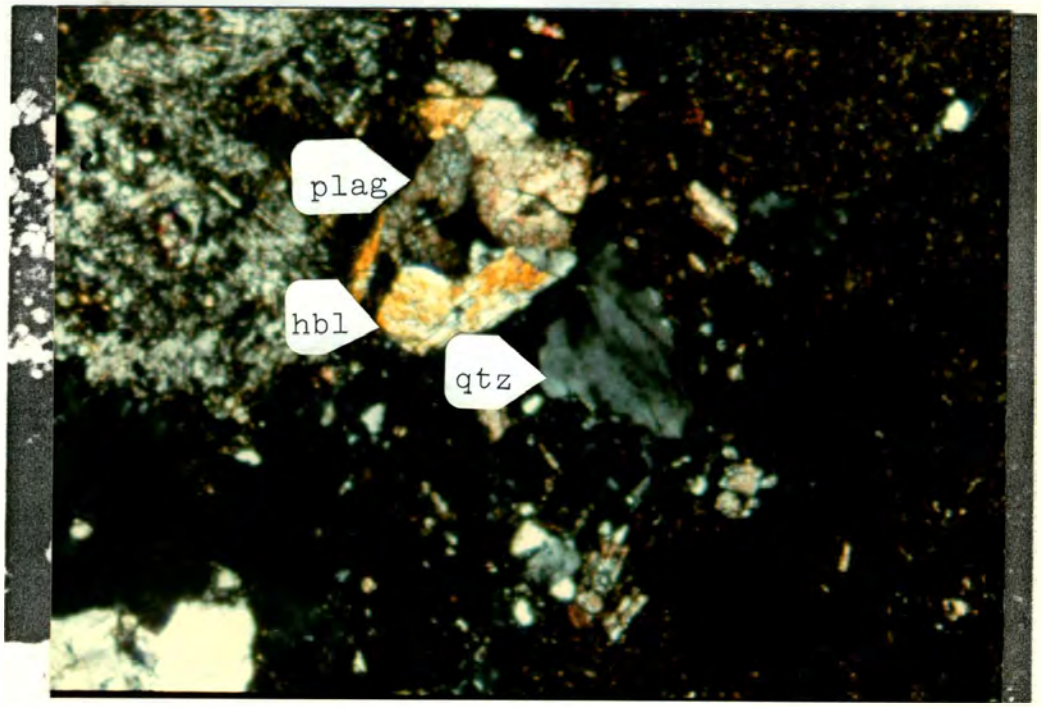


Figure 46.b. Assemblage of quartz (qtz), plagioclase (plag), and hornblende (hbl). Sample 32-11-32-9. Field of view 2.1 x 1.5 mm. Polarized light.

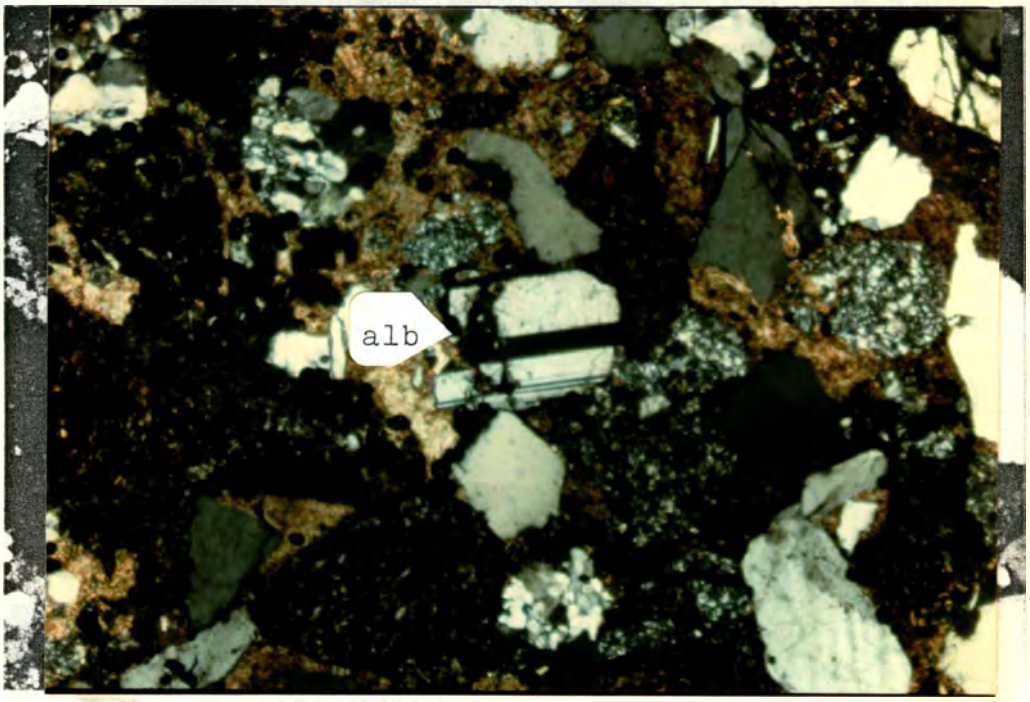


Figure 47. Euhedral fresh albite (alb). Sample 32-11-30-2. Field of view 2.7 x 1.8 mm.

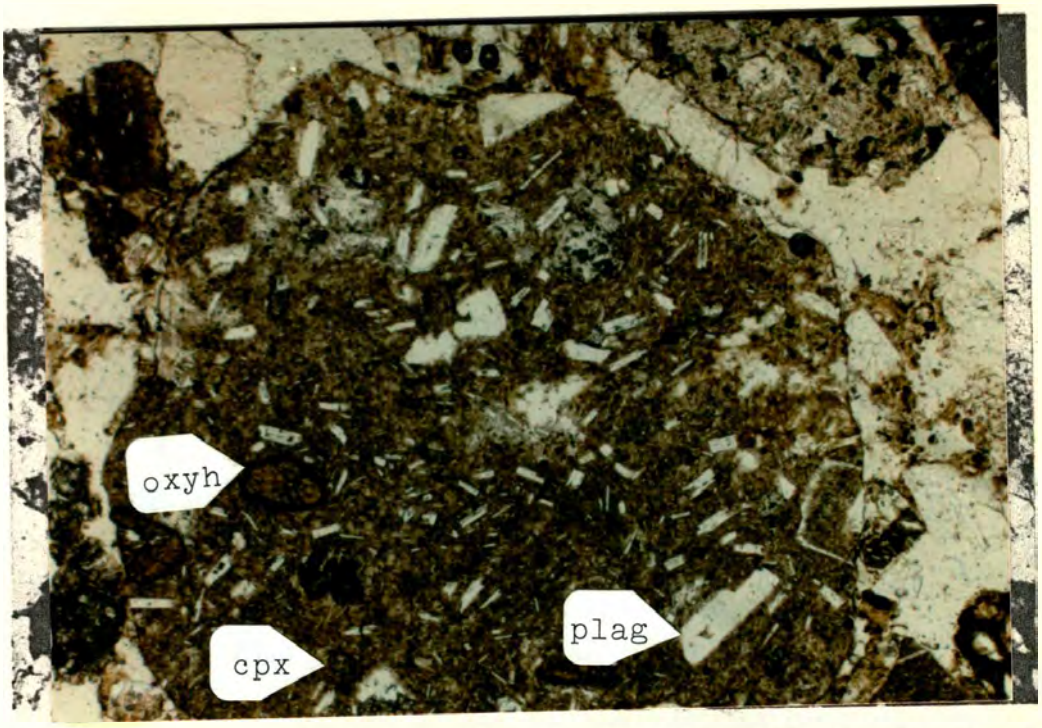


Figure 48. a. Andesitic volcanic lithic with fresh plagioclase (plag), clinopyroxene (cpx), and oxyhornblende (oxyh). Sample 32-11-32-9. field of view 3.4 x 2.3 mm. Plain light.

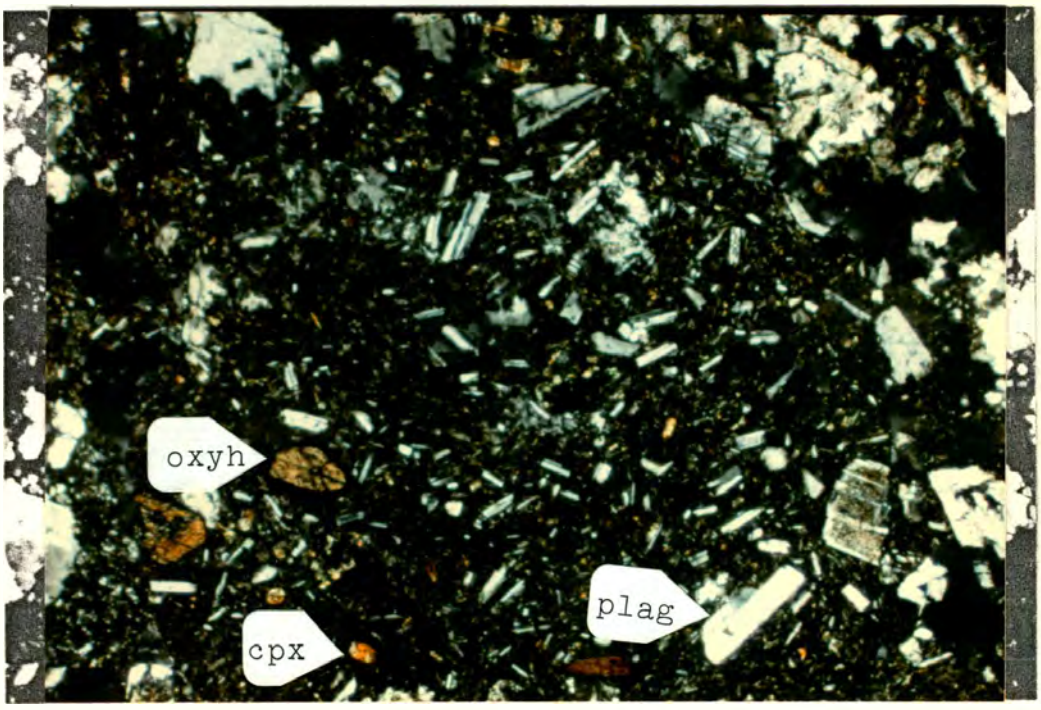


Figure 48.b. Andesitic volcanic lithic with mostly plagioclase (plag), clinopyroxene (cpx), and oxyhornblende (oxyh). Sample 32-11-32-9. Field of view 3.4 x 2.3 mm. Polarized light.

fragments.

K: Potassium Feldspar. Very little potassium feldspar is present in the samples. Most of it is oligoclase, but some microcline is present. Most of the grains are fresh. These stain yellow when treated with sodium cobaltinitrite (Figure 49). Although most potassium feldspar grains are individual, a plutonic origin is suggested by their occasional association with plagioclase or quartz.

Mafics. The primary mafic minerals are believed to have come largely from plutonic and metamorphic sources, because the mafics in the volcanic fragments have been completely altered to chlorite and clays (Figure 50). The most common mafic minerals counted were hornblende, chlorite, epidote, and biotite (Figures 51,52 and 53). Olivine being altered to chlorite, carbonate, and opaques, pyrite, hematite, garnet, zoesite, and augite are also present.

Matrix. The terminology for matrix types is after Dickinson (1970). Samples that do not contain calcite cement display psuedomatrix, protomatrix, orthomatrix, and epimatrix. Epimatrix is the least common.

Cement. Although calcite cement is present in both nonconcretionary and concretionary samples, concretionary samples contain significantly more calcite (Figures 54 and 55). When calcite cement exceeds 30 percent, it has probably replaced some detrital grains. However, differences among grain populations appear to be more closely related to grain size than to the relative amounts of calcite cementation. If a partially-altered grain could be identified, it was counted as the appropriate lithic (Figure 38). Most samples contain calcite cement, but a few are cemented by hematite (Figure 56) or have a clay matrix (Figure 57).

Misc.: Miscellaneous Grains. Grains of unknown identity or grains that fit in none of the above categories are included here. Organic matter and

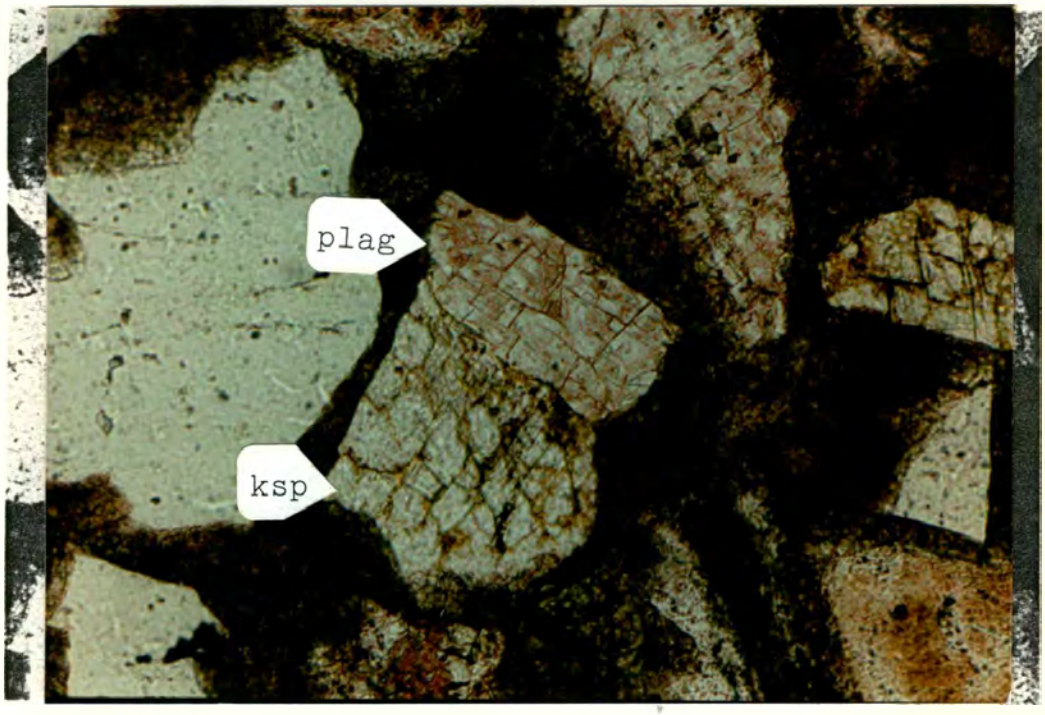


Figure 49. Yellow sodium cobaltinitrite stain in potassium feldspar (ksp), and pink amaranth stain in plagioclase (plag). Sample 32-11-31-1. field of view .85 x .58 mm. Polarized light.

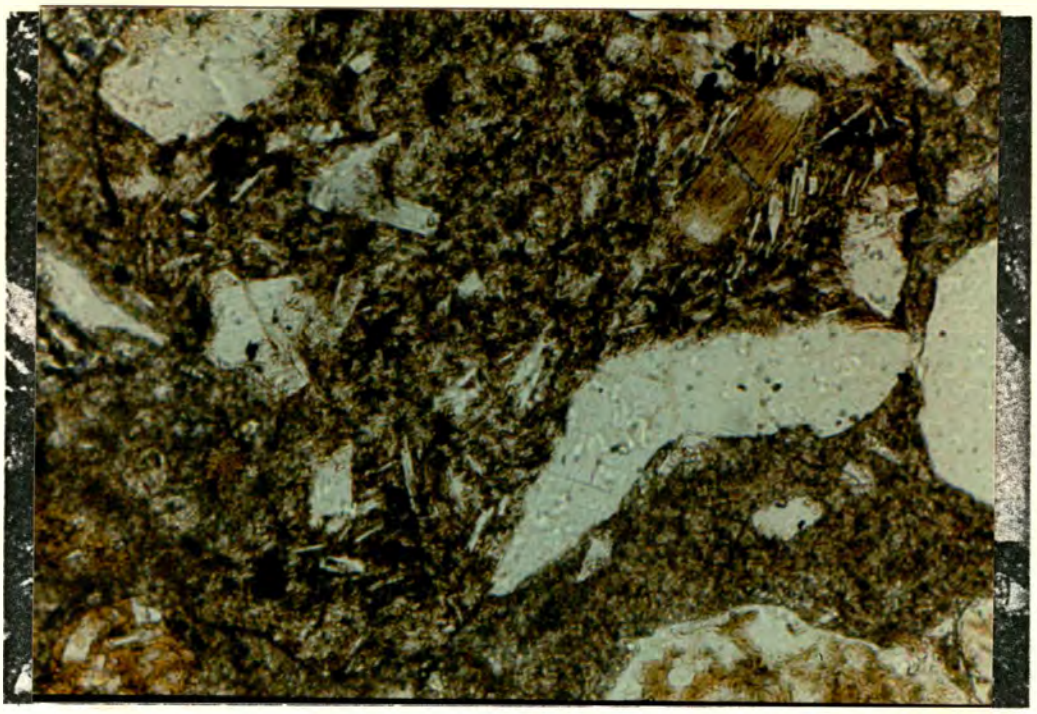

Figure 50.a. Mafics in volcanics altered to chlorite and clay. Sample 32-11-32-8. Field of view .85 x .58 mm. Plain light.

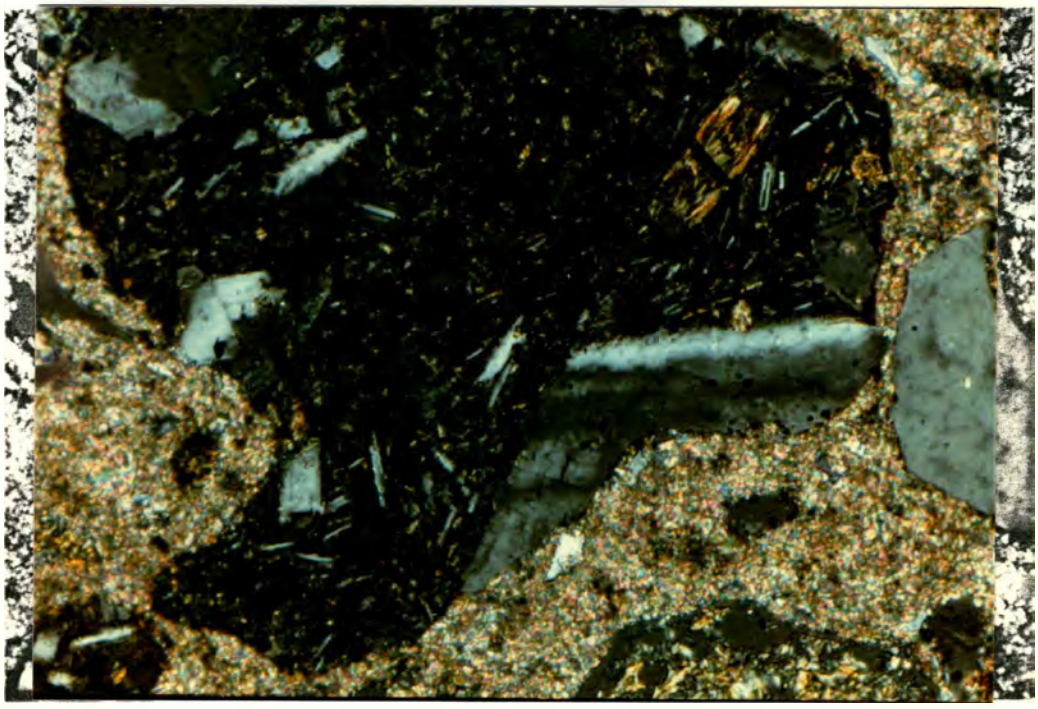

Figure 50.b. Mafics in volcanics altered to chlorite and clay. Sample 32-11-32-8. Field of view .85 x .58 mm. Polarized light.

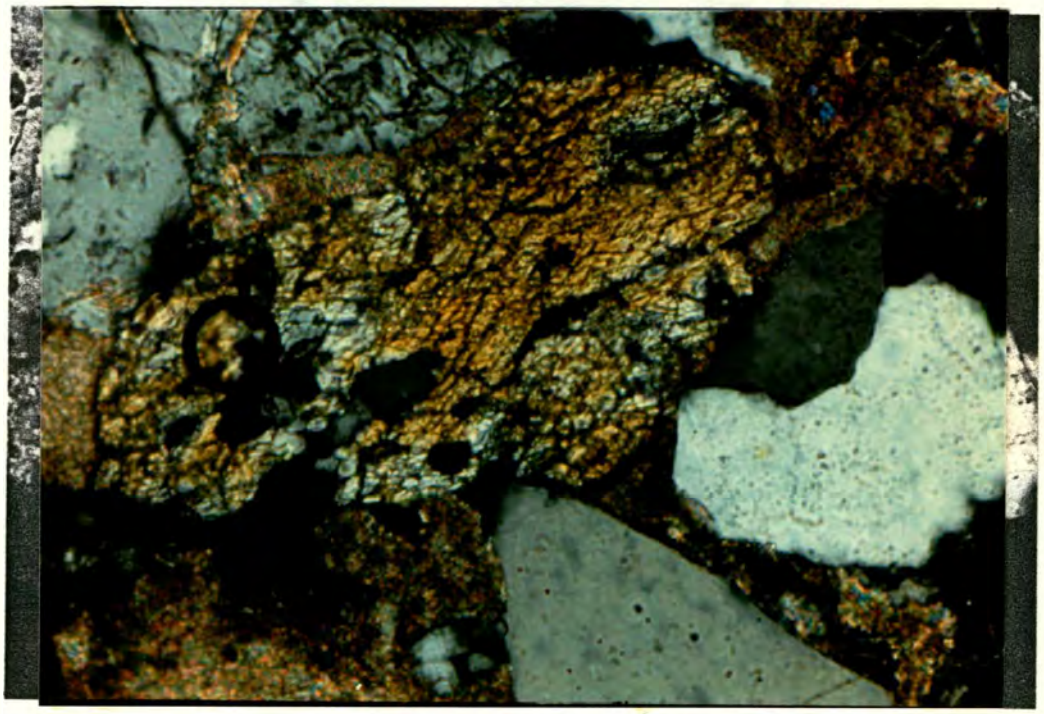

Figure 51. Hornblende grain. Samples 32-11-32-6. field of view .85 x .58 mm.

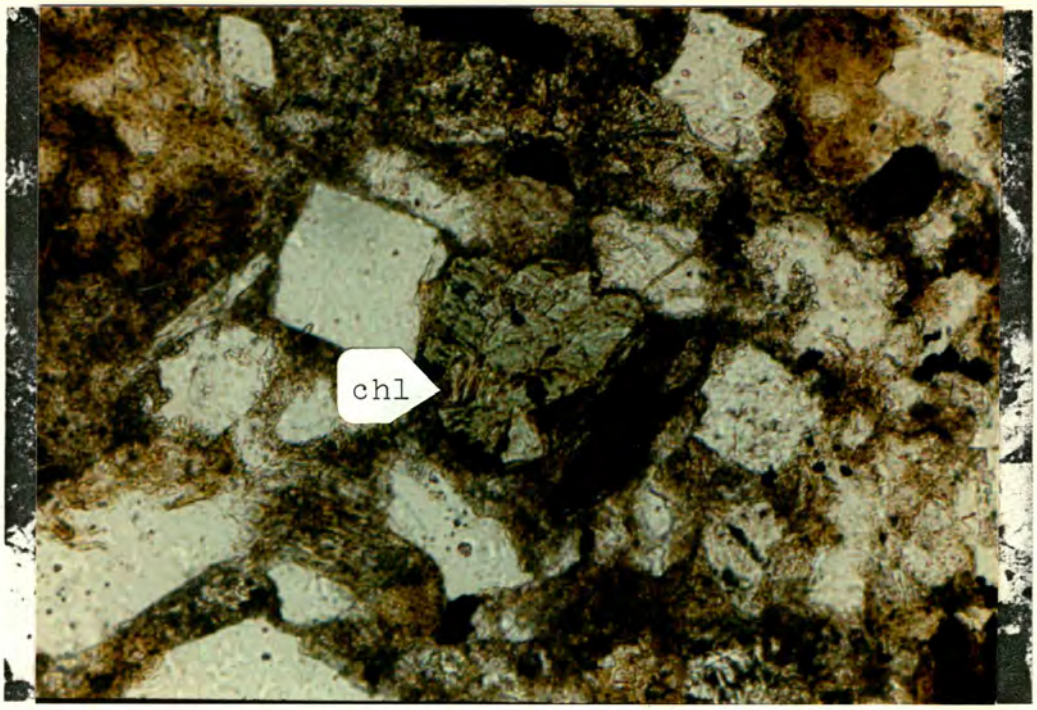


Figure 52.a. Chlorite (chl) grain. Sample 32-11-31-2. Field of view .85 x .58 mm. Plain light.

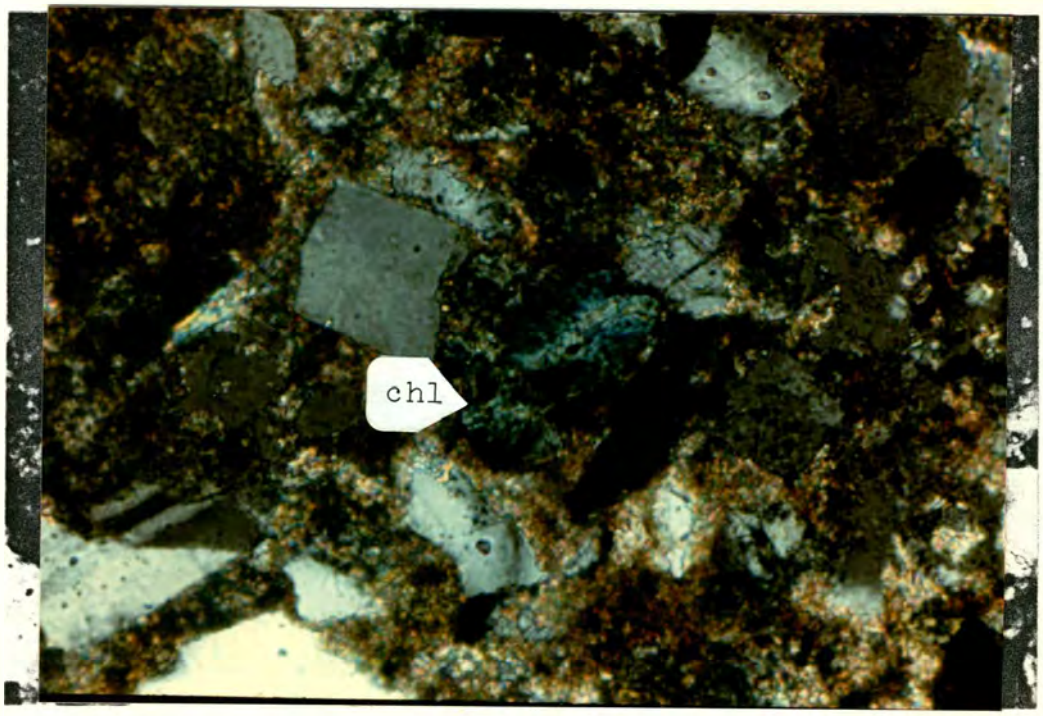


Figure 52.b. Chlorite (chl) grain. Sample 32-11-31-2. Field of view .85 x .58 mm. Polarized light.

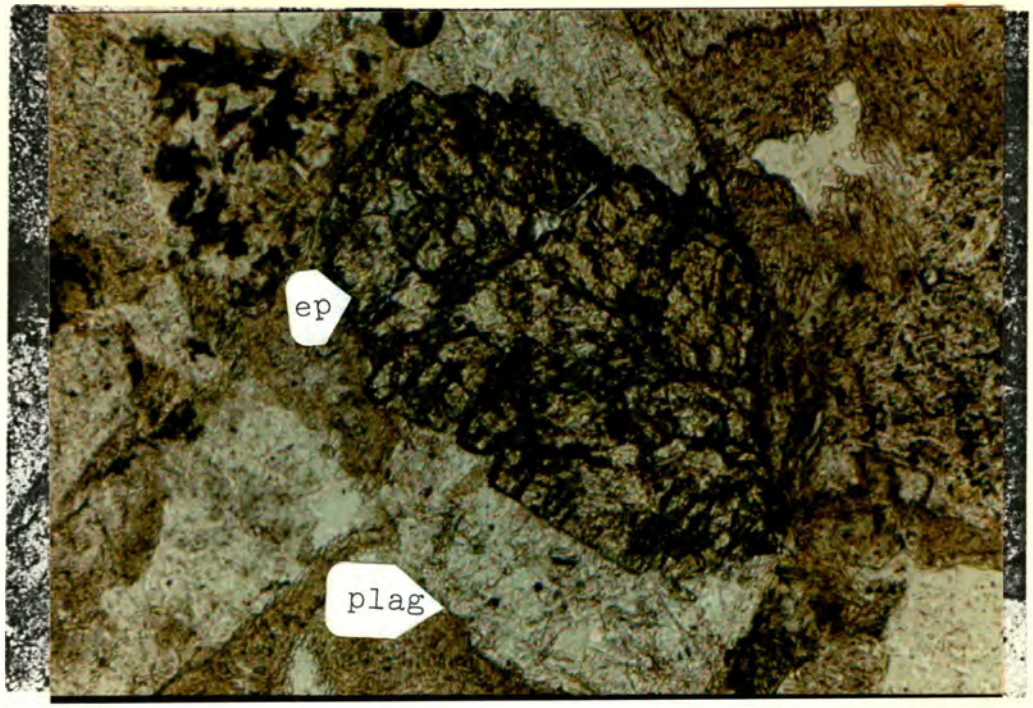


Figure 53.a. Epidote (ep) and plagioclase (plag) grain. Sample 32-11-31-5. Field of view .85 x .58 mm. Plain light.

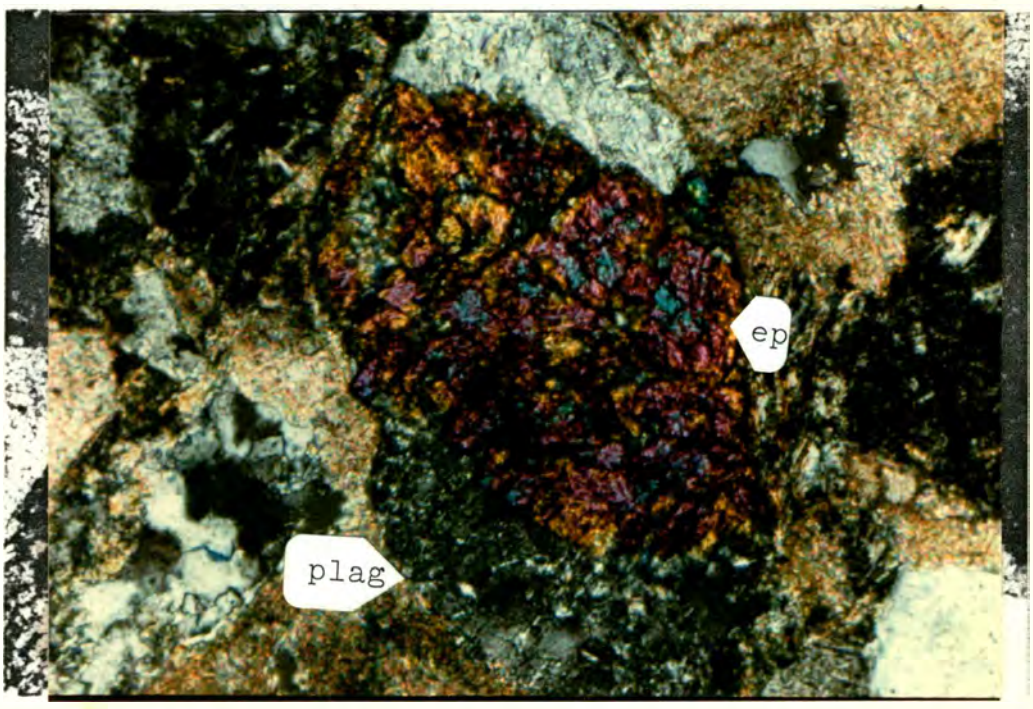


Figure 53.b. Epidote (ep) and plagioclase (plag) grain. Sample 32-11-31-5. Field of view .85 x .58 mm. Polarized light.

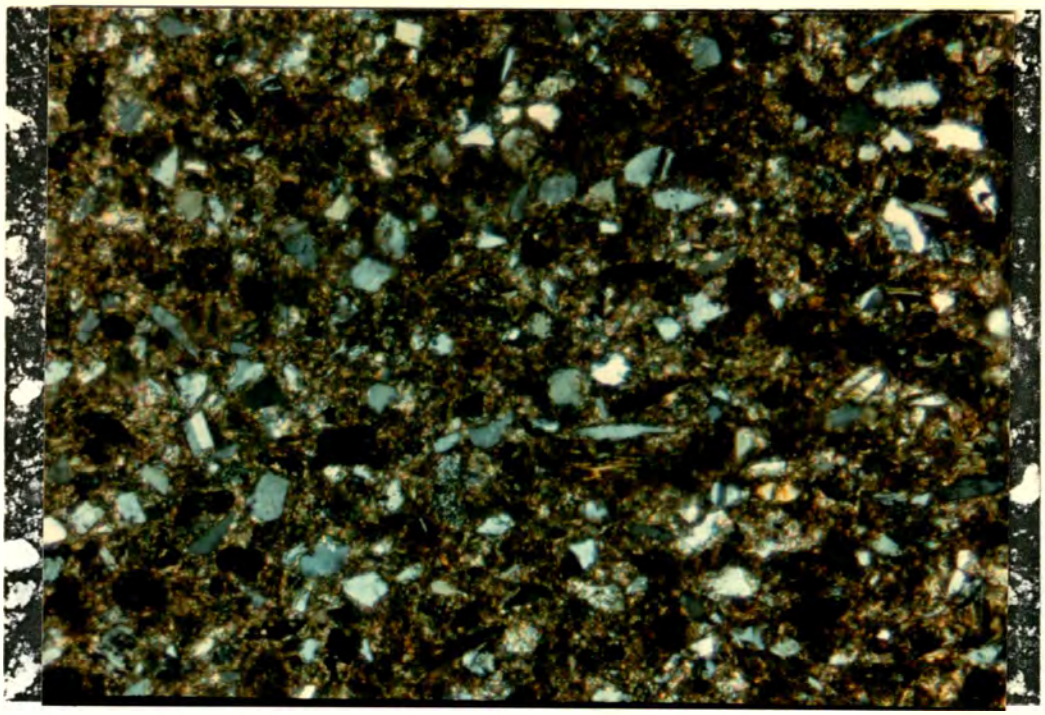

Figure 54. Calcite cement in concretionary sandstone. Sample 32-11-32-25. Field of view 2.1 x 1.5 mm.

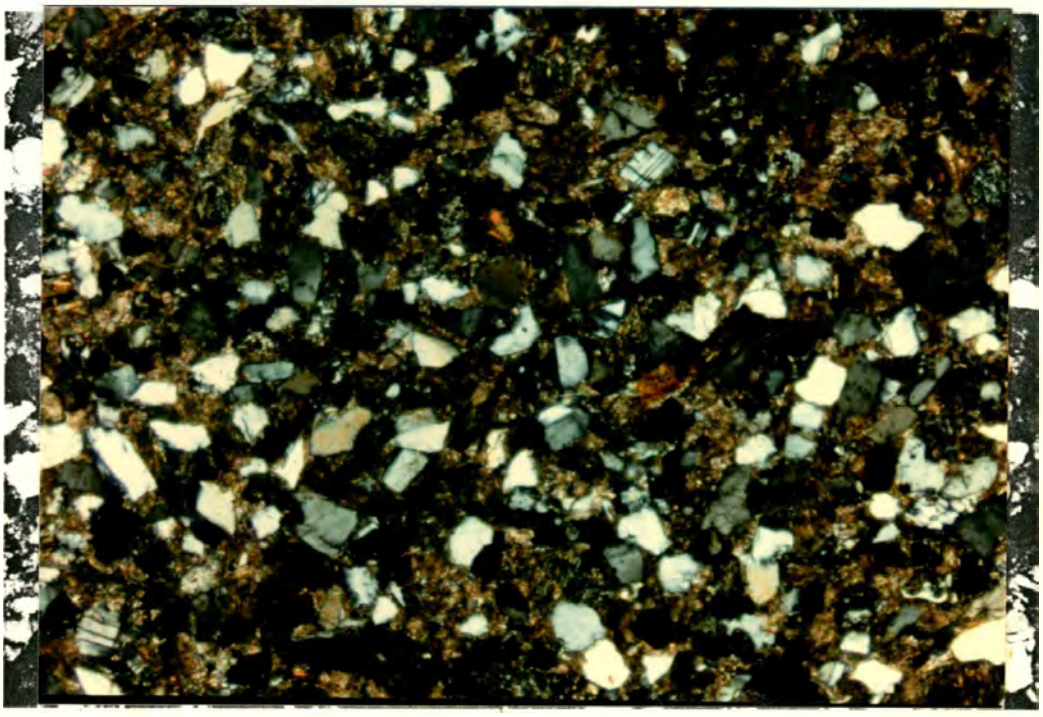

Figure 55. Calcite cement in nonconcretionary sandstone. Sample 32-11-32-26. Field of view 2.1 x 1.5 mm.

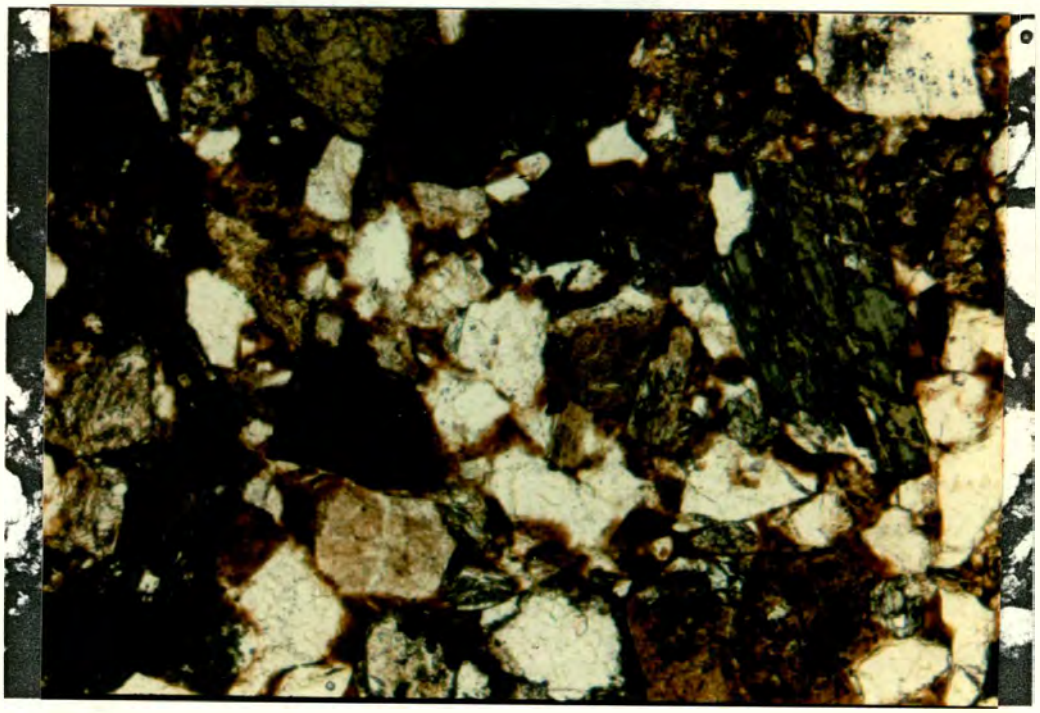

Figure 56. Hematite cement in sandstone. Sample 32-12-3-6. Field of view 2.1 x 1.5 mm.

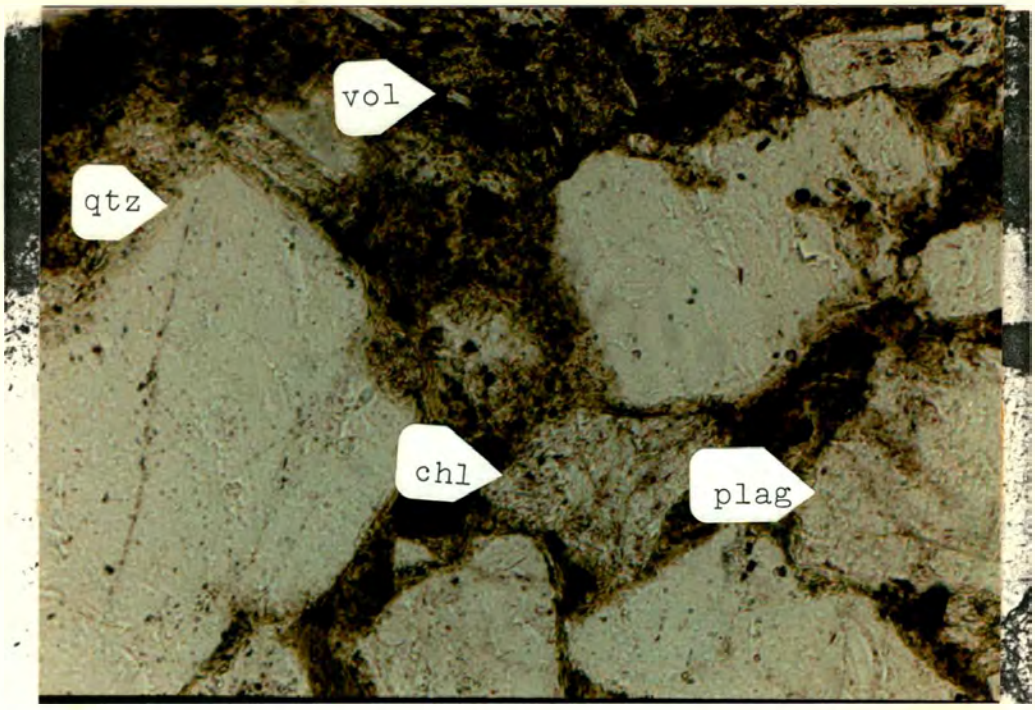


Figure 57.a. Clay matrix between quartz (qtz), plagioclase (plag), volcanic lithic (vol), and chlorite (chl) grains. Sample 32-11-30-4. Field of view .85 x .58 mm. Plain light.

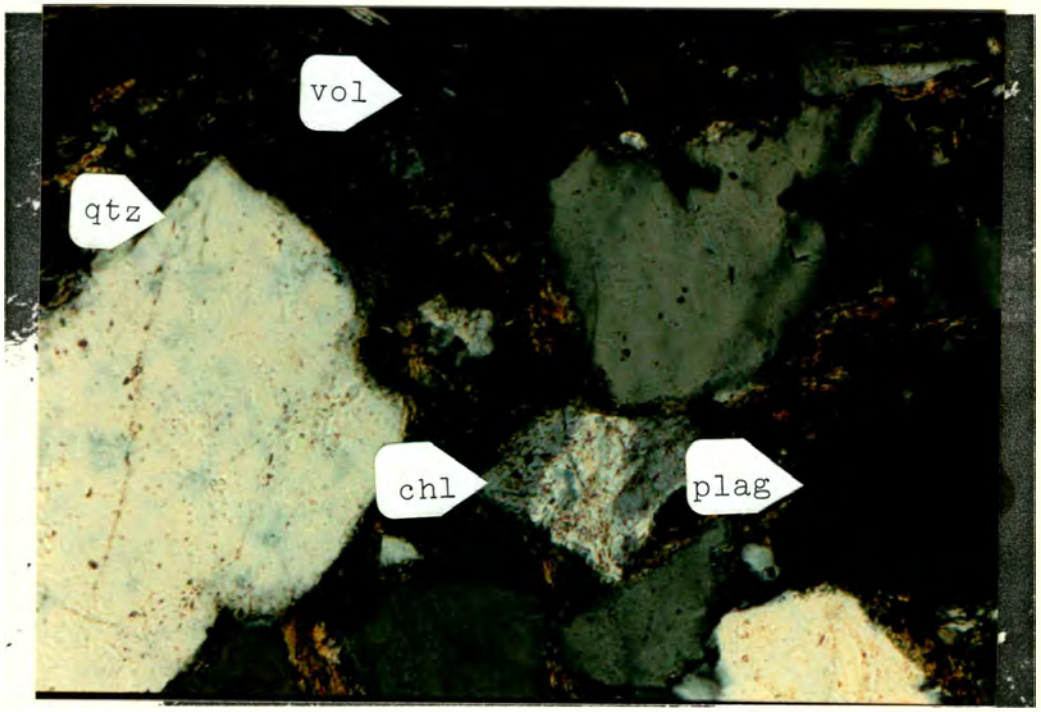


Figure 57.b. Clay matrix between quartz (qtz), plagioclase (plag), volcanic lithic (vol), and chlorite (chl) grains. Sample 32-11-30-4. Field of view .85 x .58 mm. Polarized light.

glauconite (Figure 58) are two examples.

Polycrystalline or Lithic Grains

Chert. To determine the amount of chert in individual samples, lithic counts were conducted with chert and Qa in separate categories. Some degree of error exists in point-counting fine-grained samples. In most fine-grained samples, more Qa was counted than chert; whereas all of the coarse-grained samples contain more chert than Qa (Figure 59). Because the relative amounts of Qa and chert are only used for determining the general amounts of metamorphic and plutonic polycrystalline quartz relative to chert, they do not affect the point count data.

Most chert has been recrystallized, and some contains significant percentages of impurities (Figure 60). Microcrystalline quartz with less than 15 percent impurities was counted as chert. The grains of recrystallized chert often display ghosts of radiolaria (Figure 61) and are sometimes noticeably deformed (Figure 62). Most, if not all, chert is recrystallized and was probably derived from a metamorphic terrane.

Qa: Ploycrystalline aphanitic quartz. The presence of variable crystal sizes and sutured crystal boundaries in polycrystalline quartz distinguishes it from chert (Figure 63). Small grain sizes make it difficult to distiguish the two.

Lv: Volcanic Lithics. Although a continuum of compositions, from felsic to mafic, is observed in the population of volcanic lithic grains, andesitic to dacitic volcanics account for the majority. The andesites and dacites commonly exhibit porphyritic, pilotaxitic, or trachytic textures (Figures 48 and 49). Almost all mafic constituents in the volcanics have been altered to chlorite and clays (Figure 50). A few andesite fragments containing clinopyroxene and oxyhornblende were found (Figure 48).

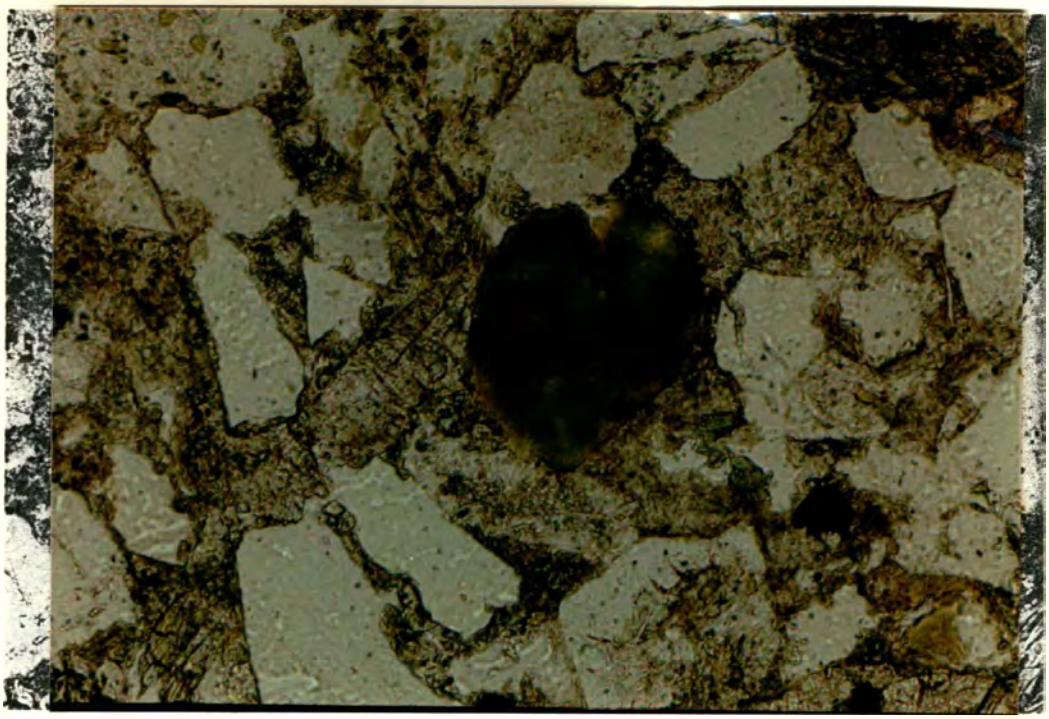

Figure 58. Glauconite grain. Sample 32-11-31-2. Field of view .85 x .58 mm.

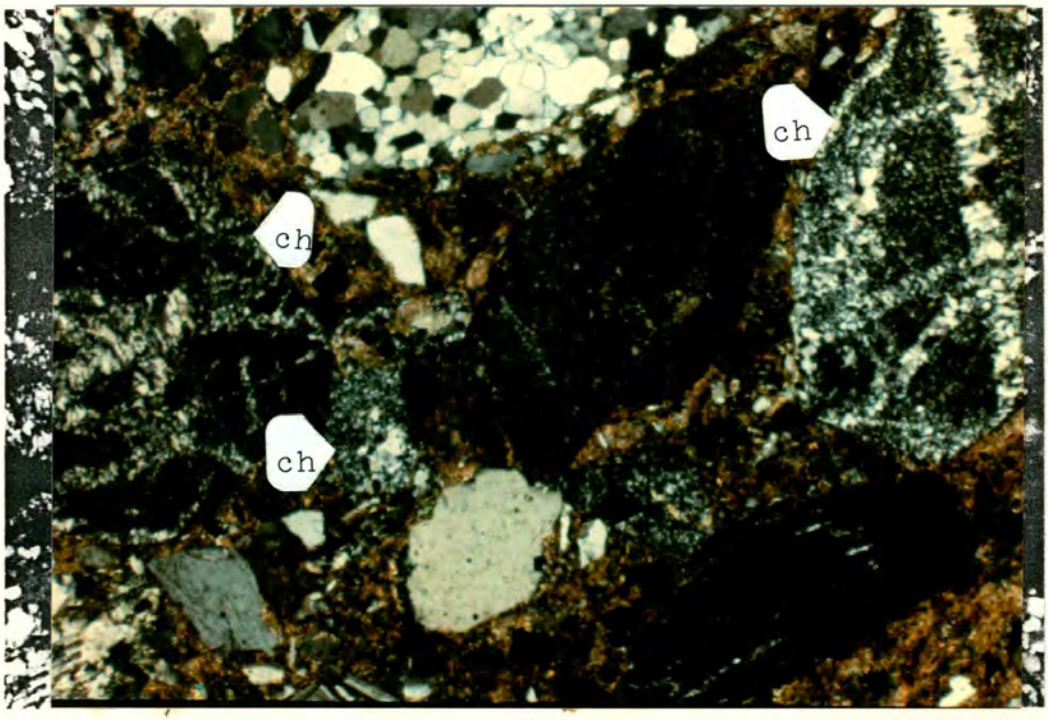


Figure 59. Chert (ch) rich sandstone. Note varying amounts of impurities. Sample 32-12-25-1. Field of view 3.4 x 2.3 mm.

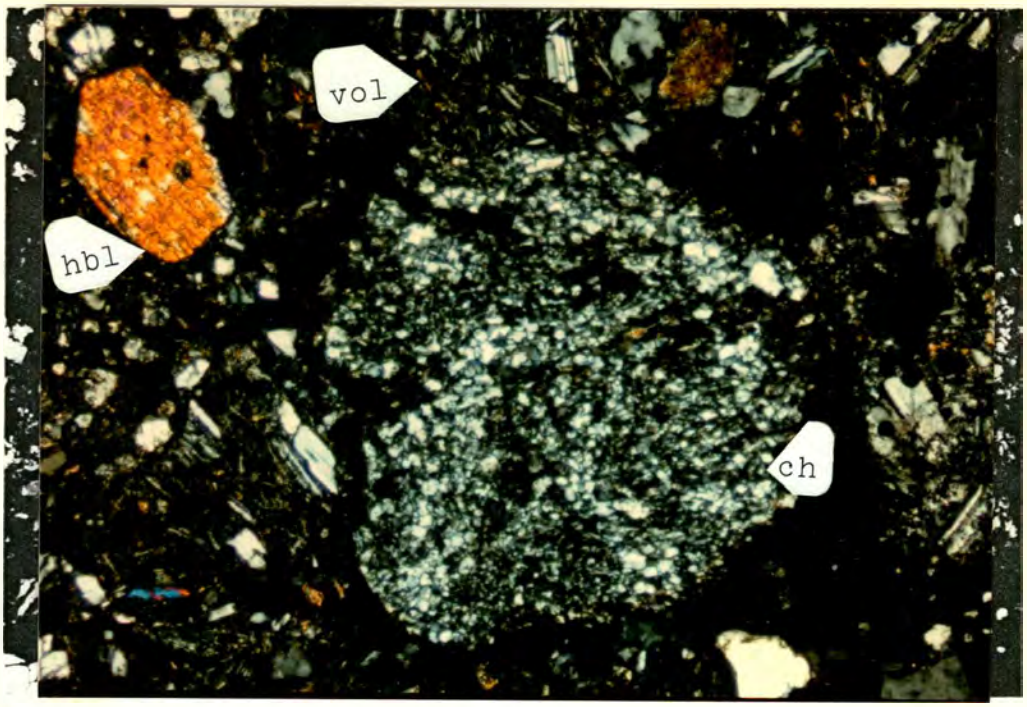


Figure 60. Chert (ch) with impurities of mica and clays. Note also hornblende (hbl) and volcanic (vol) grains. Sample 32-11-3-9. Field of view 2.7 x 1.8 mm.

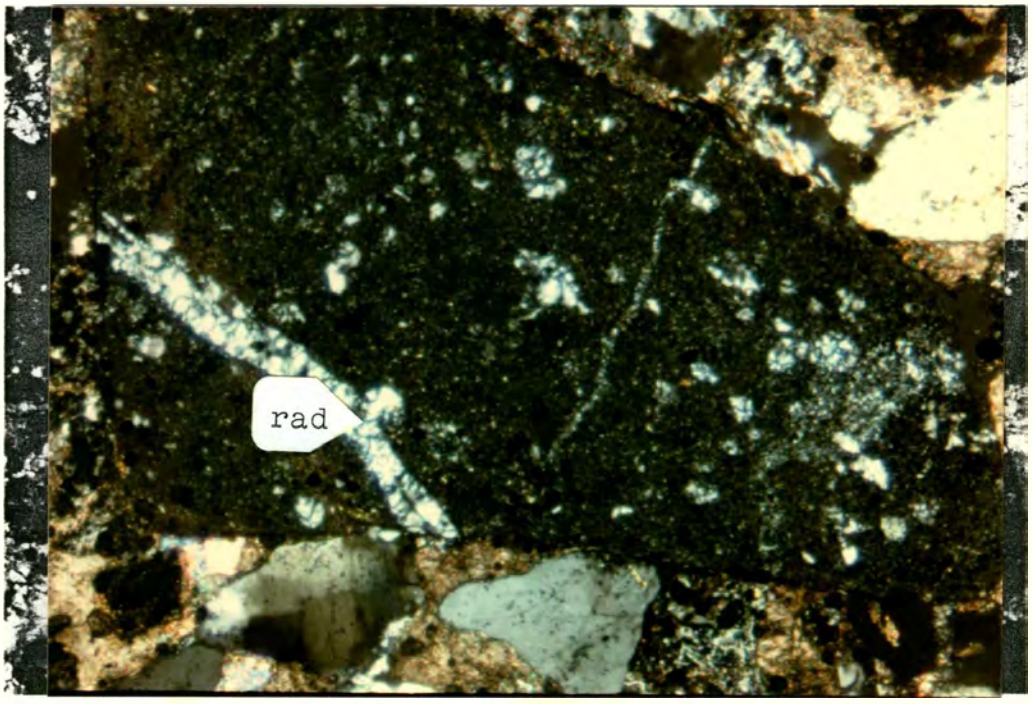


Figure 61. Chert grain with ghosts of radiolaria (rad). Sample 32-11-30-2. Field of view 2.1 x 1.5 mm.

Figure 62.a. Recrystallized and deformed chert grain. Sample 32-12-25-1. Field of view 2.1 x 1.5 mm. Plain light.

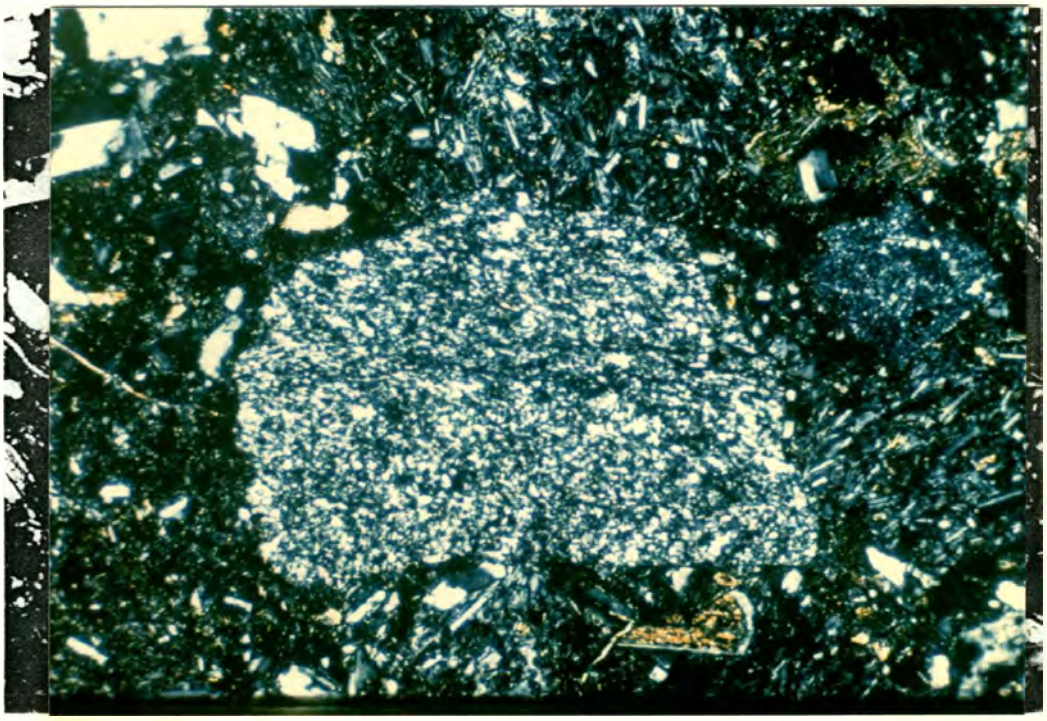

Figure 62.b. Recrystallized and deformed chert grain. Sample 32-12-25-1. Field of view 2.1 x 1.5 mm. Polarized light.

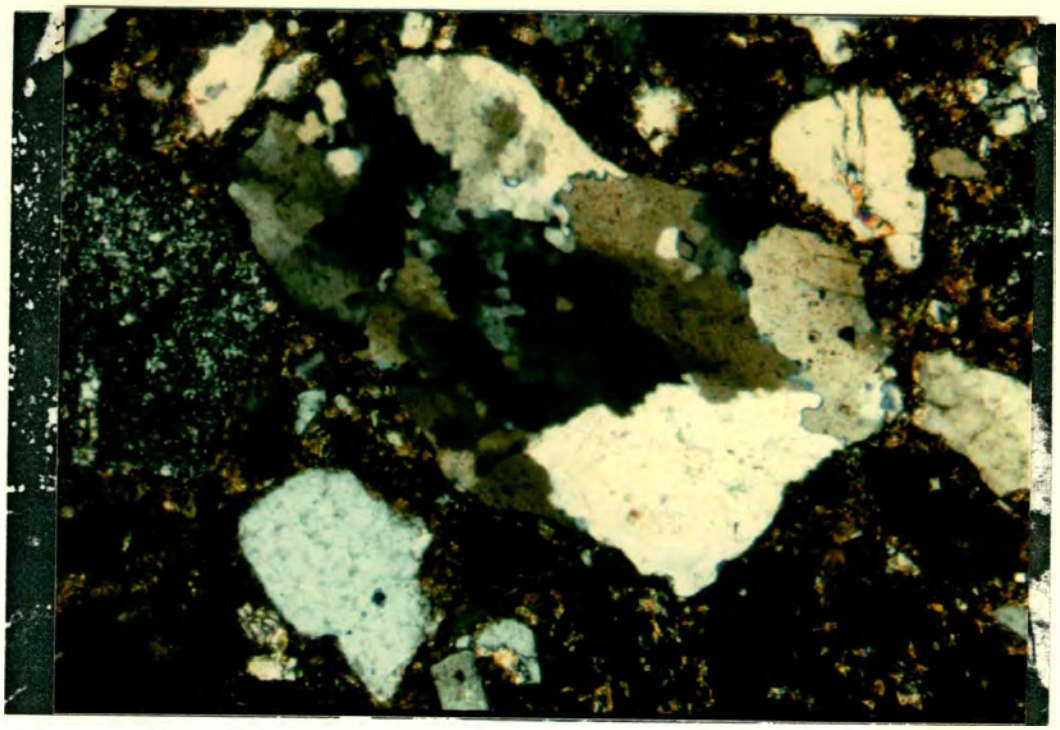

Figure 63. Polycrystalline quartz with sutured crystal boundaries and variable crystal sizes. Sample 32-12-25-1. Field of view 2.1 x 1.5 mm.

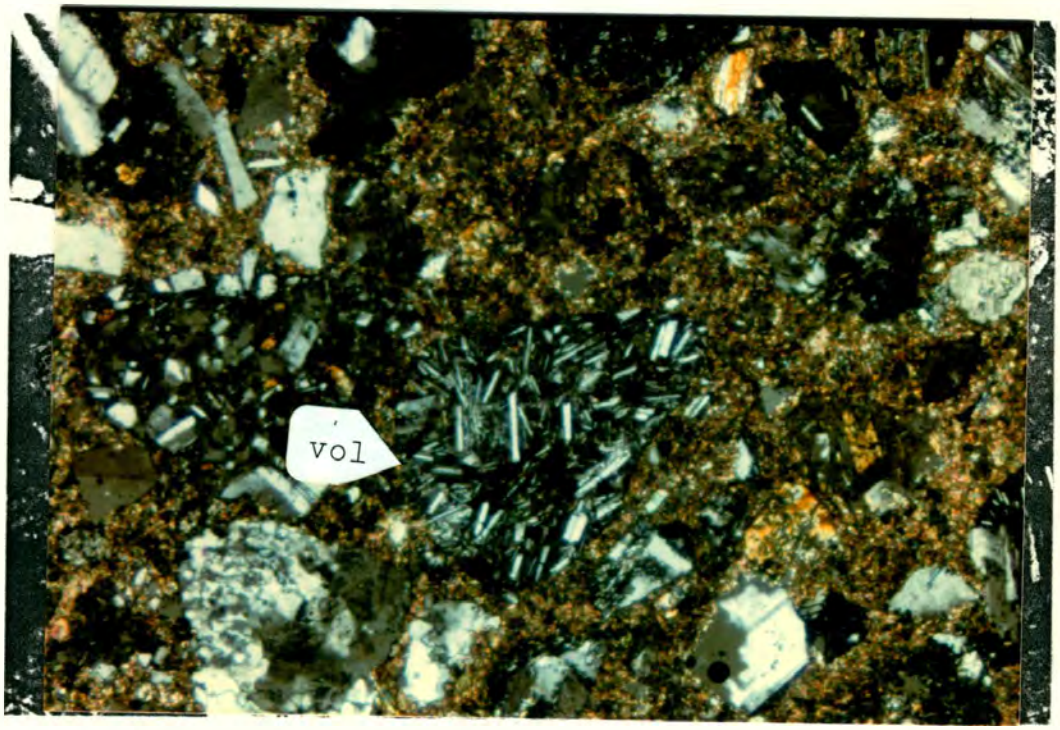


Figure 64. Pilotaxitic texture in volcanic (vol) lithic. Sample 32-11-32-8. Field of view 2.1 x 1.5 mm.

Although some potassium-rich volcanics were recognized by their susceptibility to sodium cobaltinitrite stain, the compositions of the majority of volcanic grains were determined by using the A-normal or Michael-Levy statistical method for determining plagioclase compositons. If a sufficient number of plagioclase laths was present in a pilotaxitic or trachytic grain, the Micheal-Levy method was used. The A-normal method was used on porphyritic grains. If the plagioclase composition was more sodic than $An_{50}$ the rock was classified as an andesite (using the IUGS classification).

Plagioclase phenocrysts in volcanic lithics are remarkably fresh considering the degree of alteration affecting the groundmass and mafic phenocrysts. Alteration of mafics is presumed to have resulted from either metamorphism or weathering.

Lslt: Siltstone Lithics. Siltstone lithics are rare in most samples. Some siltstone lithics are probably accumulations of intraclasts.

Lcs: Mudstone Lithics. Claystone lithics are also rare in most samples. In samples were they are not replaced by calcite cement, many of the claystone lithics are beginning to form psuedomatix. The lithics being replaced by calcite have vague grain boundries but still contain identifiable silt-sized constituents (Figure 65). Their origin appears to be largely intraformational. The division between claystone and siltstone was based on the amount of silt-sized grains: if the lithic contained less than 15 percent silt-sized fragments it was classified as a claystone.

Lm: Metamorphic Lithics. Both foliated and nonfoliated aggregates comprise the metamorphic grain populations (Figure 66 and 67). The foliated varieties include mainly quartz, clay, graphite, and phyllosilicate assemblages such as calcite-biotite schist, muscovite schist, and phyllite. The nonfoliated aggregates include assemblages such as quartz-

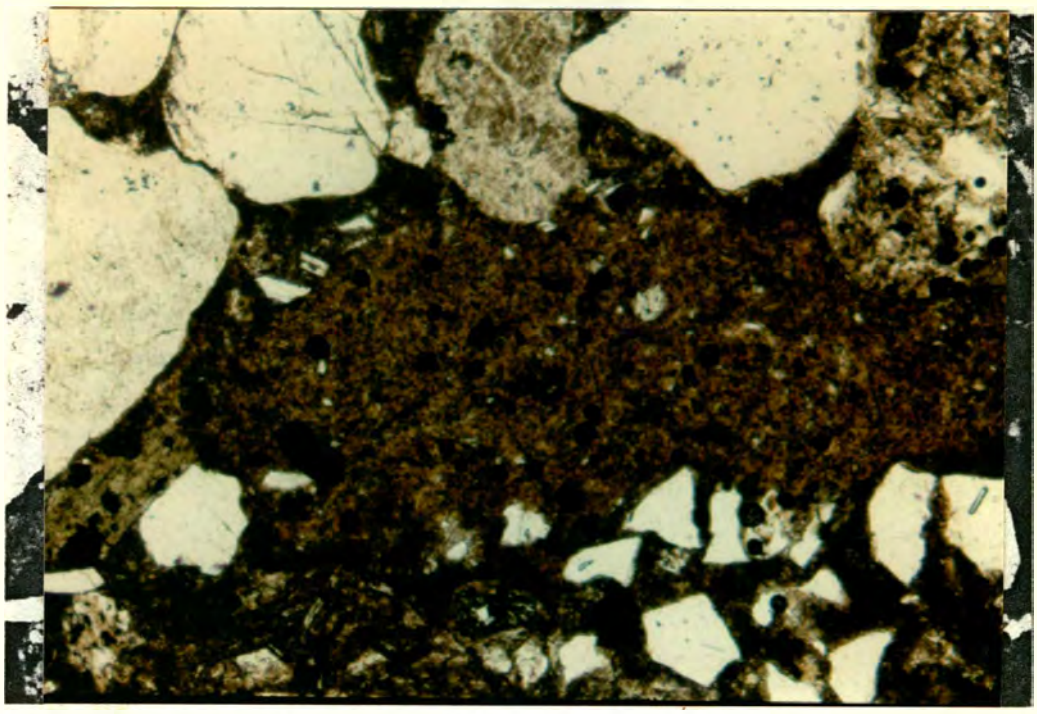

Figure 65.a. Sedimentary lithic grain being replaced by calcite. Sample 32-11-21-5. Field of view 2.1 x 1.5 mm. Plain light.

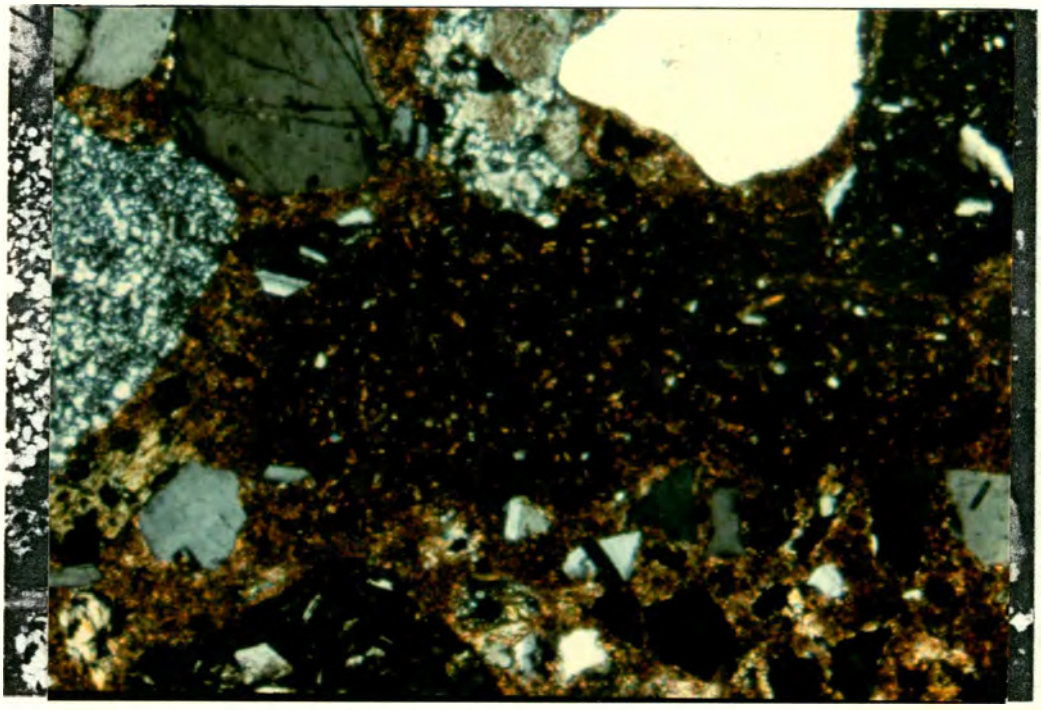

Figure 65.b. Sedimentary lithic grain being replaced by calcite. Sample 32-11-21-5. Field of view 2.1 x 1.5 mm. Polarized light.

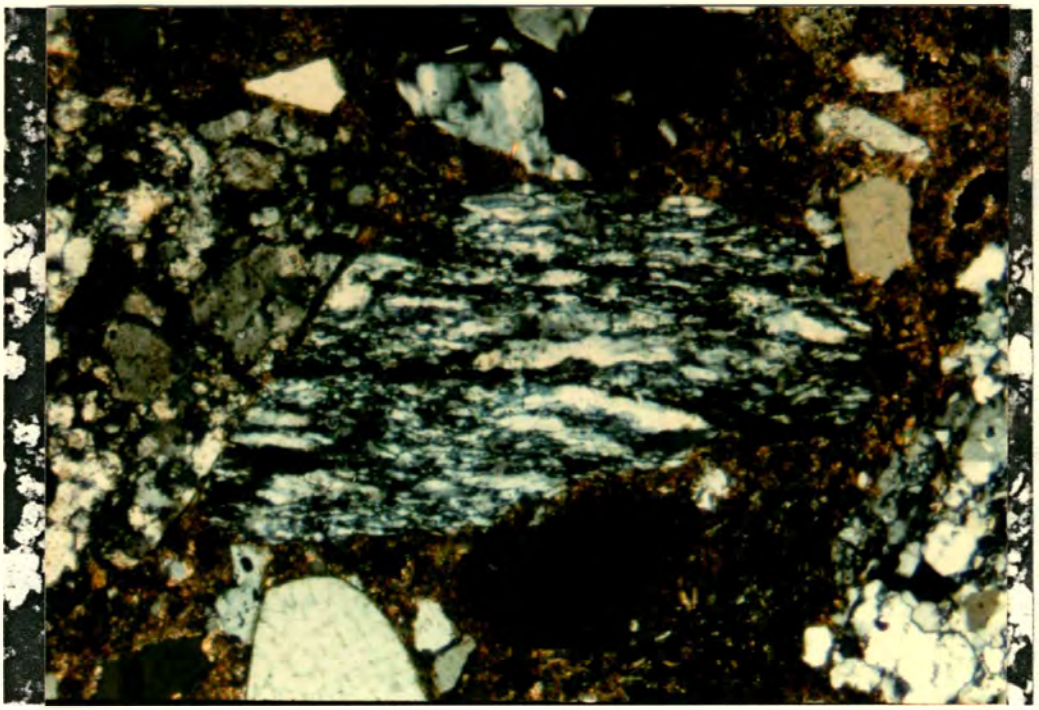

Figure 66. Foliated metamorphic lithic grain. Sample 32-12-25-1. Field of view 2.1 x 1.5 mm.

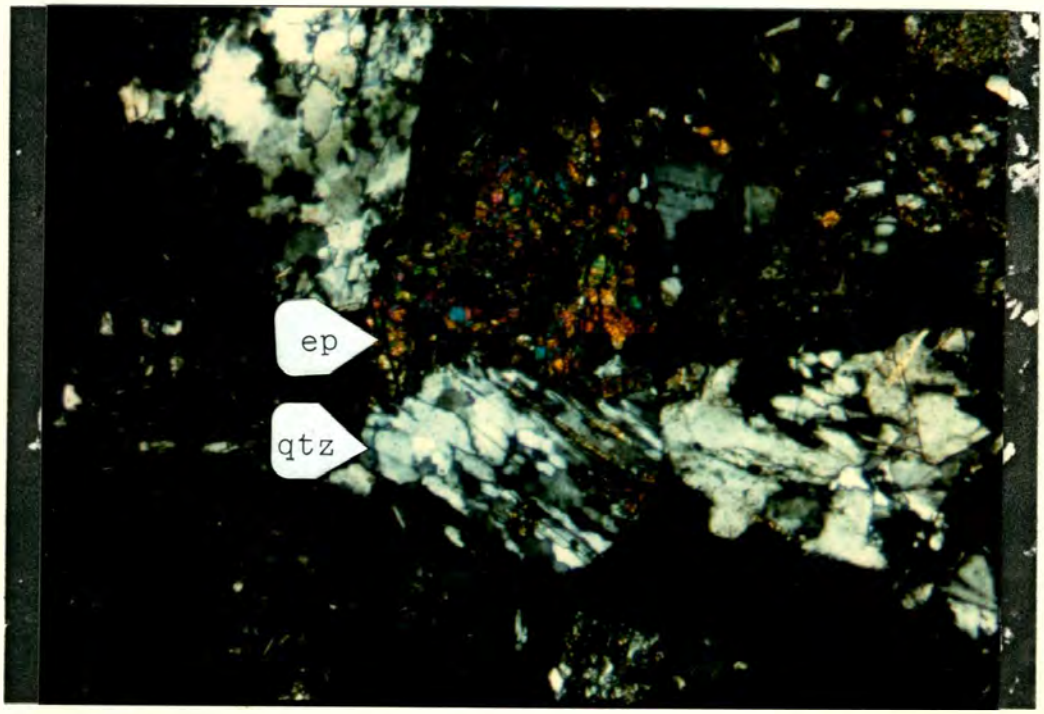


Figure 67. Epidote (ep) -quartz (qtz) metamorphic aggregate. Sample 32-11-32-9. Field of view 2.1 x 1.5 mm.

epidote-chlorite, actinolite-plagioclase-epidote-quartz, zoesite-plagioclase, and chlorite-quartz. Some detrital prehnite and pumpellyite are also present. Specific P/T conditions cannot be deduced from the metamorphic mineral assemblages.

Li: Intrusive Lithics. Most of the plutonic fragments contain coarse minerals and are therefore counted as individual grains such as quartz, plagioclase, or biotite. The grains most often counted in this category are grains that exhibite granophyric textures (Figure 68). The plutonic source rocks must have consisted of albite or oligoclase, quartz, hornblende, biotite, and minor potassium feldspar. This mineral assemblage suggests the composition of a granodiorite or quartz monzonite.

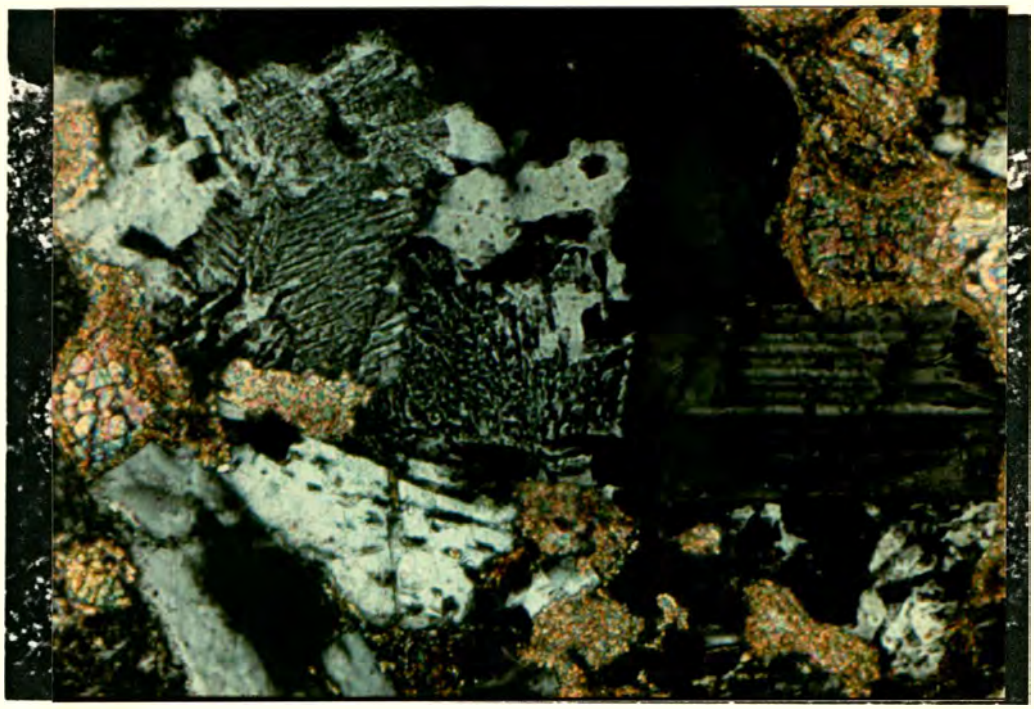

Figure 68. Granophyric texture in plutonic lithic grain. Sample 32-11-31-5. Field of view .85 x .58 mm.

APPENDIX 2: Modal analysis of samples from Facies 1.

| Total Count (300 Points) | Sample Numbers 32-11-33-1 | 32-11-33-2 | 32-12-23-1 |
|---|---|---|---|
| Qm | 19 | 19 | 10 |
| P | 17 | 15 | 11 |
| K | 2 | 1 | - |
| Lithics | 14 | 17 | 19 |
| Qp | 1 | 4 | 2 |
| Mafics | 4 | 7 | 4 |
| Matrix | - | - | - |
| Cement | 39 | 34 | 49 |
| Misc. | 4 | 3 | 5 |
| **Lithic Count (200 Points)** | | | |
| Qa | 13 | 25 | 12 |
| Chert | 5 | 4 | 15 |
| Lv | 57 | 63 | 17 |
| Lslt | - | - | 1 |
| Lcs | 13 | 5 | 29 |
| Lm | 5 | 2 | 19 |
| Li | 2 | - | 1 |
| Misc. | 5 | 1 | 6 |
| **QFL** | | | |
| Q | 37 | 41 | 27 |
| F | 37 | 29 | 27 |
| L | 26 | 30 | 46 |
| **QmFLt** | | | |
| Qm | 35 | 34 | 23 |
| F | 37 | 29 | 27 |
| Lt | 28 | 37 | 50 |
| **QpLvLs** | | | |
| Qp | 20 | 29 | 29 |
| Lv | 61 | 64 | 18 |
| Ls | 19 | 7 | 53 |

APPENDIX 3: Modal analysis of samples from Facies 2.

| Total Count (300 Points) | Sample Numbers 32-12-21-9 | 32-11-32-2 | 32-12-22-13 | 32-12-21-15 |
|---|---|---|---|---|
| Qm | 10 | 17 | 30 | 11 |
| P | 18 | 13 | 20 | 27 |
| K | 1 | 1 | 2 | 3 |
| Lithics | 17 | 10 | 7 | 9 |
| Qp | 4 | 3 | 3 | 3 |
| Mafics | 5 | 5 | 13 | 4 |
| Matrix | - | - | 23 | - |
| Cement | 42 | 49 | - | 42 |
| Misc. | 3 | 2 | 2 | 1 |
| **Lithic Count (200 Points)** | | | | |
| Qa | 11 | 25 | - | 15 |
| Chert | 6 | 13 | - | 14 |
| Lv | 69 | 37 | - | 55 |
| Lslt | - | - | - | - |
| Lcs | 1 | 8 | - | 2 |
| Lm | 11 | 13 | - | 10 |
| Li | 1 | - | - | - |
| Misc. | 1 | 4 | - | 4 |
| **QFL** | | | | |
| Q | 28 | 46 | 53 | 26 |
| F | 37 | 32 | 37 | 56 |
| L | 35 | 22 | 10 | 18 |
| **QmFLt** | | | | |
| Qm | 20 | 39 | 48 | 21 |
| F | 37 | 32 | 37 | 56 |
| Lt | 43 | 29 | 15 | 23 |
| **QpLvLs** | | | | |
| Qp | 17 | 39 | - | 30 |
| Lv | 71 | 39 | - | 58 |
| Ls | 12 | 22 | - | 12 |

APPENDIX 4: Modal analysis of samples from Facies 3.

| Total Count (300 Points) | Sample Numbers 32-11-32-25 Spacing 0.5 | 32-11-32-26 Spacing 0.5 | 32-12-26-4 | 32-11-32-10 |
|---|---|---|---|---|
| Qm | 12 | 23 | 18 | 17 |
| P | 7 | 18 | 22 | 13 |
| K | - | 4 | 2 | 3 |
| Lithics | 3 | 11 | 10 | 7 |
| Qp | - | - | 3 | - |
| Mafics | 9 | 5 | 9 | 14 |
| Matrix | - | - | - | - |
| Cement | 65 | 37 | 34 | 43 |
| Misc. | 4 | 2 | 2 | 3 |
| **Lithic Count (200 Points)** | | | | |
| Qa | - | 4 | 5 | - |
| Chert | - | 7 | 8 | - |
| Lv | - | 50 | 47 | - |
| Lslt | - | - | 1 | - |
| Lcs | - | 9 | 11 | - |
| Lm | - | 20 | 21 | - |
| Li | - | 5 | 3 | - |
| Misc. | - | 5 | 4 | - |
| **QFL** | | | | |
| Q | 56 | 41 | 38 | 42 |
| F | 32 | 39 | 44 | 40 |
| L | 12 | 20 | 18 | 18 |
| **QmFLt** | | | | |
| Qm | 54 | 41 | 33 | 41 |
| F | 32 | 39 | 44 | 40 |
| Lt | 14 | 20 | 23 | 19 |
| **QpLvLs** | | | | |
| Qp | - | 12 | 14 | - |
| Lv | - | 56 | 50 | - |
| Ls | - | 32 | 36 | - |

APPENDIX 4: Modal analysis of samples from Facies 3 (cont.).

| Total Count (300 Points) | Sample Numbers 32-11-32-5 Spacing 0.5 | 32-11-31-2 |
|---|---|---|
| Qm | 22 | 24 |
| P | 14 | 14 |
| K | 1 | 2 |
| Lithics | 8 | 15 |
| Qp | 2 | - |
| Mafics | 9 | 6 |
| Matrix | - | - |
| Cement | 40 | 37 |
| Misc. | 4 | 2 |
| **Lithic Count (200 Points)** | | |
| Qa | - | 10 |
| Chert | - | 10 |
| Lv | - | 39 |
| Lslt | - | 2 |
| Lcs | - | 22 |
| Lm | - | 11 |
| Li | - | 2 |
| Misc. | - | 4 |
| **QFL** | | |
| Q | 51 | 43 |
| F | 32 | 29 |
| L | 17 | 28 |
| **QmFLt** | | |
| Qm | 47 | 43 |
| F | 32 | 29 |
| Lt | 21 | 28 |
| **QpLvLs** | | |
| Qp | - | 21 |
| Lv | - | 41 |
| Ls | - | 38 |

APPENDIX 5: Modal analysis of samples from Facies 4.

| Total Count (300 Points) | Sample Numbers 32-11-32-30 | 32-11-32-32 | 32-11-32-38 | 32-12-22-8 |
|---|---|---|---|---|
| Qm | 21 | 18 | 20 | 16 |
| P | 28 | 26 | 10 | 20 |
| K | 3 | 1 | 3 | 1 |
| Lithics | 6 | 5 | 11 | 9 |
| Qp | 2 | 1 | 4 | 5 |
| Mafics | 10 | 7 | 13 | 7 |
| Matrix | - | - | - | - |
| Cement | 27 | 41 | 36 | 40 |
| Misc. | 3 | 1 | 3 | 2 |
| **Lithic Count (200 Points)** | | | | |
| Qa | - | - | - | 20 |
| Chert | - | - | - | 16 |
| Lv | - | - | - | 41 |
| Lslt | - | - | - | - |
| Lcs | - | - | - | 6 |
| Lm | - | - | - | 12 |
| Li | - | - | - | 3 |
| Misc. | - | - | - | 2 |
| **QFL** | | | | |
| Q | 38 | 37 | 49 | 41 |
| F | 52 | 54 | 27 | 41 |
| L | 10 | 9 | 24 | 18 |
| **QmFLt** | | | | |
| Qm | 35 | 35 | 42 | 31 |
| F | 52 | 54 | 27 | 41 |
| Lt | 13 | 11 | 31 | 28 |
| **QpLvLs** | | | | |
| Qp | - | - | - | 38 |
| Lv | - | - | - | 43 |
| Ls | - | - | - | 19 |

APPENDIX 5: Modal analysis of samples from Facies 4 (cont.).

| Total Count (300 Points) | Sample Numbers 32-12-22-10 | 32-12-22-11 |
|---|---|---|
| Qm | 14 | 19 |
| P | 21 | 22 |
| K | 2 | 4 |
| Lithics | 7 | 9 |
| Qp | 2 | 2 |
| Mafics | 9 | 22 |
| Matrix | - | 19 |
| Cement | 43 | - |
| Misc. | 2 | 3 |
| **Lithic Count (200 Points)** | | |
| Qa | - | - |
| Chert | - | - |
| Lv | - | - |
| Lslt | - | - |
| Lcs | - | - |
| Lm | - | - |
| Li | - | - |
| Misc. | - | - |
| **QFL** | | |
| Q | 35 | 37 |
| F | 51 | 46 |
| L | 14 | 17 |
| **QmFLt** | | |
| Qm | 31 | 33 |
| F | 51 | 46 |
| Lt | 18 | 21 |
| **QpLvLs** | | |
| Qp | - | - |
| Lv | - | - |
| Ls | - | - |

APPENDIX 6: Modal analysis of samples from Facies 5.

| Total Count (300 Points) | Sample Numbers 32-11-30-1 | 32-11-30-2 | 32-11-30-4 | 32-11-30-5 |
|---|---|---|---|---|
| Qm | 12 | 29 | 24 | 20 |
| P | 17 | 7 | 14 | 8 |
| K | 1 | 1 | 2 | 2 |
| Lithics | 36 | 19 | 29 | 30 |
| Qp | 5 | 21 | 7 | 14 |
| Mafics | 3 | - | 1 | 1 |
| Matrix | 10 | - | 22 | - |
| Cement | - | 22 | - | 24 |
| Misc. | 16 | 1 | 1 | 1 |
| **Lithic Count (200 Points)** | **Spacing 1.0** | **Spacing 1.0** | **Spacing 1.0** | **Spacing 1.0** |
| Qa | 3 | 6 | 4 | 3 |
| Chert | 9 | 44 | 14 | 22 |
| Lv | 66 | 26 | 60 | 55 |
| Lslt | 3 | 6 | 1 | 1 |
| Lcs | 3 | 7 | 6 | 7 |
| Lm | 14 | 4 | 10 | 8 |
| Li | 2 | 4 | 3 | 3 |
| Misc. | - | 3 | 2 | 1 |
| QFL | | | | |
| Q | 23 | 65 | 41 | 46 |
| F | 26 | 11 | 21 | 14 |
| L | 51 | 24 | 38 | 40 |
| QmFLt | | | | |
| Qm | 16 | 38 | 32 | 27 |
| F | 26 | 11 | 21 | 14 |
| Lt | 58 | 51 | 47 | 59 |
| QpLvLs | | | | |
| Qp | 8 | 53 | 19 | 26 |
| Lv | 45 | 28 | 63 | 57 |
| Ls | 47 | 19 | 18 | 17 |

APPENDIX 6: Modal analysis of samples from Facies 5 (cont.).

| Total Count (300 Points) | Sample Numbers 32-11-31-5 | 32-11-32-7 | 32-11-32-17 | 32-12-21-3 |
|---|---|---|---|---|
| Qm | 18 | 21 | 20 | 13 |
| P | 14 | 21 | 20 | 18 |
| K | 1 | 3 | 3 | 2 |
| Lithics | 36 | 25 | 16 | 20 |
| Qp | 6 | 4 | 2 | 2 |
| Mafics | 1 | 9 | 5 | 5 |
| Matrix | - | 15 | - | - |
| Cement | 23 | - | 33 | 35 |
| Misc. | 1 | 2 | 1 | 4 |
| **Lithic Count (200 Points)** | **Spacing 1.0** | | **Spacing 1.0** | |
| Qa | - | 1 | 4 | 2 |
| Chert | 9 | 7 | 7 | 7 |
| Lv | 57 | 63 | 60 | 64 |
| Lslt | 3 | 4 | 1 | 2 |
| Lcs | 8 | 10 | 9 | 5 |
| Lm | 17 | 11 | 15 | 17 |
| Li | 3 | 1 | 3 | - |
| Misc. | 3 | 3 | 1 | 3 |
| QFL | | | | |
| Q | 32 | 34 | 36 | 28 |
| F | 20 | 32 | 38 | 35 |
| L | 48 | 34 | 26 | 37 |
| QmFLt | | | | |
| Qm | 24 | 28 | 33 | 24 |
| F | 20 | 32 | 38 | 35 |
| Lt | 56 | 40 | 29 | 41 |
| QpLvLs | | | | |
| Qp | 10 | 8 | 12 | 9 |
| Lv | 60 | 65 | 63 | 67 |
| Ls | 30 | 27 | 25 | 24 |

APPENDIX 6: Modal analysis of samples from Facies 5 (cont.).

| Total Count (300 Points) | Sample Numbers 32-12-21-5 | 32-12-21-6 | 32-12-25-1 | 32-11-31-1 |
|---|---|---|---|---|
| Qm | 16 | 11 | 26 | 7 |
| P | 12 | 11 | 6 | 7 |
| K | 1 | 1 | 1 | 2 |
| Lithics | 26 | 31 | 22 | 19 |
| Qp | 10 | 10 | 13 | 2 |
| Mafics | 2 | 7 | 1 | 2 |
| Matrix | - | - | - | - |
| Cement | 32 | 27 | 31 | 61 |
| Misc. | 1 | 2 | - | - |
| **Lithic Count (200 Points)** | **Spacing 1.0** | **Spacing 1.0** | **Spacing 1.0** | |
| Qa | 8 | 3 | 3 | 2 |
| Chert | 15 | 7 | 47 | 5 |
| Lv | 59 | 74 | 30 | 57 |
| Lslt | 2 | 2 | 1 | - |
| Lcs | 5 | 2 | 10 | 4 |
| Lm | 9 | 9 | 7 | 22 |
| Li | - | 1 | 2 | 5 |
| Misc. | 2 | 2 | - | 5 |
| **QFL** | | | | |
| Q | 39 | 32 | 59 | 24 |
| F | 21 | 19 | 9 | 24 |
| L | 40 | 49 | 32 | 52 |
| **QmFLt** | | | | |
| Qm | 24 | 18 | 39 | 19 |
| F | 21 | 19 | 9 | 24 |
| Lt | 55 | 63 | 52 | 57 |
| **QpLvLs** | | | | |
| Qp | 24 | 10 | 52 | 8 |
| Lv | 58 | 75 | 30 | 64 |
| Ls | 18 | 15 | 18 | 28 |